SSI report

SSI Rapport
2008:08

Rapport från Statens strålskyddsinstitut
tillgänglig i sin helhet via www.ssi.se

SSI's independent consequence calculations in support of the regulatory review of the SR-Can safety assessment

Shulan Xu, Anders Wörman, Björn Dverstorp,
Richard Kłos, George Shaw och Lars Marklund

Statens strålskyddsinstitut
Swedish Radiation Protection Authority

SSI's Activity Symbols

Ultraviolet, solar and optical radiation
Ultraviolet radiation from the sun and solariums can result in both long-term and short-term effects. Other types of optical radiation, primarily from lasers, can also be hazardous. SSI provides guidance and information.

Solariums
The risk of tanning in a solarium are probably the same as tanning in natural sunlight. Therefore SSI's regulations also provide advice for people tanning in solariums.

Radon
The largest contribution to the total radiation dose to the Swedish population comes from indoor air. SSI works with risk assessments, measurement techniques and advises other authorities.

Health care
The second largest contribution to the total radiation dose to the Swedish population comes from health care. SSI is working to reduce the radiation dose to employees and patients through its regulations and its inspection activities.

Radiation in industry and research
According to the Radiation Protection Act, a licence is required to conduct activities involving ionising radiation. SSI promulgates regulations and checks compliance with these regulations, conducts inspections and investigations and can stop hazardous activities.

Nuclear power
SSI requires that nuclear power plants should have adequate radiation protection for the generalpublic, employees and the environment. SSI also checks compliance with these requirements on a continuous basis.

Waste
SSI works to ensure that all radioactive waste is managed in a manner that is safe from the standpoint of radiation protection.

Mobile telephony
Mobile telephones and base stations emit electromagnetic fields. SSI is monitoring developments and research in mobile telephony and associated health risks.

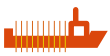

Transport
SSI is involved in work in Sweden and abroad to ensure the safe transportation of radioactive substances used in the health care sector, industrial radiation sources and spent nuclear fuel.

Environment
"A safe radiation environment" is one of the 15 environmental quality objectives that the Swedish parliament has decided must be met in order to achieve an ecologically sustainable development in society. SSI is responsible for ensuring that this objective is reached.

Biofuel
Biofuel from trees, which contains, for example from the Chernobyl accident, is an issue where SSI is currently conducting research and formulating regulations.

Cosmic radiation
Airline flight crews can be exposed to high levels of cosmic radiation. SSI participates in joint international projects to identify the occupational exposure within this job category.

Electromagnetic fields
SSI is working on the risks associated with electromagnetic fields and adopts countermeasures when risks are identified.

Emergency preparedness
SSI maintains a round-the-clock emergency response organisation to protect people and the environment from the consequences of nuclear accidents and other radiation-related accidents.

SSI Education
is charged with providing a wide range of education in the field of radiation protection. Its courses are financed by students' fees.

EDITORS / REDAKTÖRER : Shulan Xu[1], Anders Wörman[2], Björn Dverstorp[1], Richard Kłos[3], George Shaw[4] and Lars Marklund[2]

[1] Swedish Radiation Protection Authority (SSI)
[2] The Royal Institute of Technology (KTH), Stockholm
[3] Aleksandria Sciences, UK
[4] University of Nottingham, UK

TITLE / TITEL: SSI's independent consequence calculations in support of the regulatory review of the SR-Can safety assessment/ SSI:s oberoende beräkningar av radiologiska doser till stöd för granskningen av SKB:s säkerhetsanalys SR-Can.

DEPARTMENT / AVDELNING: of Nuclear Facilities and Waste Management / Avdelningen för kärnteknik och avfall

SSI rapport: 2008:08
mars 2008
ISSN 0282-4434

Statens strålskyddsinstitut
Swedish Radiation Protection Authority

Sammanfattning

Svensk Kärnbränslehantering AB (SKB) presenterade i slutet av 2006 säkerhetsredovisningen SR-Can som är en första utvärdering av den långsiktiga säkerheten för ett KBS-3-slutförvar vid Forsmark respektive Laxemar. SR-Can projektet ger en bild av SKB:s arbete med att utveckla de metoder för säkerhetsanalys som kan komma att användas för att ta fram en tillståndsansökan. Enligt SKB:s nuvarande planer kommer en ansökan om tillstånd för ett slutförvar för använt kärnbränsle att lämnas in under 2009/2010.

Denna rapport redovisar SSI:s oberoende modellering och granskning av den radiologiska konsekvensanalysen i SR-Can. Arbetet har genomförts inom SSI-projektet CLIMB (Catchment LInked Models of radiological effects in the Biosphere). Rapporten utgör ett av flera stödjande dokument för SSI:s och Statens kärnkraftinspektions (SKI) gemensamma granskning av SR-Can (se SSI Rapport 2008:04 / SKI Rapport 2008:19).

SSI initierade projekt CLIMB 2004 för att bygga upp en oberoende modelleringskompetens inför kommande granskningar av SKB:s tillståndsansökningar för geologiska slutförvar. Modelleringen inom CLIMB täcker alla aspekter av säkerhetsanalysen från utläckage av radioaktiva ämnen från de tekniska barriärerna till radiologiska konsekvenser i den ytnära miljön. Granskningen av SR-Can innebär en första möjlighet att använda CLIMB-modellerna som stöd för myndigheternas granskning av SKB:s konsekvensanalyser.

Syftet med att göra oberoende beräkningar är att få en djupare inblick i SKB:s beräkningar och att kunna identifiera eventuella svagheter i deras analyser. Genom att använda alternativa konceptuella modeler kan även osäkerheter i SKB:s modellantaganden utvärderas.

Granskningen av SR-Can omfattar tre huvuddelar:

- Reproduktion av utvalda beräkningsfall för radionuklidtransport och dosfaktorer
- Oberoende modellering av radionukliders omsättning och radiologiska doser i biosfären med två alternativa modeller:
    - GEMA (the Generic Ecosystem Modelling Approach) som är en traditionell boxmodell
    - En spatiellt endimensionell kontinuerlig representation av radionuklidtransport i kvartära avlagringar och ytvattendrag som baseras på att läckagevägarna bestäms från modeller över 3D grundvattenomsättning och ytvatten.
- Granskning av utvalda radionuklider i SKB:s databas för K_d-värden

CLIMB:s oberoende beräkningar har inneburit en omfattande användning av SKB:s data. De flesta data har erhållits från SR-Can-rapporter eller på begäran från SKB:s elektroniska databas. Informationen har dock inte alltid varit tillräcklig för att kunna reproducera SKB:s publicerade resultaten. Ytterligare kommunikation med SKB har i vissa fall varit nödvändig för att klargöra hur SKB använt data och modeller i sina beräkningar.

Resultaten från CLIMB:s beräkningar är i stora delar överensstämmande med resultaten i SR-Can. Dock kvarstår vissa avvikelser, vilket antyder att det finns brister i dokumentationen av SKB:s modeller och beräkningar. Som en del av granskningen har SSI reproducerat beräkningarna av SKB:s nyutvecklade LDF-värden (dosfaktorer för landskapsmodellen). LDF-konceptet används av SKB för att beräkna den radiologiska effekten av ett kontinuerligt enhetsutsläpp till hela landskapet. CLIMB har i sin granskning identifierat ett antal konceptuella problem i SKB:s tillämpning av LDF-konceptet i SR-Can. För det första bygger LDF-

beräkningarna på att det läcker från samtliga kapslar i förvaret, vilket leder till att radionukliderna fördelas mellan många landskapsobjekt i biosfären. Detta är inte konsistent med det riskdominerande advektions-/korrosionsscenariot där endast en eller enstaka kapslar antas vara otäta. För det andra är medelvärdesbildningen av dosberäkningen över landskapet inte teoretiskt korrekt, eftersom det saknas ett summeringssteg. I praktiken kan båda dessa problem leda till en underskattning av de beräknade doserna.

De två alternativa CLIMB-modellerna, GEMA och den spatiellt kontinuerliga transportmodellen, som använts för att beräkna doser i miljön leder till liknande slutsatser. Den senare modell visar att inflödet av radionuklider till biosfären kan ske i geografiskt mer begränsade områden än vad som antagits i SR-Can, speciellt i en begränsad del av ekosystemet. Beräknade doser från båda modellerna är en till två storleksordningar högre än SKB:s LDF värden för de flesta radionukliderna. CLIMB föreslår att SKB bör utreda skälen till dessa skillnader.

De sorptionsdata ($K_{d\text{-värden}}$) som använts i SR-Can härrör från de tidigare säkerhetsanalyserna SR 97 och SAFE. Med tanke på att flera internationella genomgångar av K_d-värden genomförts under de senaste 10 åren bör SKB nu uppdatera sin databas. SKB bör i samband med detta utnyttja de omfattande platsspecifika K_d-värden som insamlats under platsundersökningarna i Forsmark och Laxemar.

Shulan Xu (ansvarig för SSI:s modelleringsgrupp CLIMB)

Summary

With the publication of the SR-Can report at the end of 2006, Swedish Nuclear Fuel and Waste Management Co (SKB) have presented a complete assessment of long-term safety for a KBS-3 repository. The SR-Can project demonstrates progress in SKB's capabilities in respect of the methodology for assessment of long-term safety in support of a licence application for a final repository. According to SKB's plans, applications to construct a geological repository will be submitted in 2009, supported by post-closure safety assessments.

Project CLIMB (Catchment LInked Models of radiological effects in the Biosphere) was instituted in 2004 to provide SSI with an independent modelling capability when reviewing SKB's assessments. Modelling in CLIMB covers all aspects of performance assessment (PA) from near-field releases to radiological consequences in the surface environment. This review of SR-Can provides the first opportunity to apply the models and to compare the CLIMB approach with developments at SKB.

The aim of the independent calculations is to investigate key aspects of the PA models and so to better understand the assessment methodology used by SKB. Independent modelling allows critical review issues to be addressed by the application of alternative models and assumptions.

Three reviews are undertaken here:

- Reproduction of selected cases from SR-Can in order to demonstrate an adequate understanding of the PA model from details given in the SR-Can documentation.
- Alternative conceptualisation of radionuclide transport and accumulation in the surface system. Two modelling approaches have been used: GEMA (the Generic Ecosystem Modelling Approach) is a traditional compartmental model similar to that used by SKB in SR-Can but with additional functionality and flexibility. The second approach takes

continuous transport models to investigate contaminant migration through the Quaternary deposits into the surface drainage system.

- The final strand of the CLIMB investigation is a review of the radionuclide K_d database used in SR-Can since K_d is one of the most sensitive parameters used in assessment modelling.

Extensive use has been made of SKB's data, much of which is available either directly from the SR-Can supporting documentation or, on request, from the SKB electronic database. Nevertheless the available information was not sufficient to reproduce the published results. Additional communication with SKB was required to clarify data and interpretation so that the complete calculations could be reproduced.

The results produced by CLIMB show reasonable agreement with the SR-Can results. However, there remain some discrepancies, indicating that some features of the model system are not fully communicated in the SR-Can documentation. Part of the review included a derivation of the *Landscape Dose Factor* (LDF) – a concept newly developed for SR-Can by SKB. It is intended to reflect the radiological impact of a continuous unit release (1 Bq y^{-1}) to the whole landscape. The CLIMB review finds that there are conceptual difficulties with the approach as currently employed by SKB. Firstly, the LDF relates the radiological consequences of radionuclide release into the biosphere for a scenario which assumes equal probability for the failure of all waste canisters throughout the entire repository. This is not consistent with the overall risk assessment, in relation to other kinds of scenario. Secondly, even if the LDF represents an average dose from the whole landscape, the methodology presented in SR-Can is not theoretically correct because a summation step in deriving the average is missing. In practise, this leads to an underestimate of the dose rate.

Two alternative models, GEMA and continuous transport models, make different conceptualisations of the system but arrive at similar conclusions. A simple transport analysis based on a realistic description of lithography shows that the release of radionuclides to the biosphere can be expected to take place in geographically limited discharge areas or part of an ecosystem. Estimated dose rates derived using GEMA and the continuous transport model are one to two orders magnitude higher than the LDF values for most of the radionuclides considered. The CLIMB review suggests that SKB should investigate the reasons for these deviations.

The K_d database used in SR-Can dates from the SR 97 and Project SAFE assessments. A review is required since several K_d reviews have been published in the last decade. It is recommended that use be made of the extensive site database accumulated by SKB in the course of the site investigation programmes for Forsmark and Laxemar.

Shulan Xu (leader of the CLIMB modelling team)

Contents

1 Introduction

SKB has published the Main Report (SKB, 2006a) of the SR-Can project at the end of 2006 which is a complete assessment of long-term safety for a KBS-3 repository. The purpose of the SR-Can project is to prepare for SKB's assessment of long-term safety methodology to support a licence application for a final repository. According to SKB's plans, applications to construct a geological repository will be submitted in 2009, supported by post-closure safety assessments.

In order to prepare for the reviews of the forthcoming license applications SSI initiated a research and development project in the area of performance assessment (PA) modelling, called CLIMB (Catchment LInked Models of radiological effects in the Biosphere) in 2004. The goal is to develop an independent modelling capacity to allow an evaluation of SKB's calculations of radionuclide releases and dose/risk calculations. The models will cover the full spectrum of events from near field releases to dose consequences in the surface environment, but the main focus will be on redistribution and transport of radionuclides in the surface environment and dose consequence calculations.

Review of the SR-Can assessment provides the first opportunity to test our framework of models and software. The purpose of the independent calculations is to help us understand the assessment methodology used by SKB and identify critical reviewing issues/questions through testing alternative models and assumptions.

The independent calculations are being made in two parts: one is to reproduce SKB's calculations and the other is to perform calculations using alternative models. Reproducing calculations were made for selected cases, radionuclides and for one site (Laxemar) due to limited time. A deterministic, pin-hole failure case was considered for near field and geosphere transport. Calculation of activity concentrations in landscape models at Laxemar was performed for 14 selected nuclides. A Landscape Dose Factor (LDF) was calculated for ^{129}I only, as a random check from the list of LDF values.

Two alternative modelling approaches are used in the independent modelling of radionuclide transport in the surface environment and radiological dose consequences, namely a) a traditional compartmental model (Generic Ecosystem Modelling Approach, GEMA; Kłos, 2008) and b) a continuous transport model. In both calculations a simple surface environment system is constructed based on SR-Can data. We use the same parameter values presented in SR-Can documents as much as possible in our alternative modelling in order to make comparisons between models meaningful. The Ecolego Toolbox (Broed and Xu, 2008) is the software used to perform numerical calculations.

Since the solid-liquid distribution coefficient, K_d, is one of the most sensitive parameters when calculating activity concentration/dose consequences, a review of SKB's K_d database used in SR-Can was undertaken and is also included in this report.

2 Reproducing the SR-Can assessment

2.1 Near field and far field transport

2.1.1 Near field transport

In the SR-Can assessment, radionuclide transport in the near field is modelled by the compartment model COMP23 (Cliff and Kelly, 2006), which models processes related to radionuclide release and transport in the canister interior, the bentonite buffer and the deposition tunnel backfill. A schematic description of the near field, as modelled by COMP23, is given in Figure 10-13 in the Main Report (SKB, 2006a). However, the information provided describing the model and the input data is not always clear, and neither is it sufficiently complete to allow us to reproduce the results of the SR-Can assessment. Two examples are given below.

The transport resistance between bentonite buffer and a surrounding fracture comprises a) diffusion into a narrow surrounding fracture and b) the limited capacity of slow-flowing groundwater in the surrounding rock (Lindgren and Lindström, 1999; Romero et al., 1999; Hedin, 2001). According to Vahlund (2007), only the latter process is included in the transport resistance calculation, though this has not been explained in the SR-Can documentation. Data presented in the Data Report (SKB, 2006b) are not sufficiently complete to allow the calculations to be reproduced. For instance, no mean values of solubility limits are presented to allow a deterministic calculation to be performed.

We implemented the COMP23 model in Ecolego Toolbox (Broed and Xu, 2008). Three pathways are calculated, i.e., Q1, a fracture intersecting the deposition hole at the vertical position of the canister lid; Q2, an excavation damaged zone in the floor of the deposition tunnel and Q3, a fracture intersecting the deposition tunnel. According to Vahlund (2007) the flow resistances, Ω, for these three pathways are calculated as follows:

$$\Omega = \frac{1}{Q_e} \tag{2-1}$$

where Q_e is the equivalent flow.

The values of Q_e for these three pathways are given in Table 10-5 in the Main Report.

The resistance caused by advection between compartments is described by the following equation, which is not explicitly given in SR-Can documents.

$$\Omega^i = \frac{d_i}{v_i} \tag{2-2}$$

where v_i is the velocity and d_i is the length of the compartment in the direction of radionuclide transport.

The compartment geometry data within the discretised system is unchanged from SR 97 according to Vahlund (2007), although the size of the tunnel in SR-Can (Figure 10-13 in the Main Report) differs slightly from that of SR 97 (Figure 2 in Hedin, 2001). The geometrical data for the discretised system can be found in Maul et al. (2003). With all the above information and radionuclide specific and physical parameters provided by Hedin (2007a), the calculation of radionuclide transport in the near field can be performed.

The calculation we reproduced was performed for the deterministic pin-hole failure case given in Table 10-3 in the Main Report. Calculated fluxes from pathways Q1, Q2 and Q3 are shown in Figures 2-1 to 2-3 together with corresponding fluxes from SKB's calculation. The calculated peak fluxes are summarised in Tables 2-1 and 2-2 with peak fluxes from SKB, Quintessa and early results from SR 97 also presented for comparison. The calculated peak fluxes for pathway Q1 are within a factor 2 of the corresponding fluxes from SKB's calculation, except for ^{135}Cs. The peak fluxes of ^{135}Cs from two calculations differ by a factor 5 (see Table 2-1), although the tails of the curves are rather similar (Figure 2-1). Discrepancies of one to two orders of magnitude are found between the peak fluxes calculated for pathway Q3 (see Table 2-2). As mentioned by Maul et al., (2008), the reason for this might be SKB's process description for transport within the tunnel which may have been incorrectly interpreted in our calculations.

Table 2-1 shows a comparison of calculated peak fluxes for pathway Q1 between SR-Can and SR 97, which differ by about 2 orders of magnitude for Cs and Ni. The discrepancy in Ni fluxes might be due to the differences in input data used in SR-Can and SR 97, shown in Tables 2-3 to 2-5. We appreciate that the data base has been up-dated for SR-Can. However, the reason for this update is not well explained in SR-Can documents and the rationale for the update is especially important since major changes have been carried out. The reason for the large difference between Cs fluxes reported in SR-Can and SR 97 is not clear because the input data for these two calculations are rather similar.

2.1.2 Far field transport

In SR-Can, radionuclide transport in the far field is modelled by FARF31, a one-dimensional advection-dispersion model with matrix diffusion and sorption to describe groundwater radionuclide transport in fractured rock. The governing equations of FARF31 (Norman and Kjellbert, 1990), used for SR 97 and SR-Can, are identical apart from a slightly different conceptualisation for the migration path in these two assessments. The former uses a 'stream tube' concept to represent continuous transport within the rock, while the latter represents the actual open pore space and connected fracture network within the rock.

In our calculations, the FARF31 model is solved both analytically, in the Laplace domain with numerical inversion to the real domain by the Matlab code INVLAP.m (Hollenbeck 1998), and numerically, by a compartmental discretisation method implemented in Ecolego Toolbox (Broed and Xu, 2008). With input data provided by Hedin (2007a), the reproduced results for a near-field release from pathway Q1 are shown in Figure 2-4b. As can be seen, the results are compatible for two calculations.

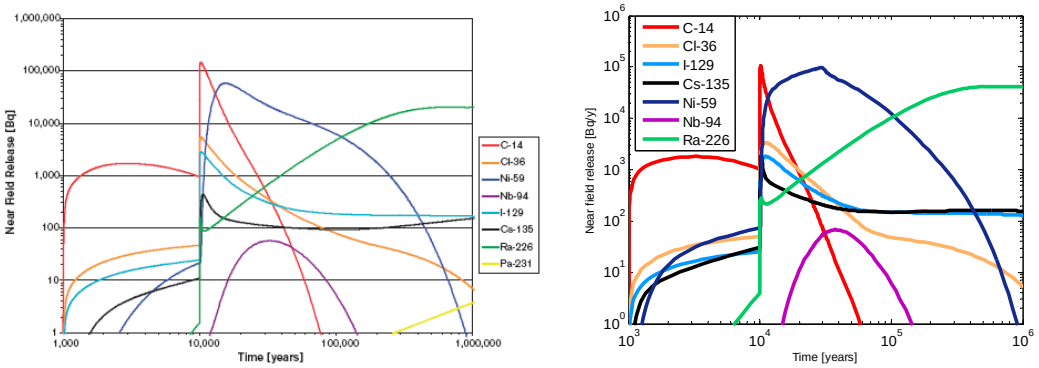

(a) (b)

Figure 2-1. Calculation of near-field releases from pathway Q1 for the deterministic pin-hole failure case, a) is SKB's calculation (SKB 2007a) and b) is our reproduced calculation from this study.

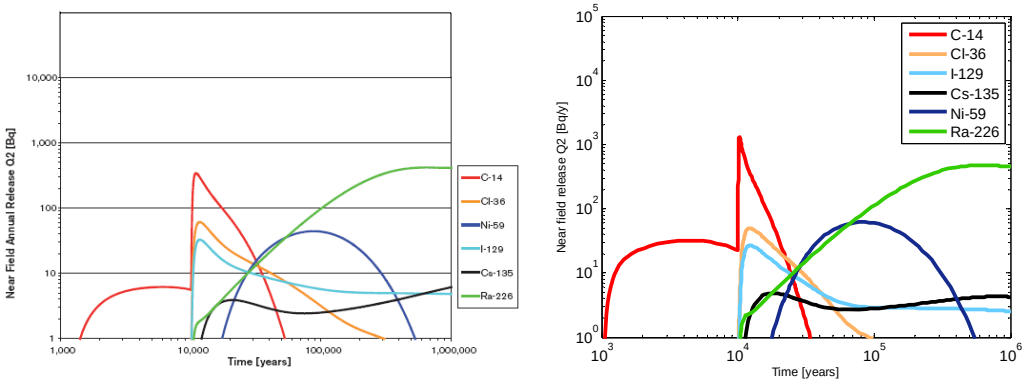

(a) (b)

Figure 2-2. Calculation of near-field releases from pathway Q2 for the deterministic pin-hole failure case, a) is from the SR-Can calculation (SKB, 2007a) and b) is our reproduced calculation from this study.

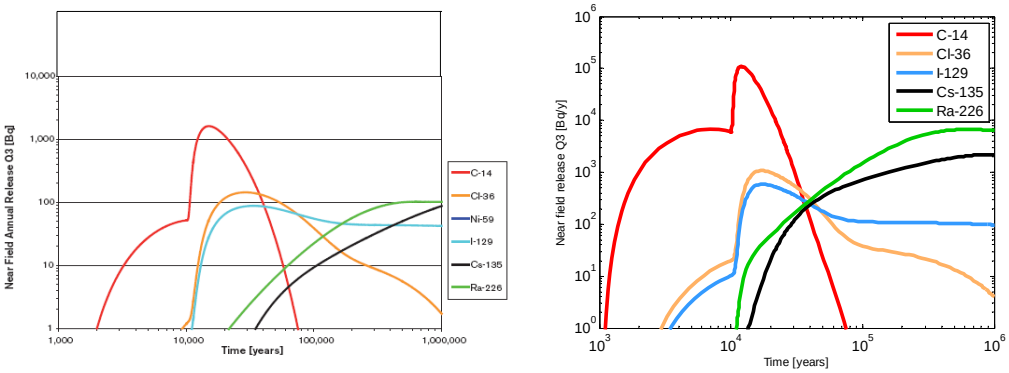

(a) (b)

Figure 2-3. Calculation of near-field releases from pathway Q3 for the deterministic pin-hole failure case, a) is from the SR-Can calculation (SKB 2007a) and b) is our reproduced calculation from this study.

Table 2-1. Peak flux (pathway Q1) [Bq/y] from near field release.

Nuclide	Time [year]	SR-Can[I]	AMBER[II]	Ecolego[III] Toolbox	SR 97[IV]
^{14}C	1×10^{4}	1×10^{5}	6×10^{4}	1×10^{5}	3×10^{5}
^{36}Cl	1×10^{4}	6×10^{3}	2×10^{3}	4×10^{3}	1×10^{3}
^{129}I	1×10^{4}	3×10^{3}	1×10^{3}	2×10^{3}	5×10^{3}
^{135}Cs	1×10^{4}	4×10^{2}	7×10^{2}	2×10^{3}	4×10^{4}
^{59}Ni	3×10^{4}	5×10^{4}	7×10^{4}	1×10^{5}	3×10^{6}
^{226}Ra	1×10^{6}	3×10^{4}	3×10^{4}	4×10^{4}	2×10^{4}

[I] Peak flux read from Figure 10-14 in the Main Report (Maul et al., 2008).

[II] Peak flux calculated using AMBER software (Maul et al., 2008).

[III] Peak flux calculated in this study.

[IV] Peak flux read from Figure 4-8 in Lindgren and Lindström, (1999) (Maul et al., 2003).

Table 2-2. Peak flux (pathway Q2 and Q3) [Bq/y] from near field release.

	Peak flux of Q2			Peak flux of Q3		
Nuclide	SKB[I]	AMBER[II]	Ecolego Toolbox	SKB[I]	AMBER[II]	Ecolego[III] Toolbox
^{14}C	1×10^{3}	4×10^{2}	1×10^{3}	2×10^{3}	4×10^{3}	1×10^{5}
^{36}Cl	6×10^{1}	5×10^{1}	5×10^{1}	2×10^{2}	5×10^{2}	1×10^{3}
^{129}I	3×10^{1}	3×10^{1}	3×10^{1}	9×10^{1}	3×10^{2}	6×10^{2}
^{135}Cs	6×10^{0}	-	5×10^{0}	9×10^{1}	1×10^{3}	2×10^{3}
^{59}Ni	3×10^{1}	3×10^{1}	6×10^{1}	-	-	-
^{226}Ra	4×10^{2}	3×10^{2}	5×10^{2}	1×10^{2}	3×10^{3}	7×10^{3}

[I] Peak flux read from Figure 10-14 in the Main Report (Maul et al., 2008).

[II] Peak flux calculated using AMBER software (Maul et al., 2008).

[III] Peak flux calculated in this study.

Table 2-3. Data used on instant release fraction (IRF) and solubilities.

Element	IRF [-] SR 97[I]	SR-Can[II]	Solubility [mol/m^3] SR 97[I]	SR-Can[II]
Ag	1	0.01	2.96×10^{-2}	1×10^{-12}
Am	0	0	6.87×10^{-4}	1×10^{-3}
C	0.15	0.05	high	high
Cl	0.06	0.05	high	high
Cm	0	0	2.22×10^{-4}	2E-4
Cs	0.03	0.01	high	high
Ho	0	0	6.27×10^{-3}	2×10^{-3}
I	0.03	0.01	high	high
Nb	1	1	1.37	4×10^{-2}
Ni	1	1	high	8×10^{-3}
Np	0	0	5.87×10^{-5}	1×10^{-6}
Pa	0	0	3.16×10^{-4}	3×10^{-4}
Pd	0.002	0.002	4.21×10^{-6}	4×10^{-3}
Pu	0	0	6.56×10^{-6}	3×10^{-4}
Ra	0	0	2.86×10^{-4}	3×10^{-4}
Se	0.03	0.0003	2.59×10^{-6}	2×10^{-7}
Sm	0	0	2.13×10^{-3}	9×10^{-5}
Sn	0.02	0.00003	4.49×10^{-6}	7×10^{-5}
Sr	0.0025	0.0025	6.88	5×10^{-1}
Tc	0.002	0.002	7.67×10^{-6}	1×10^{-10}
Th	0	0	1.22×10^{-6}	1×10^{-3}
U	0	0	1.28×10^{-4}	1×10^{-5}
Zr	0	0	2.50×10^{-6}	1×10^{-5}

[I] Lindgren and Lindström, (1999). [II] Hedin (2007a).

Table 2-4. Distribution coefficients K_d, effective diffusivities D_e and porosity used for bentonite (porosity for bentonite in SR 97 is 0.41 for all elements).

Element	Kd [m^3/kg] SR 97[I]	SR-Can[II]	D_e [m^2/y] SR 97[I]	SR-Can[II]	Porosity [-] SR-Can[II]
Ag	0	0	0.00631	0.00379	0.43
Am	3	24	0.00221	0.00379	0.43
C	0	0	0.00095	0.00032	0.17
Cl	0	0	0.00003	0.00032	0.17
Cm	3	24	0.00221	0.00379	0.43
Cs	0.05	0.03	0.01892	0.00947	0.43
Ho	1	5	0.00631	0.00379	0.43
I	0	0	0.00009	0.00032	0.17
Nb	0.2	3	0.01577	0.00379	0.43
Ni	0.1	0.07	0.03154	0.00379	0.43
Np	3	40	0.03154	0.00379	0.43
Pa	0.3	3	0.02208	0.00379	0.43
Pd	0.01	5	0.00315	0.00379	0.43
Pu	3	40	0.00946	0.00379	0.43
Ra	0.01	0.001	0.01577	0.00379	0.43
Se	0.003	0	0.00221	0.00032	0.17
Sm	1	5	0.00631	0.00379	0.43
Sn	3	40	0.00221	0.00379	0.43
Sr	0.01	0.001	0.01577	0.00379	0.43
Tc	0.1	40	0.01577	0.00379	0.43
Th	3	40	0.00221	0.00379	0.43
U	1	40	0.01577	0.00379	0.43
Zr	2	5	0.00158	0.00379	0.43

[I] Lindgren and Lindström, (1999). [II] Hedin (2007a).

Table 2-5. Solid-liquid distribution coefficients (K_d), effective diffusivities and porosities used for crushed rock-bentonite backfill (porosity is 0.3 and effective diffusivity is 0.0031536 m^2/y for all elements in SR 97).

Element	Kd [m^3/kg] SR 97[I]	Kd [m^3/kg] SR-Can[II]	D_e [m^2/y] SR-Can[II]	Porosity [-] SR-Can[II]
Ag	0.005	0	0.00221	0.36
Am	3	17.7	0.00221	0.36
C	0.0009	0	0.00221	0.36
Cl	0	0	0.00018	0.14
Cm	3	18	0.00221	0.36
Cs	0.05	0.03	0.00663	0.36
Ho	2	10	0.00221	0.36
I	0	0	0.00018	0.14
Nb	0.9	0.9	0.00221	0.36
Ni	0.03	1.47	0.00221	0.36
Np	5	18.2	0.00221	0.36
Pa	0.9	0.9	0.00221	0.36
Pd	0.01	1.5	0.00221	0.36
Pu	5	18.2	0.00221	0.36
Ra	0.02	0.0013	0.00221	0.36
Se	0.001	0	0.00018	0.14
Sm	2	10	0.00221	0.36
Sn	0.5	18.2	0.00221	0.36
Sr	0.002	0.0013	0.00221	0.36
Tc	0.9	18.2	0.00221	0.36
Th	5	18.2	0.00221	0.36
U	4	18.2	0.00221	0.36
Zr	1	1.2	0.00221	0.36

[I] Lindgren and Lindström, (1999). [II] Hedin (2007a).

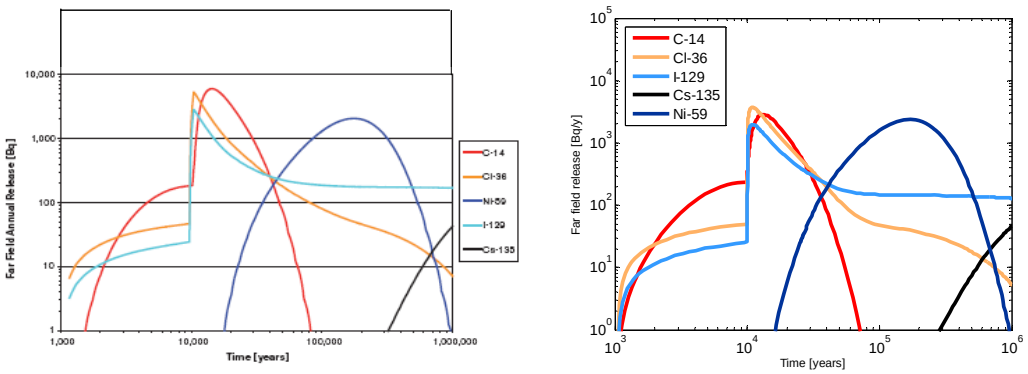

Figure 2-4. Calculation of far-field releases from pathway Q1 for the deterministic pin-hole failure case, a) is from SR-Can calculation (SKB 2007a) and b) is our reproduced calculation from this study.

Table 2-6. Peak flux (pathway Q1) [Bq/y] from far field release.

Nuclide	Time [year]	SR-Can[I]	AMBER[II]	Ecolego[III] Toolbox	SR 97[IV]
^{14}C	2×10^{4}	6×10^{3}	3×10^{3}	3×10^{3}	2×10^{4}
^{36}Cl	1×10^{4}	5×10^{3}	2×10^{3}	4×10^{3}	1×10^{3}
^{129}I	1×10^{4}	3×10^{3}	1×10^{3}	2×10^{3}	5×10^{3}
^{135}Cs	1×10^{6}	4×10^{1}	1×10^{2}	5×10^{1}	1×10^{3}
^{59}Ni	2×10^{5}	2×10^{3}	2×10^{3}	2×10^{3}	1×10^{5}

[I] Peak flux read from Figure 10-15 in the Main Report (Maul et al., 2008).

[II] Peak flux calculated using AMBER software (Maul et al., 2008).

[III] Peak flux calculated in this study.

[IV] Peak flux read from Figure 4-8 in Lindgren and Lindström, (1999), (Maul et al., 2003).

Table 2-7. Solid-liquid distribution coefficients (K_d) and effective diffusivities D_e used for the rock.

Element	Kd [m^3/kg] SR 97[I]	Kd [m^3/kg] SR-Can[II]	D_e [m^2/y] SR 97[I]	D_e [m^2/y] SR-Can[II]
Ag	0.05	0.05	2.2391×10^{-6}	1.1529×10^{-6}
Am	3.3	13	1.2614×10^{-6}	6.7815×10^{-7}
C	0.001	0.001	1.5768×10^{-6}	8.1378×10^{-8}
Cl	0	0	2.6175×10^{-6}	1.3563×10^{-7}
Cm	3	3	1.2614×10^{-6}	6.7815×10^{-7}
Cs	0.05	0.042	2.7752×10^{-6}	1.4241×10^{-6}
Ho	2	2	1.2614×10^{-6}	6.7815×10^{-7}
I	0	0	2.6175×10^{-6}	5.6287×10^{-8}
Nb	1	1	1.2614×10^{-6}	6.7815×10^{-7}
Ni	0.02	0.01	8.8301×10^{-7}	4.6114×10^{-7}
Np	5	0.018	1.2614×10^{-6}	6.7815×10^{-7}
Pa	1	1	1.2614×10^{-6}	6.7815×10^{-7}
Pd	0.01	0.01	1.2614×10^{-6}	6.7815×10^{-7}
Pu	5	5	1.2614×10^{-6}	6.7815×10^{-7}
Ra	0.02	2.1	1.1668×10^{-6}	6.0355×10^{-7}
Se	0.001	0.001	1.2614×10^{-6}	6.7815×10^{-7}
Sm	2	2	1.2614×10^{-6}	6.7815×10^{-7}
Sn	0.001	0.001	1.2614×10^{-6}	6.7815×10^{-7}
Sr	0.0002	0.00031	1.0407×10^{-6}	5.3574×10^{-7}
Tc	1	1	1.2614×10^{-6}	6.7815×10^{-7}
Th	5	1	1.9868×10^{-7}	1.0172×10^{-7}
U	5	6.3	1.2614×10^{-6}	6.7815×10^{-7}
Zr	1	1	1.2614×10^{-6}	6.7815×10^{-7}

[I] Lindgren and Lindström (1999). [II] Hedin (2007a).

Table 2-6 shows calculated peak fluxes for pathway Q1 compared with those from SKB, Quintessa and early results from SR 97. Again, the calculated peak fluxes for pathway Q1 are within a factor 2 compared with SKB's results. Peak fluxes for Cs and Ni differ by about 2 orders of magnitude between SR-Can and SR 97. Peak fluxes for Ra have not been reported in either SR 97 or SR-Can. Our calculation, using input data from SR 97 and SR-Can, shows a difference of about 3 orders of magnitude for the peak fluxes. This deviation should be due solely to differences in the input data since the models used for the two assessments are the same. Table 2-7 shows the input data for SR-Can and SR 97. The solid-liquid distribution coefficient (K_d) for Ra used in SR-Can is 100 times that used in SR 97. The K_d for ^{226}Ra is a median value adapted from sparse data, with censoring effects, from the literature (Crawford et al., 2006). Since the radiological dose is dominated by ^{226}Ra (SKB, 2006a) further investigation of appropriate site-specific K_d values for ^{226}Ra is recommended.

2.2 Landscape models and LDF

2.2.1 Our understanding of the methodology of the landscape models

SKB uses a new biosphere assessment methodology, based on a landscape model, to analyse the radiological consequences of radionuclide releases into the biosphere. The landscape model couples individual, simplified radionuclide transport models for various ecosystems. Those simplified models are mainly the models used in SR 97, with some modifications. SKB's assessment methodology uses multiple steps, culminating with the calculation of landscape dose factors (LDF) in units of Sv/y per Bq/y which express all the radiological information about individual sites and ecosystems as a single, radionuclide-specific number that can then be applied as a scaling factor to geosphere releases.

Discharge points are first identified from flow simulations, taking land rise into account and assuming that all canisters within a repository fail at the same time (ie. equal probability for each canister failure). Then, the cluster of discharge points on the map is identified and each cluster is assigned to a specific biosphere object. Biosphere objects are linked based on the current and future drainage systems. Each object can evolve from one ecosystem to another, such as a marine basin becoming a freshwater lake due to shore level movement. The LDF is decoupled from geosphere transport and is evaluated on the basis of a continuous unit release (1 Bq y^{-1}) of each radionuclide into the biosphere objects from the geosphere. The calculation period for landscape development is 18,000 years.

21 objects and 5 rivers are identified for the calculation of LDFs at the Laxemar site. Within each object, four ecosystems are possible, viz. sea, lake, mire and agricultural land. No river model is used explicitly. The activity concentrations of the radionuclides in the river water is calculated by dividing the flux of radionuclides by the water flux in the river, which is calculated by multiplying the catchment area of the river with the average runoff in the catchment.

According to the SR-Can document, the procedure for calculating LDF is as follows. The landscape model is constructed based on 21 landscape objects which can change with time from one ecosystem to another. The continuous unit release from the repository is distributed to these landscape objects. The fraction of the unit release distributed to each

object is proportional to the probability of discharge occurring to these objects, obtained from flow modelling based on a scenario with equal probability of failure for each canister. The time step for ecosystem change is 1000 years. The information on time-dependent ecosystem changes and distribution of unit release, as well as the rules for the way in which the radionuclide inventory is treated as ecosystems change, are given in Tables 2-2, 2-3 and 3-3 in Avila et al. (2006). Parameter values for various ecosystems at the Laxemar site can be found in Appendix 1, SKB (2006c). Time-varying parameter values are obtained from Kautsky (2006a). In parallel with the LDF, Avila (2006) presented the concept of the Aggregated Dose Factor (TF_{agg}) to facilitate the calculation of doses from ingestion of food produced in different landscape objects. Avila (2006) also presented a method to estimate the number of individuals sustained by landscape objects based on the whole annual demand of carbon. When the landscape model is implemented in appropriate numerical solution software with input parameters, the LDF values for various radionuclides are derived according to the five steps summarised below, from Avila et al. (2006) and SKB (2006c):

- ***Step 1.*** Simulations are performed based on the above mentioned landscape model to obtain the time dynamics of the radionuclide activity concentrations in the landscape resulting from continuous unit release rates.

- ***Step 2.*** Dose rates to individuals for specific ecosystems are estimated by multiplying the TF_{agg} of that particular ecosystem with the corresponding radionuclide activity concentrations in soils or waters obtained from the simulations in step 1. For each radionuclide and evaluation time (every 1000 years from the start of the simulation) a complementary cumulative distribution function (CCDF) is obtained by plotting the number of individuals sustained by all landscape objects against the dose rate for the corresponding objects.

- ***Step 3.*** The CCDFs obtained in step 2 are fitted to lognormal distributions using the weighted means and standard deviations of the dose rates over all landscape objects as parameters. The fitted distributions (see blue lines in Figure 2-6) for each time and radionuclide are used to calculate the effective dose rate to the most exposed individual at each reference time and for each radionuclide

- ***Step 4.*** From the fitted distributions, the dose rate to an individual representative of the most exposed group is determined. The most exposed group is defined as the group including individuals receiving a dose rate between the maximum value defined by the effective dose rate that one person exceeds (see vertical black dashed lines in Figure 2-6) and one tenth of that value (see vertical green dashed lines in Figure 2-6). The dose rate to a representative individual from this group was assumed to equal the arithmetic mean of the fitted lognormal distribution between the maximum dose rate and one tenth of the maximum (see vertical red dashed lines in Figure 2-6). The size of the group is estimated by finding the fraction of the CCDF falling between the maximum and one tenth of the maximum.

- ***Step 5.*** The maximum dose rate to a representative individual over all time periods considered is determined for each radionuclide. These values were selected as LDF values.

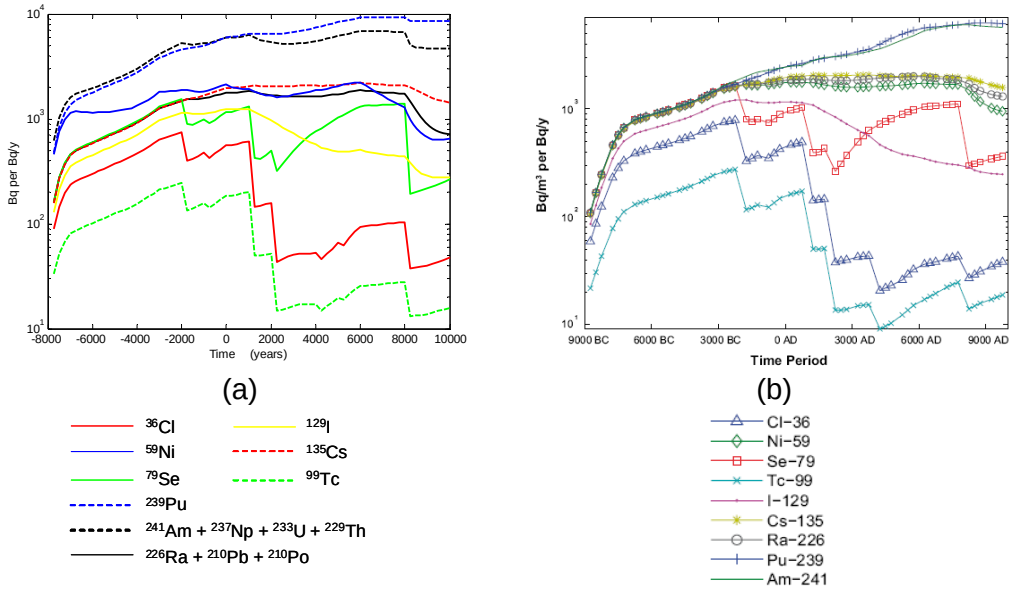

Figure 2-5. Total inventory in all objects calculated for Laxemar site for continuous release rates of 1 Bq y^{-1} to all objects of the landscape, a) reproduced inventory from this study, b) from SR-Can calculation (after Avila et. al., 2006). It is believed that there is a printing error in the original report: the units on Y-axis should be Bq per Bq y^{-1}.

2.2.2 Reproducing results

It is confusing that the parameter values for ecosystems given in Appendix A in Avila et al., (2006) and Appendix I in SKB (2006c) are different, even though the same models and results (LDF values for various radionuclides) are presented in both reports. As an example, the density of the soil at Laxemar site is 2650 kg/m^3 in Avila et al. (2006) and 700 kg/m^3 in SKB (2006c) although both are stated to be site-specific values. However, no further reference has been given to allow the original source to be traced. After contact with SKB it was established that data given in SKB (2006c) are used in the final SR-Can calculation.

In the SR-Can documentation there is a lack of information on how different objects in the landscape model are connected at different times. We obtained an additional explanation about these model connections (Kautsky 2006b), as follows: When all the objects are sea those sea objects exchange with the one located at coast (for Laxemar case it is object 2) no matter where other objects are located. When several agricultural land objects are located downstream of each other, the release from an agricultural land object is transported to the river and then to the next object if that one is not an agricultural land.

Using the above information and input data, the landscape model is implemented in Ecolego Toolbox (Broed and Xu, 2008). The calculated total inventories in all objects for various radionuclides versus time for a continuous release rate of 1 Bq/y over 18,000 years are shown in Figure 2-5. The calculated results are comparable with those shown in Figure 3-13 in Avila et al., (2006). It is assumed that the inventories of ^{241}Am and ^{226}Ra include their daughter nuclides, as indicated in the legend to Figure 2-5 a).

A sample calculation for LDF was performed only for ^{129}I. According to the five steps described previously, Figure 2-6a to 6f show example distributions of dose rates for ^{129}I over landscape objects at Laxemar at various time points beginning at 8000 BC. This is based on the assumption that SKB's radiological consequence analysis was performed only for the interglacial periods (temperate domain), therefore the calculation of LDF started from the last interglacial (8000 BC), which means the LDF is decoupled from geosphere release. The highest dose rate, at 250AD, is approximately 0.25× SKB's LDF value for ^{129}I. The precise reason for this is difficult to identify since the landscape model is so complex (consisting of 21 objects, 80 models, more that 300 compartments and over 6000 input parameter values). However, a possible explanation is as follows.

Figure 3-21 in Avila et al. (2006) indicates that the calculated activity concentration of ^{129}I in object 25 (a stream object) in the Laxemar landscape model is 8×10^{-6} Bq/m^3 at 10,000 AD based on release distributions given in Table 3-3 in Avila et al. (2006). This means that less than 1 Bq/y is released to this river because the unit release is distributed to all objects. It is not explicitly stated in Avila et al. (2006) which river is associated with object 25. Thus, we calculated activity concentrations of ^{129}I in all rivers at Laxemar based on the data given by Kautsky (2006a) assuming 1 Bq/y was released to each river. The activity concentration of ^{129}I was calculated assuming complete mixing of the released radionuclide with the total flow. The flow was calculated from the catchment area multiplied by the run-off coefficient for each river. The results are shown in Table 2-8, from which it can be seen that none of the rivers had an activity concentration higher than that of object 25. Thus, the activity concentrations in rivers seem to be overestimated by Avila et al. (2006). This might be the reason to increase the dose rates a factor of 4 because the dose rates for the river are the highest in the log-normal distributions.

2.2.3 Discussion

Unlike SR 97, SR-Can considers several ecosystems in the assessment instead of a single ecosystem at a time in the early assessments. System characteristics also change over time. Novel developments in SR-Can also include Landscape Dose Factors, Aggregated Dose Transfer Factors, the lognormal distribution method to identify the most exposed population group and modifications of sub-models used in SR 97 and SAFE. However, if these concepts/methods are to be used in SR-site the comments given in the following sections should be considered by SKB.

2.2.3.1 Landscape models and the LDF concept

The first major concern with the LDF approach is in connection with the spatial distribution of leakage points and the assumptions of probability of leakage of individual canisters. The LDF is calculated from a large number of distributed leakage points at repository level assuming a) that any canister position can give rise to leakage and b) that the LDF should include the probabilities for canister failure (equal for each canister). Hence, the LDF relates to the flux of radionuclides into the biosphere in a scenario in which all canisters leak simultaneously, or with equal probability, without considering cross-correlations with other probabilities in the overall risk analysis. For example, the buffer erosion scenario is considered to occur for only for a few canisters in the deposition holes under the condition with highest flow rates. The probability for this scenario should be

obtained by flow modelling based on a number of realizations of stochastic discrete-fracture networks. Unfortunately, the flow modelling used to estimate the probability for the discharge points in LDF was not done in this way. In this sense, the LDF concept is not consistent with the overall assessment. This probabilistic aspect is taken out of its context in a fully probabilistic scenario analysis in which each scenario (realization) is evaluated fully and averaged after the full consequences are calculated. The probabilistic aspects are now constrained by the assumption that each canister fails with equal probability and difficulties to combine this with the overall probability of failure analysis including conditional probabilities for the entire scenario.

Another major concern with the LDF approach is the way in which dose rates are averaged across the biosphere objects which, together, comprise the landscape. Even if, as SKB states, the LDF is intended to represent an average dose from the whole landscape due to a scenario of equal probability of canister failure with a continuous unit release (1 Bq y^{-1}), the mean dose $\langle D \rangle$ mathematically might be described as a sum of functions of the concentrations at all the objects:

$$\langle D \rangle \propto \sum_{i=1:n} f\left(\omega_i \frac{1}{V_i} \right) \tag{2-3}$$

where V_i is the volume of the object, ω_i is the distribution fraction of the scenario and $f(\text{-})$ is the symbol of the function.

In SKB (2006c), when the dose is calculated for each biosphere object a lognormal distribution method is used to obtain the mean dose for that time step and then many time steps are evaluated to find the highest dose. We should note that none of these biosphere objects individually receives 1 Bq/y but, summed together as the landscape, they receive 1 Bq/y. In practise this leads to an underestimate of the dose rate due to unit release (1 Bq/y) distributed over all objects. It has been mentioned in Avila et al. (2006) that peak dose rates in the cases in which the releases are directed to single objects are between 5 and 50 times higher than the peak dose rates when releases are distributed to all objects. Theoretically the average dose from the whole landscape should be the sum of the weighted doses from individual landscape objects as shown in Eq. (2-3).

In addition to the major concerns about the LDF concept described above, there are several other concerns outlined below.

The use of aggregated transfer factors, TF_{agg}, in dose calculations is useful because of their simplicity. However, certain diets are not included when deriving the TF_{agg} values which, furthermore, do not consider some potentially significant environmental media, which may lead to an under-estimation of doses. For example, fish was the only component of the diet considered when calculating the TF_{agg} for aquatic ecosystems, whereas freshwater invertebrates, with a higher bioaccumulation factor for ^{210}Po than fish (Karlsson and Bergström, 2002), were included as part of the diet in earlier assessments. If the TF_{agg} is to be used in future assessments a systematic evaluation of the method is needed. Similarly, the lognormal distribution method to find the most exposed group is innovative but does not appear to have been properly used in this case, as mentioned

earlier, because the summation step was missing. We also question the goodness of fit of lognormal distributions to the calculated CCDFs for dose as a function of population.

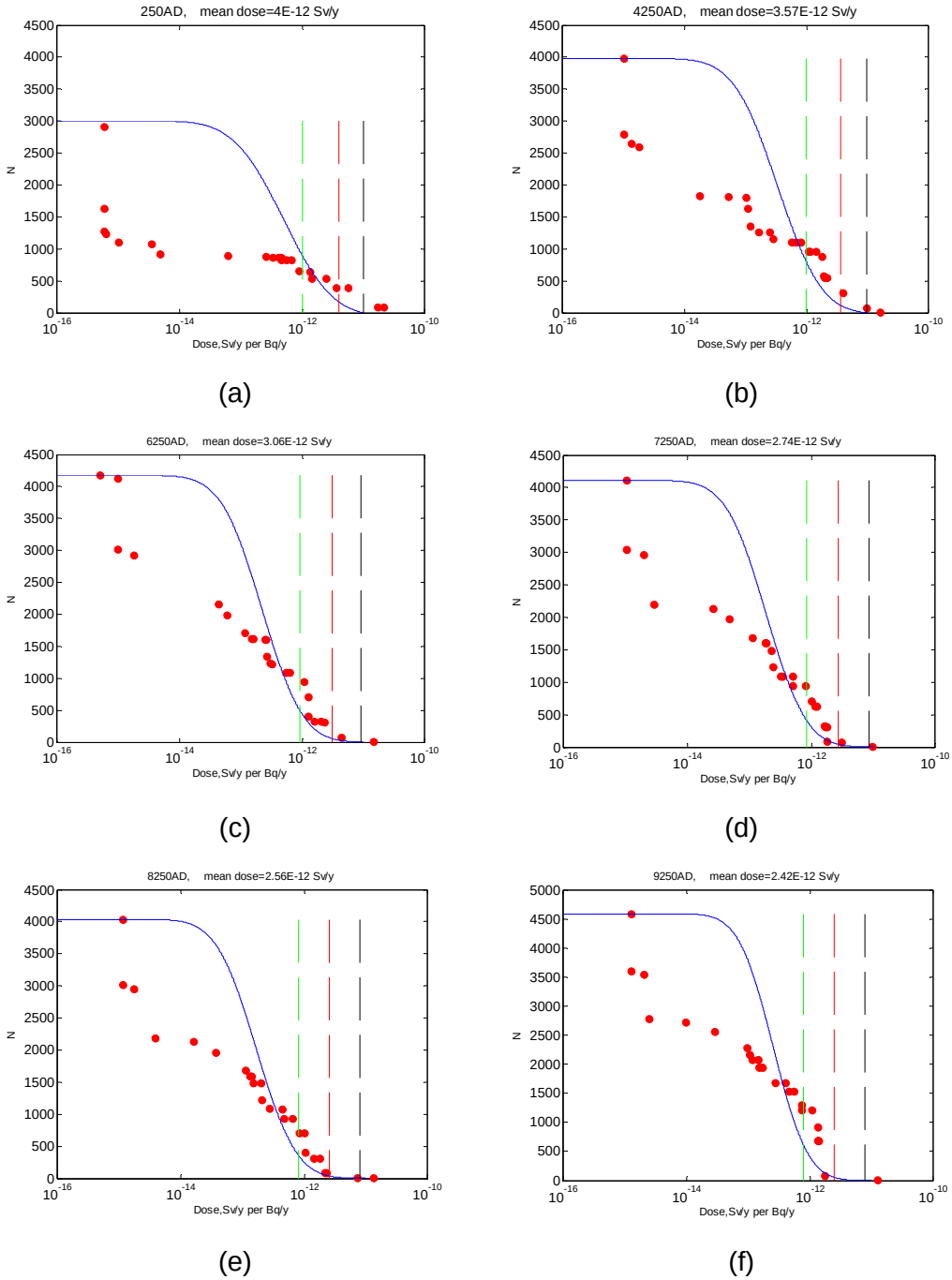

Figure 2-6. Distribution of ^{129}I dose rates for objects at Laxemar vs. corresponding complementary cumulative sustainable population (based on food yield) at different time points (denoted as red dots). The blue line is the fitted log-normal distribution. The dashed black line indicates the maximum value of the dose rate; the dashed green line indicates 1/10 of the maximum value; the dashed red line indicates the mean value.

Table 2-8. Calculated ^{129}I activity concentrations in river water assuming continuous unit release [1 Bq/y] directly into each river. River data presented here are the average values given by Kautsky (2006a).

Object[I]	River	Average area of the catchment [m^2]	Concentration [Bq/m^3]
25	Ekerumsån	2.9×10^{6}	2.2×10^{-6}
22	Gästerbäcken	2.5×10^{6}	2.6×10^{-6}
23	Laxemarån	6.0×10^{7}	1.1×10^{-7}
24	Mederhultsån	2.0×10^{6}	3.3×10^{-6}
26	Misterhultsån	2.8×10^{7}	2.3×10^{-7}

[I] this is our best interpretation of the object number corresponding to rivers in the Laxemar landscape.

LDFs are evaluated on the basis of unit releases (1 Bq y^{-1}) into the biosphere, which are decoupled from geosphere release flux. Thus, it is difficult to evaluate the dose rate for radionuclides with decay chains (^{241}Am and ^{226}Ra) although this may not affect the total dose rate in the end. For instance, the calculated dose rate for ^{226}Ra only accounts for its daughter nuclides, not the dose contributions from its ancestors.

There are no probabilistic simulations for LDF and a single value of LDF is used in the risk assessment. SKB's argument seems to be *"... several conservative assumptions have been made in dose calculations and for selection of the LDF values that are used in SR-Can"* (Avila et al., 2006). It is hard to believe that the LDF values are conservative by considering that the LDF value for ^{129}I is lower than the Ecosystem Dose Factor EDF value for the well scenario. The EDF value for ^{129}I is obtained by scaling the EDF value for ^{129}I from SR 97 with the ratio of well capacity 2000 and 7884 [m^3/y] used for SR 97 and SR-Can, respectively (see Table 2-9).

We recommend that assessment starts by evaluating dose rates in the cases in which radionuclide release is directed to a single biosphere object, connected to several other objects, to obtain a range of possible dose rates. Then, if full probabilistic weighting factors are available for each biosphere object, the average dose rates across the landscape can be averaged with greater confidence. Models used to describe radionuclide transport in individual ecosystems should be validated using site specific data as extensively as possible, and process models used, where possible, to increase the understanding of processes of radionuclide distribution in the surface environment.

2.2.3.2 Simplified radionuclide models

Four ecosystem types are identified at the Laxemar site. These are represented by what SKB terms "simplified radionuclide models" (SKB, 2007c). These models are slightly modified from the models used in previous safety assessments such as SR 97 and SAFE (Bergström et al., 1999; Karlsson et al., 2001).

Table 2-9. Comparison of Landscape Dose Factors (LDF) [Sv/y per Bq/y] with Ecosystem Dose Factors (EDF) [Sv/y per Bq/y] for a 'well' scenario calculated in SR-Can and scaled from SR 97 data (in the table LDF and EDF Well (SR-Can) are taken from Table 10-2 in SKB (2006a), EDF Well (SR 97) is taken from Table 4-1 in Bergström et al., (1999)).

Radionuclide	LDF	EDF Well (SR-Can)	EDF Well (SR 97) well capacity 2000 [m^3/y]	EDF Well (scaled from SR 97) well capacity 7884 [m^3/y]*
Cl-36	8.10×10^{-15}	3.70×10^{-14}	9.80×10^{-13}	2.49×10^{-13}
Ca-41	5.60×10^{-14}	5.50×10^{-15}		
Ni-59	4.40×10^{-15}	2.50×10^{-15}	7.90×10^{-14}	2.00×10^{-14}
Ni-63	3.80×10^{-15}	5.90×10^{-15}	8.20×10^{-14}	2.08×10^{-14}
Se-79	1.10×10^{-12}	1.20×10^{-13}	3.60×10^{-12}	9.13×10^{-13}
Sr-90	8.00×10^{-13}	1.10×10^{-12}	1.70×10^{-11}	4.31×10^{-12}
Zr-93	2.90×10^{-14}	4.30×10^{-14}	2.00×10^{-13}	5.07×10^{-14}
Nb-94	2.10×10^{-11}	4.70×10^{-13}	4.60×10^{-12}	1.17×10^{-12}
Tc-99	3.10×10^{-15}	2.60×10^{-14}	7.40×10^{-13}	1.88×10^{-13}
Pd-107	2.20×10^{-15}	1.40×10^{-15}	3.10×10^{-14}	7.86×10^{-15}
Ag-108m	1.00×10^{-10}	4.50×10^{-12}	1.80×10^{-12}	4.57×10^{-13}
Sn-126	2.00×10^{-12}	3.20×10^{-13}	5.20×10^{-12}	1.32×10^{-12}
I-129	1.60×10^{-11}	4.40×10^{-12}	1.20×10^{-10}	3.04×10^{-11}
Cs-135	2.30×10^{-12}	7.90×10^{-14}	2.60×10^{-12}	6.60×10^{-13}
Cs-137	4.10×10^{-12}	1.90×10^{-12}	7.90×10^{-12}	2.00×10^{-12}
Sm-151	2.00×10^{-16}	4.00×10^{-15}	4.10×10^{-14}	1.04×10^{-14}
Ho-166m	2.90×10^{-11}	1.40×10^{-12}	2.70×10^{-12}	6.85×10^{-13}
Pb-210	5.30×10^{-12}	2.70×10^{-11}	2.50×10^{-10}	6.34×10^{-11}
Ra-226	4.70×10^{-11}	1.10×10^{-11}	1.60×10^{-10}	4.06×10^{-11}
Th-229	3.20×10^{-12}	2.00×10^{-11}	5.10×10^{-10}	1.29×10^{-10}
Th-230	1.00×10^{-10}	8.30×10^{-12}	2.60×10^{-10}	6.60×10^{-11}
Th-232	1.20×10^{-12}	9.10×10^{-12}	2.90×10^{-10}	7.36×10^{-11}
Pa-231	7.60×10^{-12}	2.80×10^{-11}	8.50×10^{-10}	2.16×10^{-10}
U-233	3.70×10^{-13}	2.00×10^{-12}	2.80×10^{-11}	7.10×10^{-12}
U-234	2.40×10^{-12}	1.90×10^{-12}	2.80×10^{-11}	7.10×10^{-12}
U-235	3.20×10^{-13}	2.10×10^{-12}	2.60×10^{-11}	6.60×10^{-12}
U-236	3.40×10^{-13}	1.80×10^{-12}	2.60×10^{-11}	6.60×10^{-12}
U-238	3.20×10^{-13}	1.80×10^{-12}	2.50×10^{-11}	6.34×10^{-12}
Np-237	8.70×10^{-13}	4.50×10^{-12}	8.70×10^{-11}	2.21×10^{-11}
Pu-239	9.50×10^{-13}	9.90×10^{-12}	2.80×10^{-10}	7.10×10^{-11}
Pu-240	9.10×10^{-13}	9.90×10^{-12}	2.30×10^{-10}	5.83×10^{-11}
Pu-242	8.90×10^{-13}	9.40×10^{-12}	2.90×10^{-10}	7.36×10^{-11}
Am-241	6.30×10^{-13}	8.00×10^{-12}	9.10×10^{-11}	2.31×10^{-11}
Am-243	5.60×10^{-12}	5.90×10^{-12}	7.30×10^{-11}	1.85×10^{-11}
Cm-244	6.60×10^{-14}	4.70×10^{-12}	4.10×10^{-11}	1.04×10^{-11}
Cm-245	7.00×10^{-13}	8.50×10^{-12}	2.10×10^{-10}	5.33×10^{-11}
Cm-246	7.50×10^{-13}	8.10×10^{-12}	1.80×10^{-10}	4.57×10^{-11}

* The median well capacity taken from Appendix I in SKB (2006c) was used in the calculation.

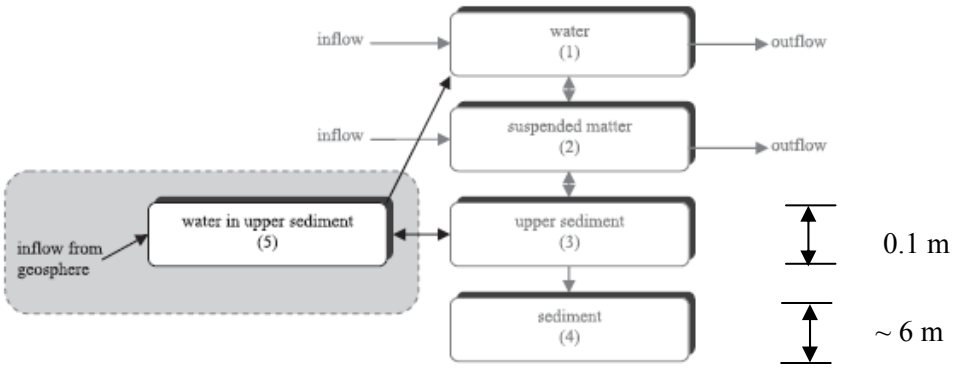

Figure 2-7. Schematic description of compartment model for ‘sea’ and ‘lake’.

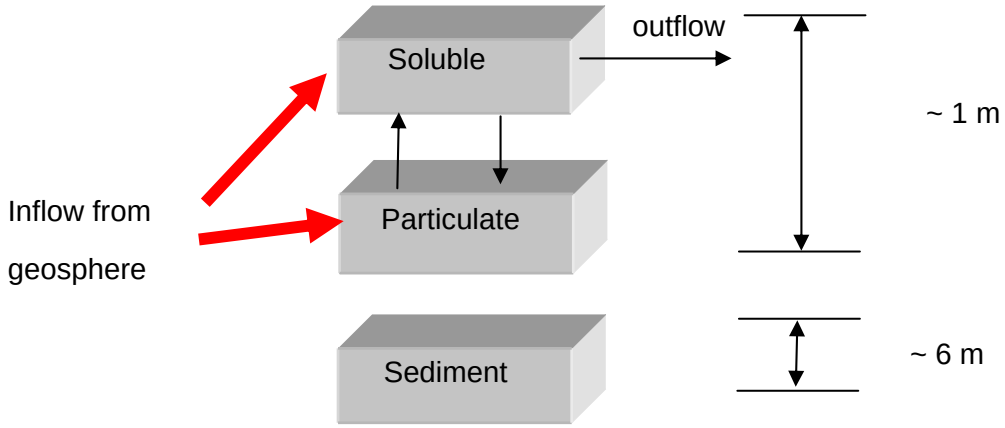

Figure 2-8. Schematic description of compartment model for ‘mire’.

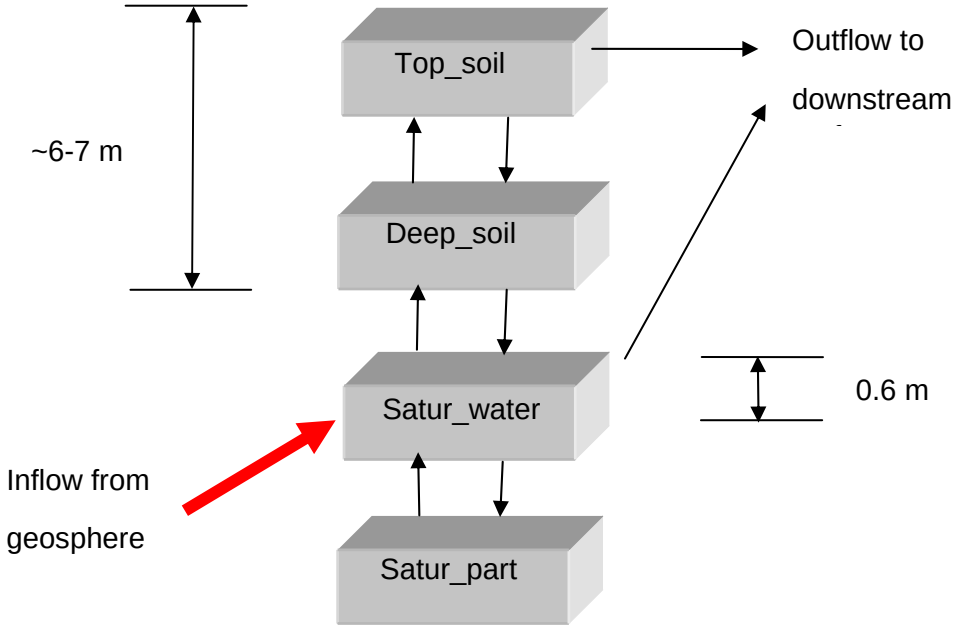

Figure 2-9. Schematic description of compartment model for agricultural land.

The models used for ‘sea’ and ‘lake’ are, structurally, the same (see Figure 2-7). These models differ from the ‘sea’ and ‘lake’ models used in SR 97 and SAFE in that an extra compartment called “water in upper sediment” has been added to account for the geosphere-biosphere interface. Radionuclides moving across this interface somehow avoid the 6 m thick “sediment” and enter the 0.1 m thick upper sediment directly. It is not clear to us why this simplification is necessary or whether it is justified. Another concern about this model is the description of the fraction of ‘accumulation bottoms’. In the model description the sediment is divided into ‘accumulation bottoms’ and ‘transport bottoms’. No particles will be accumulated in ‘transport bottoms’. Logically, two compartments are needed to represent the transport and accumulation bottoms. However, in SR-Can only one compartment is used to represent the upper-sediment, which leads to a dilution of activity concentration in the accumulating bottom sediment.

The objects of ‘mire’, ‘agricultural land’ and ‘lake’ models were all modified to include run-off through the whole catchment area around each object, rather than just the run-off on the object itself in the earlier assessment. This additional flow increases the water turnover by a factor of 100 for ‘lake’ and ‘mire’ and 10 for ‘agriculture land’. The effect of this modification compared with the earlier assessment is that the radionuclide residence time in the object can be variable, depending on retention. However, this modification has not been evaluated in the SR-Can documentation.

The process modelling study for mire shows that the mire can not be modelled by a uniform flat peat surface, “*instead, it is assumed that the large inflows from upstream catchments will keep quite large water courses open where the velocities are higher, while the actual mire develops around the main stream where the velocities are smaller*” (Vikström and Gustafsson, 2006). This means a large part of the water body in the mire is rather slow-moving or stagnant. If the radionuclides from the geosphere are transported through sediments into this slow/stagnant water body the residence time of radionuclides in the mire will differ significantly from what is calculated based on the average water flow from the whole catchment. The current mire model used in SR-Can (see Figure 2-8) has not taken this process into account and the radionuclides introduced into the mire are only considered to originate from overland sources, not from the geosphere.

For the agricultural land model it is seems unlikely that radionuclides will be transported from the saturated zone up to the upper soil layers via processes such as capillary rise and diffusion through a 6 – 10 m thick soil (see Figure 2-9). For running waters, as stated by SKB, “a compartment model was not used. Instead, instantaneous and complete mixing of the released radionuclides with the running water was assumed”. However, SKB has developed a retention model for streams (Jonsson and Elert, 2005) but this model was not used in the assessment. The reason SKB provided for this was that “the model does not contribute to any direct results, but serves to justify the use of the simplified model” (Hedin 2007b). Our independent calculations show that the sediment within running water can be a sink for radionuclides (discussed in greater detail in Section 3.2). The sediment within running water is not included in the LDF concept, therefore it is not clear how SKB can justify this argument. This is an example where transition processes are not evaluated.

3 Independent calculations using alternative models

3.1 GEMA calculations

3.1.1 GEMA overview

Within CLIMB the Generic Ecosystem Modelling Approach (GEMA) has been developed as an independent biosphere assessment modelling tool. GEMA extends the techniques discussed in BIOMOVS (1993) and BIOMOVS II (1996), and employed in Nagra's *TAME* model (Kłos *et al*., 1996) combining a review of SKB's ecosystem models up to and including SR 97 (Bergström *et al*. 1999) and Projekt SAFE (Karlsson *et al*. 2001). A detailed description of GEMA is given by Kłos (2008).

Flexibility is a key requirement of the modelling framework. Many ecosystems need to be represented in a network representing the surface drainage system, the nature of which may change in time. Review of SKB models in 2004 suggested that a module comprising eight compartments (*aquatic*: deep sediment, top sediment, lower water, upper water, *terrestrial*: Quaternary material, deep soil, top soil and litter) would be suitable for modelling the broad range of Swedish ecosystem types both in the present day and in the future. In a GEMA landscape model, each GEMA module – a flow path element (FPE) – is representative of a well defined spatial location within the overall surface drainage system. Intercompartment contaminant transfers are calculated on the basis of local water and solid material transport giving a close link to drivers of material transport.

GEMA uses a traditional foodweb of 17 exposure pathways comprising *agricultural pathways*: meat, milk (both derived from pasture land and animals' drinking water), root vegetables, green vegetables and cereals; *natural foodstuffs*: fungi, fruit, nuts and game animals (derived from animals' drinking water and natural foods); *aquatic pathways*: invertebrates, freshwater and sea fish; *drinking water*: well and surface sources; *non-foodstuff pathways*: soil ingestion, external irradiation and dust inhalation. The pathways are selected from the earlier SKB models and include some judged to be significant in the earlier assessments because of high dose consequences or because of high accumulation factors in the existing databases (Karlsson & Bergström, 2002). Additional data for fruit, nuts and fungi have been added from the literature, to complement the pathways used by SKB up to SR 97. The preliminary database for these is taken from BIOMASS (IAEA, 2003) and Kłos & Albrecht (2005). Consumption rates are taken from Karlsson *et al*. (2001) combined with Kłos & Albrecht (2005). When a pathway is active it is assumed that it is consumed at the maximum rate defined by the consumption rate. If the pathway is not active in a particular module it is assumed that uncontaminated produce is obtained from elsewhere.

3.1.2 Purpose of calculations

The CLIMB numerical review, using GEMA, investigates the impact of alternative modelling assumptions on dose calculations. Rather than repeating the full landscape model assessment of SR-Can, this review encompasses the following:

1. interpretation of landscape features in assessment models

2. review of internal structures of ecosystem models and how they influence calculated dose, including aspects of the evolution of both landscape and ecosystems
3. comparison of biosphere dose conversion factors calculated using GEMA with the LDFs calculated in SR-Can, including a discussion of the use of the newly developed aggregated transfer factor (TFagg) approach.

A subset of the overall landscape is used for this purpose: two bays in the present day Laxemar biosphere are used for this purpose (Borholmsfjärden and S Getbergsfjärden). Doses from alternative GEMA interpretations of these objects are compared with the LDFs calculated for the whole Laxemar area. The system is shown in Figure 3-1.

3.1.3 System description for the SR-Can review

3.1.3.1 Surface drainage system

Several of SKB's GIS datasets have been provided to SSI for use in CLIMB and these are the basis for the definition of the GEMA models (Lindborg, 2006):

- Topography – SDEADM.UMEU_SM_HOJ_2102
- Thickness of Quaternary deposits (QD) – SDEADM.POS_SM_GEO_2653
- Present day catchments (excluding present-day coastal catchments) – SDEADM.POS_SM_VTN_3286.

Release points identified by SKB determine the primary objects from which GEMA's surface drainage system is constructed. Combined with catchment areas, an initial interpretation of the flowpath elements in the GEMA model can be made.

An important factor in the choice of the Laxemar site is that more detailed information concerning the Quaternary deposits at Laxemar is available than at Forsmark. Lindborg (2005; 2006), and the references therein, provide the basis for the GEMA model interpretation. Only subsequent to the publication of SR-Can did details of the SKB PA model interpretation become available (SKB 2006cd).

With a land uplift rate of 1 mm y^{-1} in the Laxemar area a conceptual model of the bays and their evolution can be developed. Global Mapper (2007) was used to extract numerical data.

Table 3-1 lists the FPEs used in the GEMA calculations and illustrates the alternative interpretations of the surface drainage system evaluated in GEMA. The SR-Can system discretisation assumes that Borholmsfjärden can be treated as a single object. Two calculations have been made for this object – one a GEMA interpretation and a second in which the internal dynamics of the GEMA module have been modified to emulate the processes in the SR-Can interpretation. The GEMA conceptualisation treats Borholmsfjärden, alternatively, as either one, two or three objects. Additionally, there is a small isolated catchment to the NE of Borholmsfjärden which potentially receives radionuclide releases. This is much smaller than the other objects and is identified here as BRH_x; *Borholmsfjärden extreme*. SR-Can included this object within landscape object 13 to the north of the system considered here. However, it can justifiably be treated independently as it receives input from the geosphere and is at the head of a drainage flowpath. Appendix I gives the database for northern Borholmsfjärden (LF2:01). Kłos (2008) gives a more complete discussion of the site data.

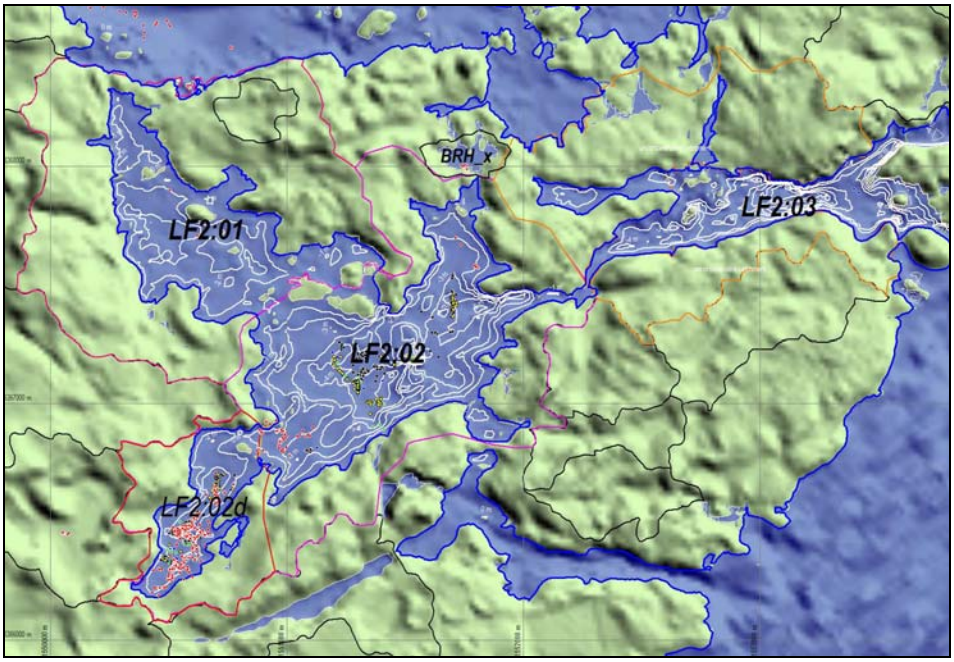

Figure 3-1. Elements of the Laxemar drainage system used in GEMA. Three flowpath elements are shown: LF2:01, LF2:02 (Borholmsfjärden) and LF2:03 (S Getbergsfjärden) together with their catchments. Contours at 1m intervals below sea level area indicated. Release points identified by SKB are shown as coloured dots. Subsidiary objects also considered are the objects LF2:02d and BRH_x.

Table 3-1. Summary of GEMA flowpath elements and numerical evaluation scenarios. Naming convention: LF is Laxemar Flowpath, this being the second Laxemar flowpath to be analysed. The three objects then comprise the first element – LF2:01 – the second LF2:02 and the third LF2:03. SKB's objects are identified as LO4 = Getbergsfjärden and LO5 = Borholmsfjärden (all sub-basins).

GEMA FPE	Object name	Total Catchment [m^2]	Source of water and solid inflows			
LF2:01	North Borholmsfjärden	1466594	No external inflow			
LF2:02	Borholmsfjärden (Central & West)	1799383	LF2:01	Laxemar 8	Laxemar 9	Laxemar 10
LF2:03	S Getbergsfjärden (SKB Object LO4)	1212399	LF2:02			
LF2:02a	Borholmsfjärden (SKB Object LO5)	3265977	Laxemar 8	Laxemar 9	Laxemar 10	
LF2:02d	West Borholmsfjärden	262062	Laxemar 8	Laxemar 9	Laxemar 10	
LF2:02c	Central Borholmsfjärden	3003915	LF2:01	LF2:02d		
BRH_x	Small catchment NE of Borholmsfjärden	36341	No external inflow			

Catchments Laxemar 8, 9 and 10 are defined by SKB (Lindborg, 2006).

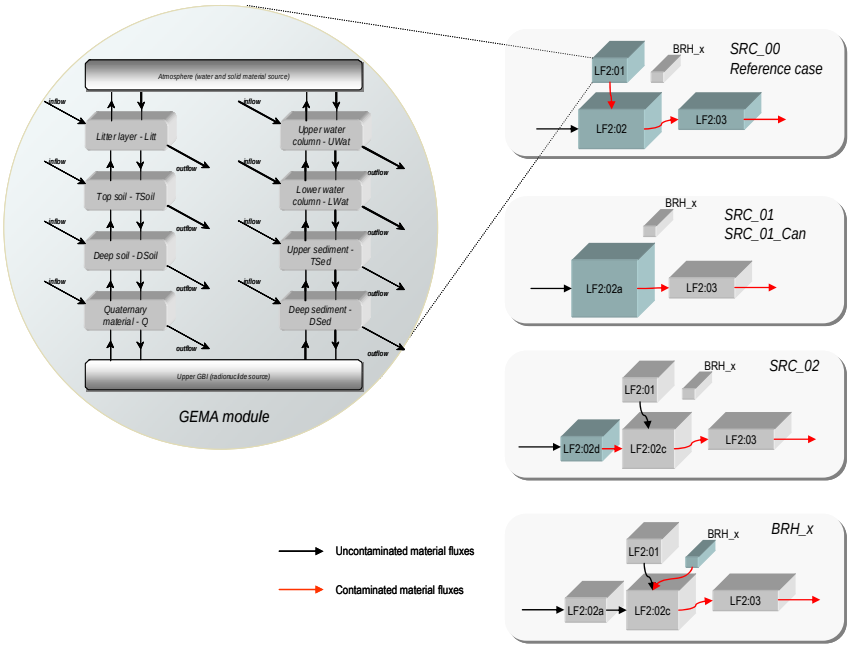

Figure 3-2. The GEMA module and the alternative interpretations of the surface drainage system modelled at Laxemar. The blue boxes denote modules for which calculations have been carried out. There are for sets of calculations: SRC_00, SRC_01, SRC_02 and BRH_x. Additionally a variant on SRC_01 was evaluated with the GEMA parameters set to model FEPs as closely as possible to the SR-Can implementation. This was the variant SRC_01_Can.

GEMA uses an interpretation of hydrological conditions within each flowpath element. Water fluxes entering the sub-catchment are balanced by those leaving. The interpretation of local topography and near-surface geology determines the fluxes through the compartments of the GEMA module. Not all parts of the system are contaminated so the *uncontaminated* catchment represents a source of water and solid material which enters the contaminated system, as part of local water and sediment balance. Flow through the system from upstream catchments (as surface drainage) is also considered – inputs from Laxemar catchments 8, 9 and 10 (see Lindborg, 2006) are noted in Table 3-1.

Stages in the evolutionary development of the modelled area are shown in Table 3-2. This identifies the ecosystem type for each of the GEMA FPEs. For each stage of the evolution the local characteristics must be identified as conditions change. Figure 3-3 shows a cross section across the Bay LF2:01 at 2000 AD and 3000 AD. Radionuclide release is to the bay bed sediment. By 3000 AD there is contaminated terrestrial material, which has originated during the earlier phase of the release. Nevertheless, this could give rise to dose due to activities on the contaminated soil. For a full description of the interpretation of local hydrology, see Kłos (2008).

Table 3-2. State of flowpath elements in the landscape as a function of time.

	Flowpath elements - GEMA objects						
date	LF2:01	LF2:02	LF2:03	LF2:02a	LF2:02d	LF2:02c	BRH_x
2000 AD	BCS	BCS	BCS	BCS	BCS	BCS	LNS
3000 AD	LNS	LNS	LNS	LNS	LNS	LNS	WNS
4000 AD	WNS	LNS	LNS	LNS	WNS	LNS	SAS
5000 AD	SAS	WNS	LNS	WNS	SAS	WNS	SAS
6000 AD	SAS	WNS	LNS	WNS	SAS	WNS	SAS
7000 AD	SAS	WAS	LNS	WAS	SAS	WAS	SAS
8000 AD	SAS	WAS	LNS	WAS	SAS	WAS	SAS
9000 AD	SAS	SAS	WNS	SAS	SAS	SAS	SAS
10000 AD	SAS	SAS	WNS	SAS	SAS	SAS	SAS

key	Aquatic	Terrestrial
BCS	Bay	Coastal / Natural soils
LNS	Lake	Natural soils
WNS	Wetland	Natural soils
WAS	Wetland	Agricultural soils
SAS	Streams	Agricultural soils

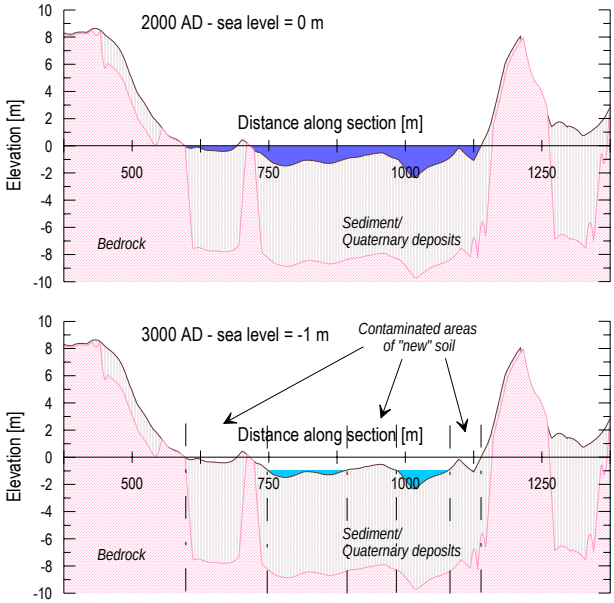

Figure 3-3. Cross section SW-NE across northern Borholmsfjärden (LF2:01) at 2000 and 3000 AD. The bedrock and thickness of Quaternary material are indicated illustrating that the present day terrestrial area would remain as uncontaminated catchment. The topography of the bay shoreline for other objects is similar. Emergent soils are indicated.

3.1.3.2 Radionuclides and releases

For the numerical evaluations presented here a set of nine radionuclides was modelled. Six are fission products (^{36}Cl, ^{59}Ni, ^{79}Se, ^{99}Tc, ^{129}I and ^{135}Cs). Additionally, ^{226}Ra was released and ingrowth of its progeny, ^{210}Pb and ^{210}Po, taken into account. Release rates were 1 Bq y^{-1} for all radionuclides except ^{210}Pb and ^{210}Po which were present in the system only as decay products. Radionuclide data are listed in Appendix I.

The location of the release points suggests the geosphere-biosphere interface is located at the lower parts of the system. As modelled here, radionuclide release is to aquatic deep bed sediment during 'bay', 'lake' and 'wetland' phases (see Figure 3-2). During agricultural conditions (assumed to be under human control) the aquatic system is limited to a small hyporheic zone (ie. beneath the stream bed). Release is then assumed to be to the Quaternary material.

The LDF concept used in SR-Can assumes that a fraction of the overall radionuclide flux to the landscape is released into each landscape object. It has been argued above (section 2.2.3) that evaluation of the LDF would be better if unit release to each landscape object were considered in turn. The volume of the object is then a key determinant of overall radiological impact.

3.1.4 GEMA results

3.1.4.1 Reference case – release to northern Borholmsfjärden

GEMA results are illustrated in Figure 3-4 for the three flow path elements in calculation case SRC_00 (defined in Figure 3-2). The plots show the dynamics of biosphere dose conversion factors (BDCF[1]) from 2 000 AD to 10 000 AD for are release starting at 2000 AD. Evolution of the FPEs is modelled as a step change each 1 000 years, as detailed in Figure 3-2. Prominent spikes in BDCF appear to coincide with these changes in FPE characteristics whereas, when FPE characteristics are held constant (ie. between step changes) the system responds smoothly.

The significance of the transient responses of BDCF to step changes in FPE characteristics can be questioned. In reality, change between states would be gradual as the bays evolve into first lakes and then wetlands. The exception is the transition to agricultural land in which human action is implicitly involved. An abrupt transition for this aspect of landscape evolution cannot be ruled out. Whereas the spikes in most cases must be interpreted with caution, the transient effects associated with conversion of wetlands to agriculture could conceivably give rise to high doses. In all cases studied, the highest indicated doses originate from the step-transition to agricultural land. However, neither the current GEMA models nor the SR-Can models are sufficiently detailed to deal with these processes satisfactorily. The reason is that sediments beneath the wetland, formed during the bay, lake and wetland periods, are converted to soil and the accumulated radionuclide inventory can then give rise to dose via a broad range of exposure pathways.

[1] The BCDF of a radionuclide is defined here as the annual individual dose arising from a cumulative release of 1 Bq y^{-1} of the radionuclide to the biosphere model.

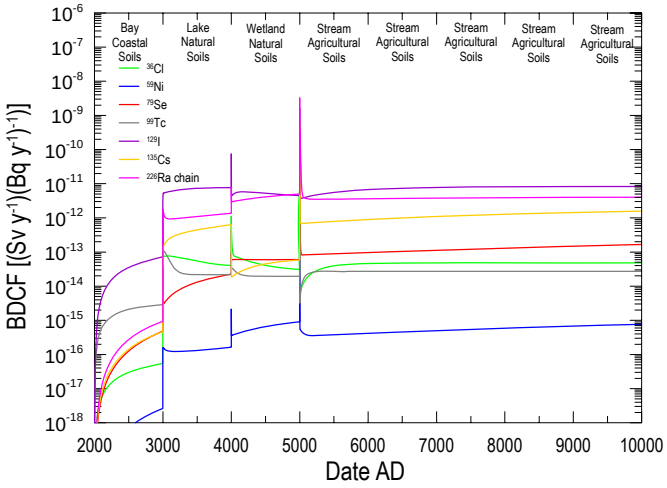

(a) LF2:01 – Northern Borholmsfjärden

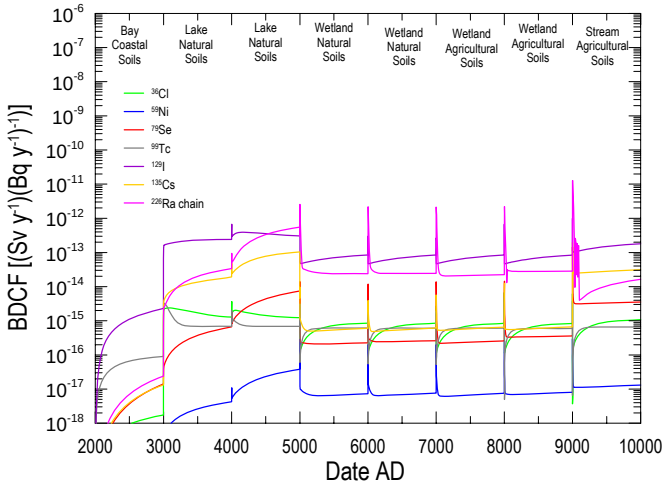

(b) LF2:02 – Borholmsfjärden (Central & West)

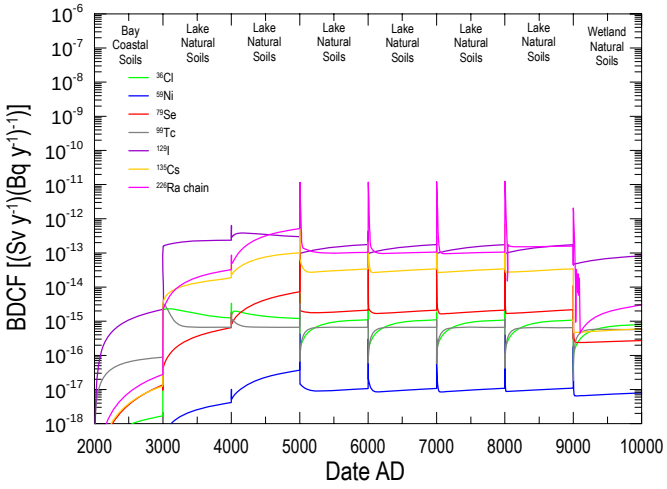

(c) S Getbergsfjärden

Figure 3-4. Reference results – SRC_00: Biosphere Dose Conversion Factors calculated for GEMA flowpath elements LF2:01, LF2:02 and LF2:03, arising from a release of 1 Bq y^{-1} to LF2:01.

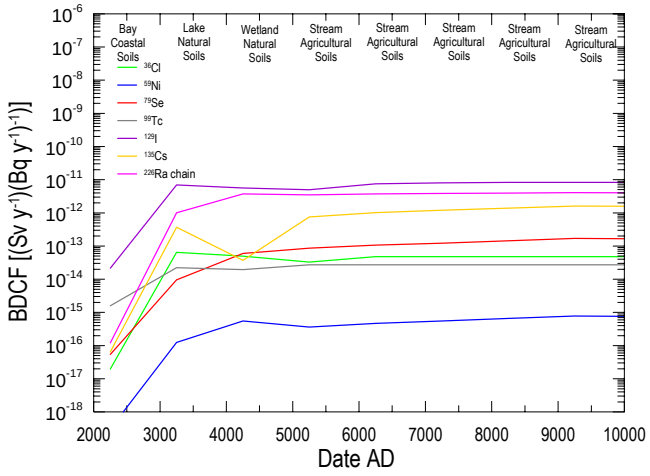

Figure 3-5. 'Smoothed' results for LF2:01 (northern Borholmsfjärden – SRC_00). The plot corresponds to Figure 3-4(a) but doses are plotted at each 1 ka starting at 1250 AD. The results are representative of the typical radiological hazard arising for the release.

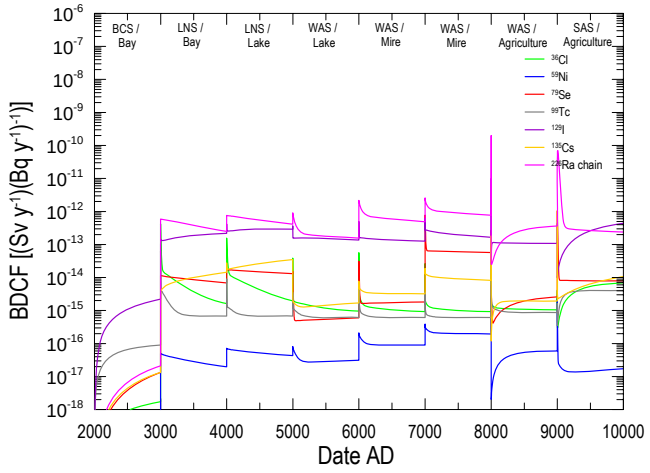

(a) Standard GEMA interpretation – LF2:02a – SRC_01

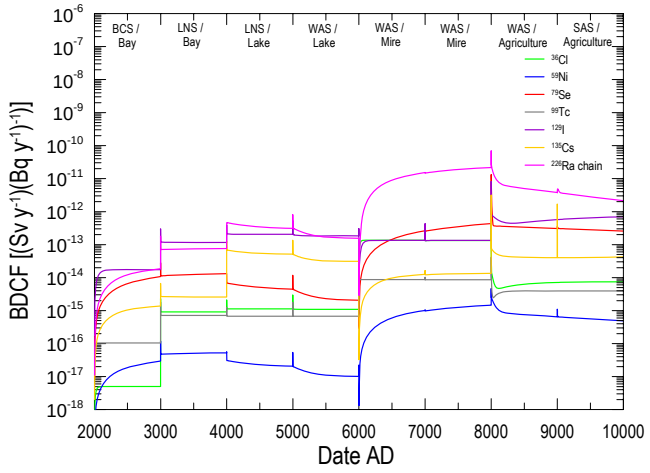

(b) GEMA interpretation of the SR-Can ecosystem models – LF2:02a – SRC_01_Can

Figure 3-6.Results for radionuclide release to the whole of Borholmsfjärden using the standard GEMA modelling approach and an emulation, using GEMA, of the SR-Can ecosystem models.

A ‘smoothed’ plot from GEMA is shown in Figure 3-5 in which BDCFs are plotted at 250 y after each transition. This view of the system response is more indicative of the long term radiological risk. Results from GEMA are discussed as a range between the maxima of the transition-peaks and the maxima of the smoothed results.

Long term behaviour of the BDCFs calculated by GEMA indicates that, as might be expected, doses arising in the ecosystems receiving direct influx of radionuclides are higher than those downstream. Typically, dose per unit release in the receiving ecosystem is around 10^{-11} Sv Bq^{-1} for ^{129}I and 10^{-15} Sv Bq^{-1} for ^{59}Ni. BDCFs for the other radionuclides lie between these results. If the spikes following the wetland/agricultural transition are taken into account, the highest dose factor might be up to ~ 3×10^{-9} Sv y^{-1}. Downstream from the first ecosystem (which receives radionuclide input from the geosphere) the doses are lower, spanning 10^{-17} to 2×10^{-13} Sv Bq^{-1}. Doses in central and western Borholmsfjärden (LF2:02) being slightly higher than in S Getbergsfjärden (LF2:03).

In part, the limited importance of objects downstream from the object which receives the release is a consequence of the limiting assumptions for sediment transport in the GEMA models. The potential consequences of contaminated sediments accumulating at the inflow to a lake might be significant. Such a build-up of sediment is seen in the modelled system, for example where Laxemar catchments 8, 9 and 10 discharge into the western end of Borholmsfjärden (into GEMA object LF2:02d).

3.1.4.2 Release to Borholmsfjärden as a single object

The SR-Can discretisation of the Laxemar system differs from GEMA in that the whole of Borholmsfjärden is treated as a single object. Two GEMA versions of the SR-Can discretisation have been modelled. The first takes a modified form of the flowpath, combining northern, west and central Borholmsfjärden as the flowpath element LF2:02a. A second variant uses GEMA’s flexibility to emulate the SR-Can ecosystem models.

The SR-Can models are structurally simpler than the GEMA module (see Appendix I). The main differences being that the objects in SR-Can have the following properties:

- Objects are either aquatic (marine/lakes) or terrestrial (agricultural land, forests). There is no transport between the two types. Mires provide a bridge between the two types, comprising water and soils compartments.
- In aquatic compartments release is to top sediment rather than to deep sediment in the reference GEMA interpretation.
- There are no sediments in wetlands, releases are therefore to the ‘top soil’ compartment. Sediment concentrations accumulated during bay and lake phases are stored until agricultural land is formed at which point the inventory is partitioned into the agricultural soils.

The intention is **not** to reproduce SR-Can results, but to determine the effect of conceptual differences in the models on calculated BDCFs compared with the standard GEMA conceptualisation. In both cases a 1 000 years evolutionary timestep is assumed. Results are shown in Figure 3-6.

Compared with the release to northern Borholmsfjärden (Figure 3-4), radionuclide release to the whole of Borholmsfjärden results in lower BDCFs, typically by at least an order of

magnitude. Higher activity concentrations are to be expected in the LF2:01 release scenario since the release area of LF2:01 is lower than that of the whole Borholmsfjärden by a factor of approximately 2.5.

The alternative conceptualisations produce some noteworthy results. Release to top sediment, rather than deep sediment, leads to higher doses in the bay phase up to 3 000 AD. Thereafter, the fact that GEMA considers soils from which radionuclide exposure may result at the earlier stages means that the doses from lakeside soils give rise to higher dose consequences. Doses in GEMA are slightly higher up to the onset of the wetland phase. During the wetland phase, doses in the SR-Can interpretation are around a factor of 10 higher than those obtained using the standard GEMA model. This is a consequence of radionuclide release being directly to the top soil compartment, and strongly sorbing radionuclides (the ^{226}Ra chain, ^{135}Cs and ^{59}Ni) illustrate this effect most strongly. Results for this type of release are certainly conservative.

System change in the SR-Can emulation is simpler than in the reference results for SRC_00 in Figure 3-4. Transitions are restricted to volume changes with the exception of the transition from wetland to agricultural soils, where there is a spike similar to those seen in the output from the standard GEMA model.

3.1.4.3 Dose as a function of object size

Using the maximum BDCFs from the smoothed results and the peak BDCFs from the agricultural land 'transient' to represent a range of doses from the FPEs, Figure 3-7 shows the influence of object area on the range of potential BDCFs. Results are shown for the different interpretations of the Laxemar objects together with results for a model of the Puttan object, a small sub-catchment northeast of lake Bolundsfjärden in the Forsmark landscape.

Evidently, the size of the modelled object is important, as is the size of the local uncontaminated catchment which contributes runoff to local soils. The largest object considered is the whole of Borholmsfjärden (LF2:02a) whereas the other objects are considerably smaller than this. For example, Puttan has an area 16 times less than Borholmsfjärden while, for the BRH_x object, the ratio is 80:1.

In SR-Can, Laxemar object 5 (Borholmsfjärden) has an area defined by the initial size of the bay. When doses from the agricultural land are calculated, the area of the object is further constrained to be 3.04×10^5 m^2. Nevertheless, this area of agricultural land can support a population of 597 individuals (Avila et al., 2006). On this basis the Puttan object could support more than 160 adults and the smaller BRH_x object more than 30 adults. It is therefore not possible to rule out such small objects, for which radiological consequences are significantly higher than for the larger objects.

This conclusion may reflect the relative differences in the application of the LDF technique. The Puttan catchment is evaluated independently in the Forsmark landscape model (as object 23) whereas the BRH_x area at Laxemar is assigned to a much larger bay. The difference may be that Puttan is identified as a distinct subcatchment in its own right whereas BRH_x is part of a coastal catchment.

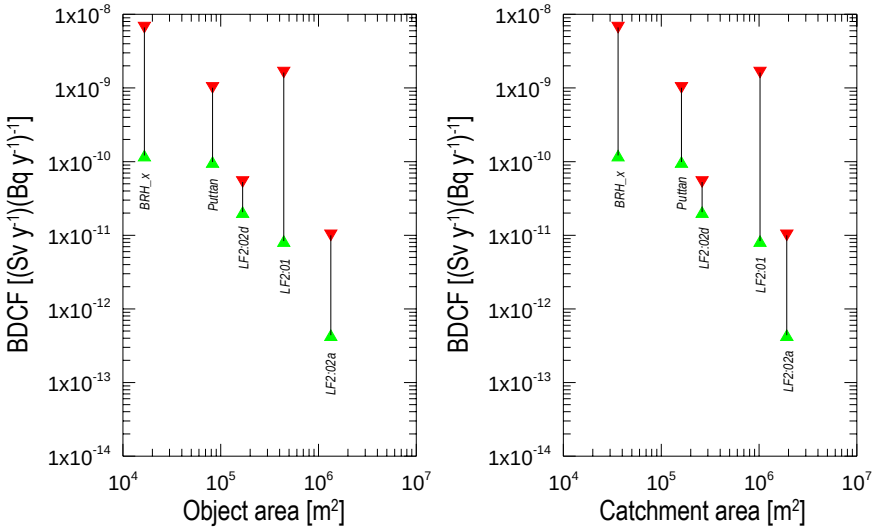

(a) ^{129}I

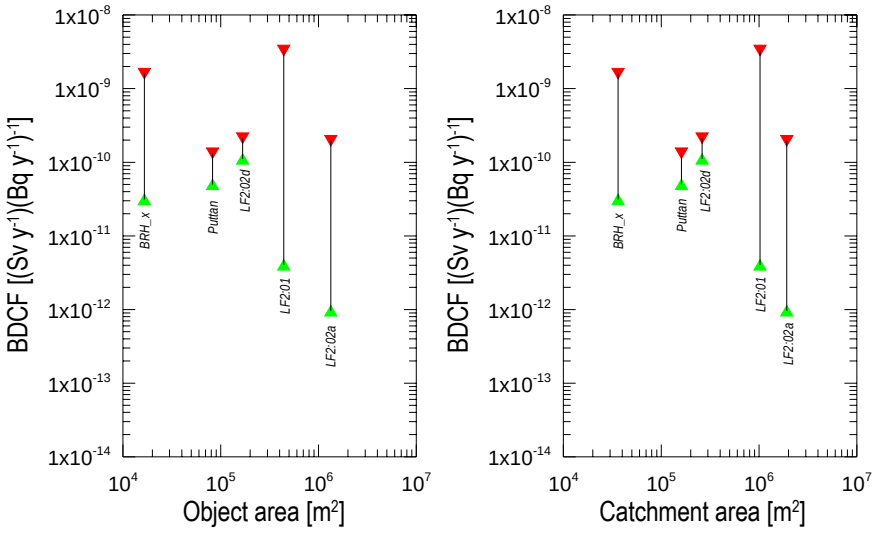

(b) ^{226}Ra chain

Figure 3-7. The range of BDCFs for a number of objects is presented for ^{129}I and the ^{226}Ra chain. Five GEMA objects are shown – four from Laxemar and one (Puttan) from Forsmark. Plots are shown for the dose vs. contaminated object area and vs. the uncontaminated local catchment. The upper data (red symbols) are the peak BDCFs on transition to agricultural land, the lower (green symbols) the maximum BDCFs from the smoothed BDCF plot.

A review of the subcatchments around Bolundsfjärden shows there are several small catchments of similar size to Puttan. A large number of small catchments may be the norm for the relatively low relief at Forsmark. It may be that the objects selected for study in the Forsmark and Laxemar sites are too large to give representative radiological consequences, notwithstanding the conservatism implicit in the LDF technique.

As noted, coastal catchments are not included in the available SKB datasets and the methodology for determining future catchments is currently poorly documented. Details of the procedure should be published and the details added to the SKB database.

Object size and the resulting dilution of radionuclide activity concentrations is not the whole story, however. Local hydrology and topography each play a part suggesting that detailed characteristics of individual objects are important. Even though, for ^{129}I, the highest calculated BDCF is for the smallest object (BRH_x), the LF2:01 (northern Borholmsfjärden) object has a peak BDCF of around 2×10^{-9} Sv Bq^{-1}, only four times smaller than the peak BDCF from BRH_x. In the case of the ^{226}Ra chain, LF2:01 also has a high peak BDCF, in this case higher than the peak BDCF of BRH_x.

3.1.4.4 SR-Can LDF and GEMA biosphere conversion factors

The alternative conceptualisation described above leads to a range of calculated biosphere dose conversion factors (BDCFs) for the objects studied. These can be compared to the Landscape Dose Factors (LDFs) calculated in SR-Can. Caution is needed because the LDF is derived from the BDCF using detailed reasoning (see Section 2.2.2). Over the range of objects considered, the LDF for each nuclide is taken to be the highest such factor calculated for the landscape as a whole. It might therefore be expected that the published LDFs would be at the high end of the ranges calculated from the limited subset of objects modelled using GEMA. A comparison of the Laxemar LDFs and the GEMA BDCFs (shown in Figure 3-8) suggests that this is not always the case.

In most cases the smoothed results for northern Borholmsfjärden are similar to, or lower than, the landscape dose factors, whereas the results for the whole of Borholmsfjärden are typically lower. On this basis the LDFs can be said to be a reasonable expression of the radiological sensitivity of the landscape. However, the smaller BRH_x object gives doses that can be an order of magnitude higher than the LDFs suggesting that the smaller objects are of greater importance than has been accounted for in SR-Can. These results are radionuclide-dependent: the dose from ^{226}Ra in BRH_x is similar to the LDF whereas for ^{129}I the BDCF obtained using GEMA is higher.

The TFagg approach, pioneered in SR-Can (Avila, 2006), is expected to be quite conservative and this is confirmed for ^{129}I and the ^{226}Ra chain. Environmental activity concentrations taken from GEMA's smoothed results are used with the TFaggs to calculate the BDCFs plotted as diamonds in Figure 3-8. On this basis the LDFs are exceeded by around two orders of magnitude for ^{129}I and more than one order of magnitude for the ^{226}Ra chain in the case of BRH_x.

Peak transient results obtained using GEMA are considerably higher than LDFs. The origin of these results is the treatment of the transition between states. Step change from one ecosystem type to another (Table 3-2) requires that the inventories accumulated in one ecosystem at earlier times are distributed in the new ecosystem. According to the model

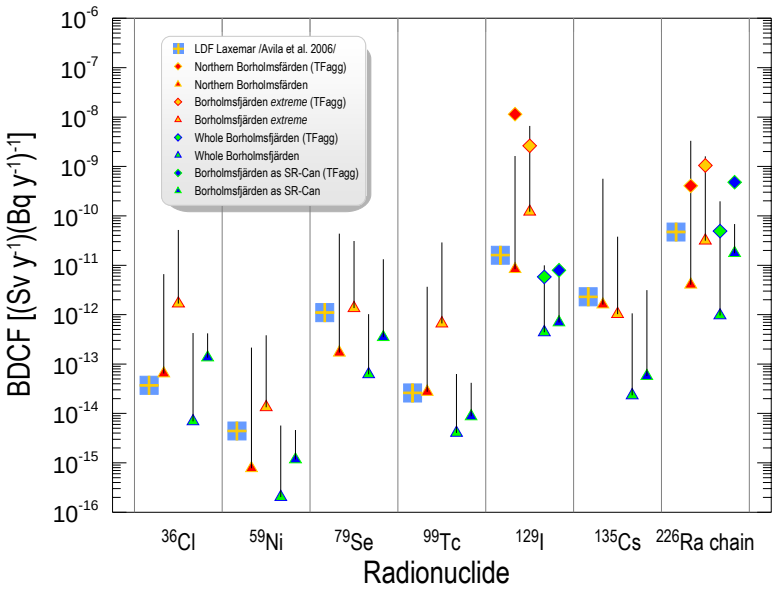

Figure 3-8. Comparison of biosphere dose conversion factors (BDCFs) from alternative interpretations of Borholmsfjärden with LDFs for Laxemar (Avila et al., 2006). Plotted BDCFs are the peaks of the smoothed results and error bars indicate the range suggested by the transient response described in section 3.1.4.1. BDCFs for ^{129}I and the ^{226}Ra chain are also calculated using the SR-Can TFaggs combined with activity concentrations calculated using GEMA.

used here (the transition matrix described in Appendix I). the water body inventory in the earlier state is transferred to the water body of the new system. This is acknowledged to be an unsatisfactory arrangement since there would be gradual change in the system characteristics in the evolution from bay to lake to wetland.

It may be argued that the simple translation of water body inventory from wetland to stream is still physically unrealistic and than, in any case, the effect is transitory. However, as noted in Section 2.2.3.2 in the comments by Vikström and Gustafsson (2006), the

water body of the wetland might remain relatively isolated from the object's hydrology. The imposition of agricultural drainage might well lead to the flushing of the wetland water content through the stream system in a short period of time. In short, the processes acting during such a transition are not well represented in either the GEMA models or the SR-Can models. The vertical bars shown in Figure 3-8 give an indication of the range of potential radiological impact, but further review of the processes involved in the evolution of one ecosystem into another is recommended.

3.1.5 Discussion

3.1.5.1 Dilution: identification and justification of landscape objects

The role of the biosphere model in PA is to represent situations and locations where radionuclides returning to the surface environment might accumulate. Dilution of radionuclides will inevitably occur within the biosphere, but it is acknowledged that the biosphere cannot be assumed to serve a safety function by diluting contaminant inflows. Furthermore, the biosphere cannot be designed or controlled. Assessment of repository safety should adequately address those features of the biosphere which act to concentrate potential releases. The identification and justification phases of biosphere model development should ensure an adequate representation of these key elements.

Development of SR-Can's landscape modelling approach has taken precedence over a detailed review of the FEPs represented in each ecosystem module and the FEP analysis of the biosphere system has not been made available. Instead, ecosystem models developed for SKB's earlier PA models have been implemented with minor modifications to allow them to function as part of a distributed landscape model. This approach is not unreasonable as a good deal of effort has been put into the models since the mid 1980s. However, the lack of a detailed identification and justification phase, for example compared with the BIOMASS Reference Biospheres Methodology (IAEA 2003), is evident in the selection of landscape objects.

Figure 3-7 shows that smaller objects – with a smaller capacity to dilute radionuclides – are radiologically more sensitive. This is also, unsurprisingly, the finding of SR-Can in that the higher LDFs are associated with smaller objects. The supportable human population is a key factor in the calculation of LDFs and this suggests a lower limit for an agricultural object size. For example, a small farmstead covering slightly more than 5 000 m^2 could support ten adults and might be a reasonable estimate of the smallest area. Depending on local hydrology, significantly less dilution than is assumed as standard in SR-Can might be possible.

The basis for SR-Can's selection of objects appears to be the use of the catchment identification mechanism in the ARC-tools landscape analysis package (Brydsten, 2006). This may not be sufficient without further refinement of the technique, especially with regard to future catchments. This is seen in the discrepancies between the modelling of the Forsmark and Laxemar sites. The example of the *Puttan* catchment, north east of Lake Bolundsfjärden at Forsmark, is relevant. This small, isolated sub-catchment of the Bolundsfjärden area is identified as a discrete object, whereas the object identified here as BRH_x is treated as part of a much larger lake. Two questions are therefore prompted. i) Does the SR-Can methodology identify all such potentially relevant small objects? ii) Are all such small objects correctly represented?

3.1.5.2 Dispersion: retention and the geosphere-biosphere interface

GEMA originated from a review of the structures of the SKB ecosystem models existing at the start of the 2000s. The main functional difference between the GEMA and SR-Can models is that both aquatic and terrestrial subsystems are available in each GEMA module. Practically, this means doses from terrestrial exposure pathways are calculated at earlier stages of GEMA's evolution scenarios as soils emerge from the parent water body.

This accounts for the higher doses estimated by GEMA at earlier times. In contrast, the SR-Can models remain as pure aquatic systems at these times.

The geosphere-biosphere interface in SR-Can assumes that groundwater discharges directly to the water content within the top sediment, which is essentially the top sediment compartment in the GEMA implementation. Radionuclides are retained in the top sediment but the reservoir is small and most are transported to the water column where turnover is fairly rapid. There is sedimentation to deeper sediments, but accumulation in the deep sediment within the SR Can models is much less than in the case of the GEMA models where radionuclide release is directly to the deep sediment. An important difference between the two conceptualisations, therefore, is retention in the local system.

Analysis of the losses from the whole Borholmsfjärden object in Figure 3-9 shows that the location of the release can make a large difference to the modelled results. The plot shows the inventory *lost* to the receiving ecosystem as a function of time. The strongly sorbing ^{226}Ra is lost most slowly under GEMA's assumption of release to the bay/lake/wetland deep sediment. There is a relatively large volume available for ^{226}Ra sorption and accumulation as this deep sediment is over 7 m in thickness. When release is to the top sediment (0.1 – 0.2 m thick) the activity is more rapidly transported to the water column and transported out of the system since there is less interaction with the deep sediment. The weakly sorbing ^{129}I is more rapidly dispersed. In both cases, the retained activity is transferred to soils as a result of land uplift and soil formation.

These results focus attention on the assumptions for the geosphere-biosphere interface. In GEMA, because activity is transferred to land from radionuclide accumulations in aquatic sediment, there is immediate interaction with deep sediment material and the assumptions about local hydrology allow flow through the bed sediment into the water column. The assumptions inherent in compartment models mean there is instantaneous mixing throughout the entire volume of the bed sediment.

Given that groundwater discharge from fractures in the underlying crystalline bedrock enters the biosphere it is difficult to envisage no interaction whatsoever of radionuclides in groundwater solution with the porewater of deeper bed sediments. The advective storage path model, described in Section 3 below, illustrates the potential for a diffusive flux of radionuclides through the bed sediment.

For the geosphere-biosphere interface there are three alternative interpretations:

- No interaction between contaminated groundwater and deep bed sediment (SR-Can).
- Full mixing of contaminated groundwater in the volume of the bed sediments (GEMA).
- Diffusive flux of contaminated groundwater from the bedrock, through the bed sediment and into the top sediment.

Of these, the latter is probably the most realistic, with the SR-Can and GEMA models being at opposite ends of the conceptual spectrum.

Clearly, a better understanding and representation of processes at the geosphere-biosphere interface is essential. This also relates to the size of the compartments assumed. The estimated discharge area contaminated by radionuclides from a leaking canister is about 25,000 m^2 (see Section 3.2.1). A more realistic area of the geosphere-biosphere interface might therefore be almost 20 times smaller than the value assumed in the GEMA models

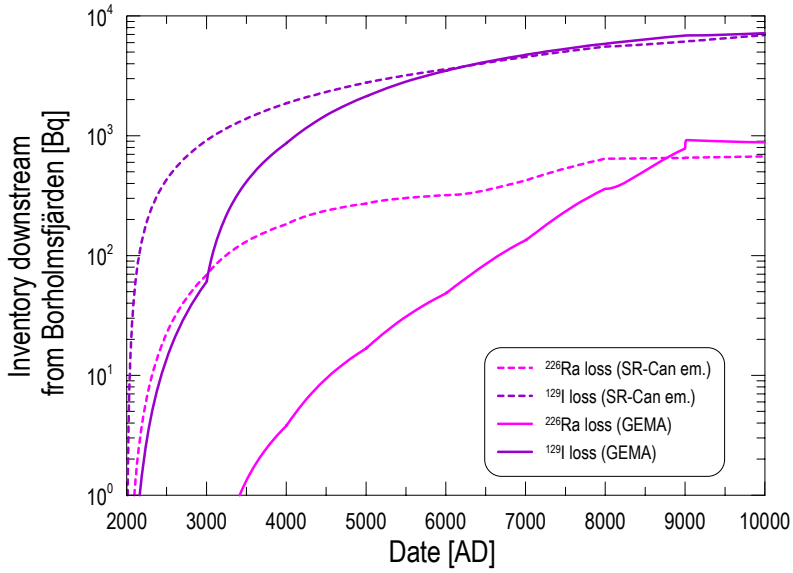

Figure 3-9. As a measure of radionuclide retention in the modelled system the activity of ^{129}I and ^{226}Ra lost from the Borholmsfjärden object (LF2:02a) is shown. 1 Bq y^{-1} is released to the object, and the plotted curves show how much of this has been transported downstream as a function of time. The cases illustrated are the GEMA interpretation of Borholmsfjärden (solid curves) and the GEMA emulation of SR-Can for the same object (broken curves).

here. The width of the geosphere-biosphere interface depends on the water flows. As well as the input from bedrock fractures there is also the question of the influence of meteoric water fluxes to be considered. Here, there is a relatively large lateral component to the water flux scheme caused by infiltration through the uncontaminated catchment. A better understanding of water balance on the catchment scale is necessary in assessment modelling.

3.1.6 Conclusions and recommendations

Starting from the same basic data it is possible to produce alternative conceptualisations of objects within the Laxemar landscape model and Biosphere Dose Conversion Factors (BDCFs) exceeding the published LDFs can be calculated. A detailed analysis of the Forsmark site has not been carried out here, but it is relevant that the GEMA interpretation of the Puttan catchment, based on the Forsmark topographic map (Lindborg, 2005), led to an

object with similar characteristics to those for the Puttan object in the SR-Can model. In contrast, the GEMA review of the landscape around Borholmsfjärden identified the small, isolated catchment BRH_x as a potentially important object, whereas this small present-day lake was subsumed into a much larger object in SR-Can.

We conclude that the methodology employed in SR-Can is not yet mature and, in particular, the procedure for identifying and characterising objects in the current and future landscapes requires further development. The volumes of the landscape objects are criti-

cal to the assessment model calculations. The absence of detailed object identification and associated documentation suggests that it is likely that the SR-Can models overestimate the size of objects.

The compartment models employed by SKB include a smaller subset of FEPs than those included in the GEMA models for the same objects. A review of SKB's compartmental modelling approach is recommended to justify the simple representation of ecosystems processes, with particular attention being paid to the modelling of mires. More generally, a better understanding of water balances within the landscape model elements is needed.

Evolutionary transitions between ecosystem states have been modelled simplistically in both SR-Can and in GEMA. The GEMA results show high transient BDCFs though it is not expected that these transients represent realistic physical responses of the biosphere. What they do tell us is that modelling of these processes requires further development.

Concerns about the interpretation of the geosphere-biosphere interface are also raised here. As well as a better representation of material fluxes, the interaction of water flows bearing radionuclides from the bedrock into the deeper Quaternary deposits should be reviewed. This should lead to a review of the necessary and sufficient extent of compartments in the models

The GEMA modelling would not have been possible without access to the detailed site characterisation data collected by SKB. Essential to this has been the database of catchment areas: however, what has not been available is a description of the coastal catchments at Laxemar (though they are available for the present-day Forsmark site). Also, so far unavailable are the derived details of future catchments. According to SKB (2006cd) these are not yet in the site database. Neither are details given in the recently published report by Brydsten (2006). Full and complete access to the available data is essential.

The aggregated transfer factor approach used by SKB is a useful development. This requires further development in terms of the range of pathways considered, and site-specific uptake factors should be developed from extensive biochemical databases in existence (Lindborg, 2005; 2006).

3.2 Transport calculations

3.2.1 Gaps in prediction of contaminated area

Prediction of radionuclide activity concentrations in the environment due to leakage from a damaged canister(s) depends on how large the contaminated/discharge area is. The analysis performed in section 3.1 shows that the radiological consequence is strongly influenced by the assumed size of the biosphere object, in other words how large the contaminated area is. However, not much effort has been made in SR-Can to explore detailed descriptions of how the biosphere objects are "identified" based on the process understanding for radionuclide distribution in the discharge area. The considerations are as follows:

– the effect of model resolution (discretisation) on the focusing of the size of the discharge area;

– the impact of the representation of processes in hyporheic zones (where surface water and groundwater exchange with each other) on radionuclide transport;

– the impact of subsurface chemical zonation (differences between deep chemistry and near-surface chemistry) on the accumulation of radionuclides in subsurface horizons at the margins of geochemical zones, (eg. regions of high organic matter content or where redox conditions change sharply), and

– the possible impacts of delayed bulk release of radionuclides in response to temporal changes in chemistry.

We propose a schematic analysis to explore these processes. Based on the models for groundwater and surface water flows, one can derive distributions of residence times for flow parcels from their origin at a leaking canister to a defined control section, which would enclose the central discharge point in a watershed as shown schematically in Figure 3-10. The stream tube associated with the passive travel of solute elements will theoretically be very narrow, in the order of the same size as the mixing cross sectional area of the stream tube at the repository depth. A stream tube is defined as the surface created by the streamlines going through a closed contour and streamlines are the curves defined by tangency to the velocity field (Norman and Kjellbert, 1990). However, diffusion and dispersion due to fracture intersections along the whole stream tube spreads radionuclides over a larger area, A, that can be estimated if we know the mean path length in the stream tube L and the associated velocity u. The spatial variance of the solute concentration in both longitudinal and transverse components can be expressed according to

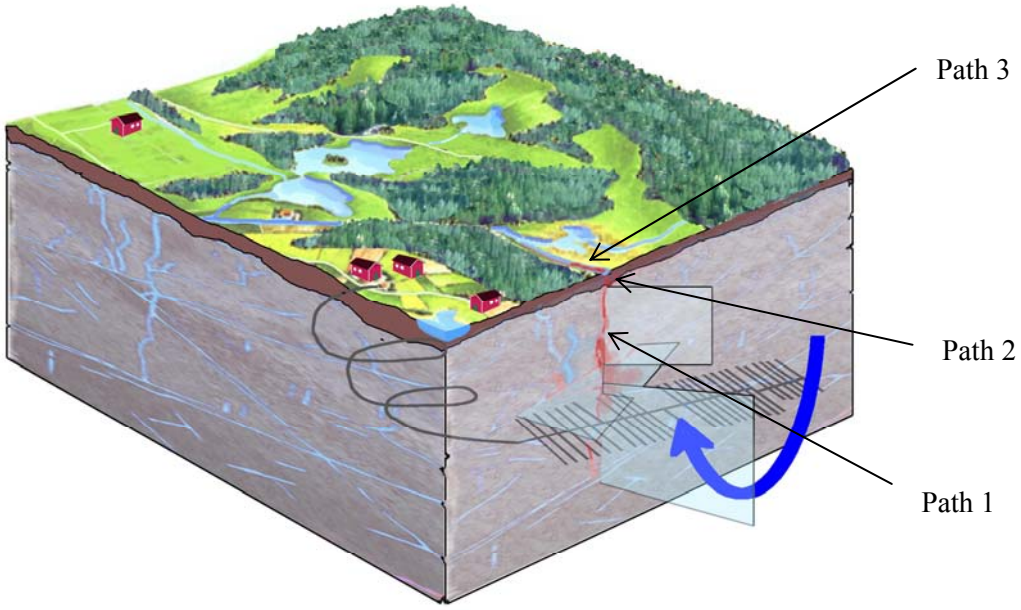

Figure 3-10. Schematic of the separation of pathway segments identified in the modelling approach. Path 1 – crystalline bedrock, Path 2 – Quaternary deposits, Path 3 – surface drainage system.

Fischer et al., (1979):

$$\sigma_L = \sqrt{2D_L\tau}$$
$$\sigma_T = \sqrt{2D_T\tau} \qquad (3\text{-}1)$$

where D_L *and* D_T are combined diffusion plus fracture dispersion coefficients in the longitudinal (L) and transverse (T) directions, respectively, and τ is the water residence time = *L/u*. Further, for fluid velocities sufficient for kinematic dispersion to dominate over molecular diffusion, the local dispersion coefficients are expressed as (Marsily, 1981):

$$D_L = \alpha_L|u|$$
$$D_T = \alpha_T|u| \qquad (3\text{-}2)$$

where α_L and α_T, which both have the dimension of length, are known as intrinsic dispersion coefficients or dispersivities.

Dispersivities can range from one to hundreds of metres in fractures and a few centimetres in sand (Marsily, 1981). A rough estimation of the spread of radionuclide in a length of fracture beneath the Quaternary deposits (QD) can be expressed as 4σ. By assuming the water residence time in the geosphere to be 40 y (SKB, 2006a), the velocity to be 12.5 m/y and α_T in fractures to be 130 m (Marsily, 1981), we obtain from equations 3-1 and 3-2 a spreading-length along the sub-Quaternary deposits fracture of 1500 m. The radionuclide spreading-width due to transport through the QD to the ground surface becomes 15 m, by assuming the water residence time in the QD to be 100 y, the velocity to be 0.06 m/y and α_T in the QD to be 1 m. We thus obtain a contaminated area of 25,000 m^2 by accounting for both the spreading-length in the fracture and the QD. It may be argued that such a "hot spot" will have limited radiological consequences because it is concentrated in a very narrow area. However, the accumulated radionuclides in the biosphere may subsequently be dispersed over a wider area by various processes such as hydrological transport, human activity (farming) and changes in chemistry or hydrological conditions. The more important question is how large the discharge area will be so that the radiological consequences can be evaluated, and neglected if this is justifiable.

In the following analysis we use hydrological/solute transport models with the above estimated discharge area of 2.5×10^4 m^2 to predict environmental activity concentrations and radiological dose consequences. The transport models used in the analyses are described in the next section.

3.2.2 1D transport and reaction along combined subsurface-surface pathways

Time dependent transport along a single pathway (defined by *x*) can theoretically be analysed using

$$C(x,t) = \int_0^t \frac{g(\xi)}{Q} \delta S(x, t-\xi) d\xi \quad (3\text{-}3)$$

where $C(x,t)$ is concentration of radionuclide in unit [Bq/m^3], $g(\xi)$ is the release of radioactivity [Bq/y] expressed as a boundary condition at the repository and δS is the solute response resulting from a unit pulse at the boundary $\delta(t)$ [y^{-1}]. The discharge of water, Q [m^3/y], is associated with a defined stream tube in which the release is assumed to initially mix and flow. Further, this discharge can be expressed as $Q = uA$, where u is water velocity [m/y] and A is the area of the stream tube [m^2]. The flux of radioactivity, q [Bq/y], at a control section defined by the transport distance x can more directly be expressed as

$$q(x,t) = \int g(\xi) \delta S(x, t-\xi) d\xi \,. \quad (3\text{-}4)$$

A modelling study has previously shown that discharge points are predominantly located in low-lying areas of the catchments where the layers of QD often are relatively deep (Marklund et al., 2007). Such areas include riparian zones, wetlands and lakes (Figure 3-11).

In order to compare our results with LDF values we adopt a unit release to the biosphere (1 Bq/y), which means our analysis starts from Path 2 using a unit continuous radionuclide release as the boundary condition. For simplicity, we assume that the transport of radionuclides along Path 2 through the QD enters a stream directly and that Path 3 represents transport within this stream. The system described in Section 3.2.1 is further simplified to the one shown in Figure 3-12.

It is assumed that reactions are constant along transport pathways and that the flow field is steady. These are crude assumptions since, for instance, we do not take into account the changes in redox potential at the geosphere-biosphere interface, which can affect solid-liquid distribution coefficients (K_d) (Ashworth and Shaw, 2005) and transient flow due to land rise. However, the latter effect was approximated by calculating the latent dose rates, i.e. the transformation of former QD and river sediments into agricultural land.

The radionuclide activity concentration along Path 2 is estimated by an advection-dispersion model (Van Genuchten and Cleary, 1979) assuming constant moisture content and one-dimensional flow:

$$\frac{\partial C(x,t)}{\partial t} + \frac{\rho}{\varepsilon}\frac{\partial C'(x,t)}{\partial t} = D\frac{\partial^2 C(x,t)}{\partial x^2} - v\frac{\partial C(x,t)}{\partial x} - \lambda\left[C(x,t) + \frac{\rho}{\varepsilon}C'(x,t)\right] \quad (3\text{-}5)$$

where $C(x,t)$ is activity concentration of radionuclide in pore water [Bq/m^3], $C'(x,t)$ is activity concentration sorbed to the soil solid matrix [Bq/kg], D is the dispersion coefficient [m^2/y], v is the mean pore water velocity [m/y], ρ is the bulk density of the QD [kg/m^3] and ε is porosity [-]. Assuming a linear adsorption isotherm $C'(x,t)$ can be described by

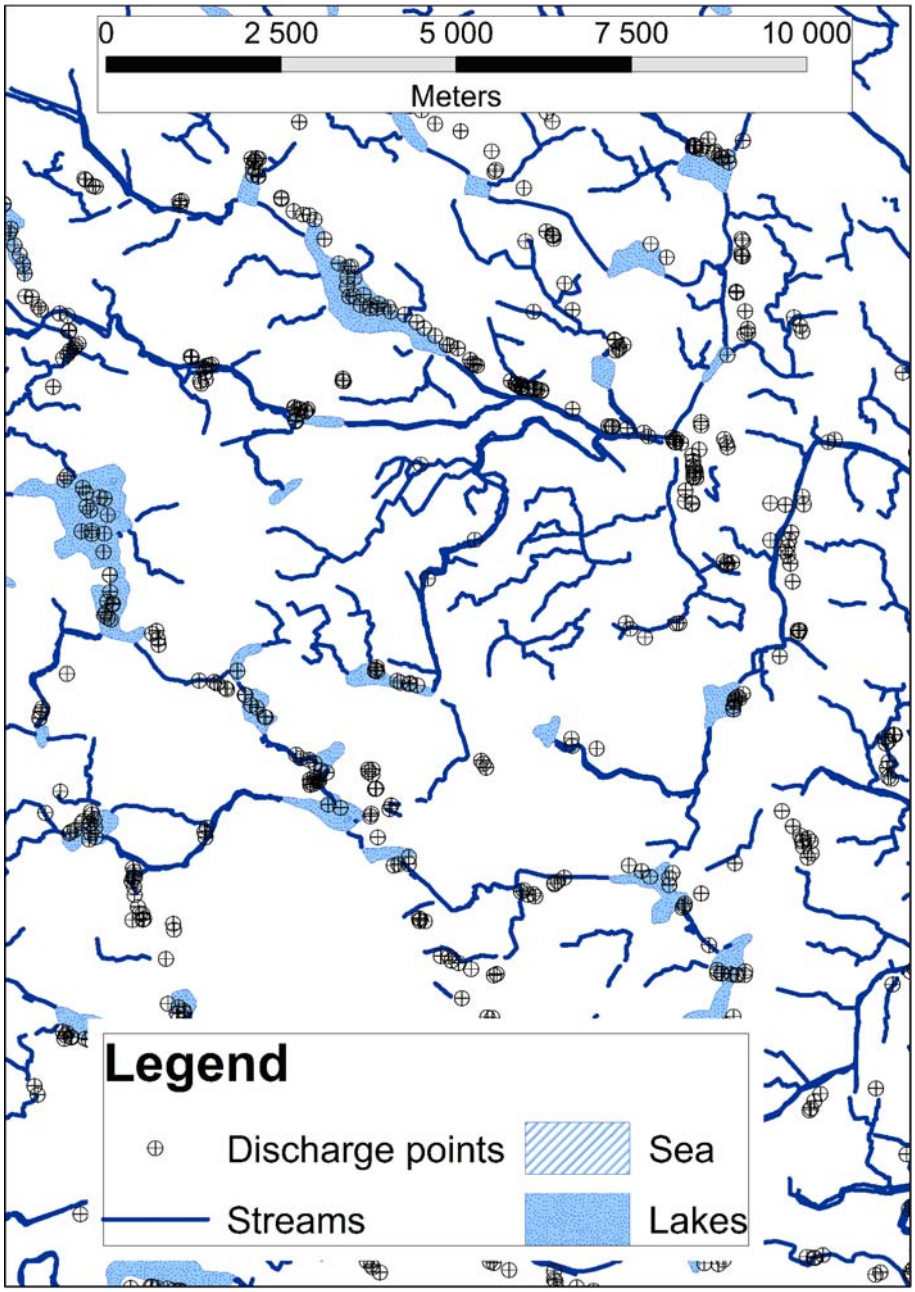

Figure 3-11. Discharge points are closely related to the hydrological drainage system in a landscape. Flow paths of deep groundwater predominantly emerge in low-lying areas where surface water accumulates. A related issue stems from the coupling between topography and the characteristics of the QD. Low-lying parts of the catchment coincide with areas where the layers of QD are often relatively deep. For Oskarshamn, the mean thickness of QD at the discharge areas is 2.2 times their average thickness over the entire area. Since fracture zones tend to be correlated with topographic lows in most geologic settings, this may further enhance the significance of the QD.

$$C'(x,t) = K_d C(x,t) \tag{3-6}$$

where K_d is the solid-liquid distribution coefficient [m^3/kg].

Combining (3-5) and (3-6), equation (3-5) can be written as:

$$\frac{\partial C(x,t)}{\partial t} = \frac{D}{R_{QD}} \frac{\partial^2 C(x,t)}{\partial x^2} - \frac{\nu}{R_{QD}} \frac{\partial C(x,t)}{\partial x} - \lambda C(x,t) \tag{3-7}$$

where R_{QD} is the retardation factor which quantifies the effect of radionuclide sorption on transport velocity, defined as

$$R_{QD} = 1 + K_d \frac{\rho_{QD}}{\varepsilon_{QD}}.$$

The initial and boundary conditions of the problem are defined as

$$C(x, t=0) = 0 \tag{3-8}$$

$$C(x=0, t) = \delta(t) \frac{M}{Q} \tag{3-9}$$

where M is activity [Bq].

The unit release response can thus be written as

$$\delta S(x) = \frac{C(x)}{M/Q} \tag{3-10}$$

Radionuclide transport in streams can be described in terms of advection, dispersion, exchange with hyporheic zones and adsorption to sediments (e.g. Bencala and Walters, 1983; Elliott and Brooks, 1997). Under the past two decades different models describing transport processes in streams have been developed, such as the first-order mass transfer model (FOT model), the impermeable model (IS model), the water infiltration model (WI model) and the advective-storage-path model (ASP model). By using temporal moments of residence time, the relationships between the parameters of different models can be determined (Wörman, 2000), which leads to identical model predictions up to the first three temporal moments. Thus, selection of any of these models is not critical for the pre-

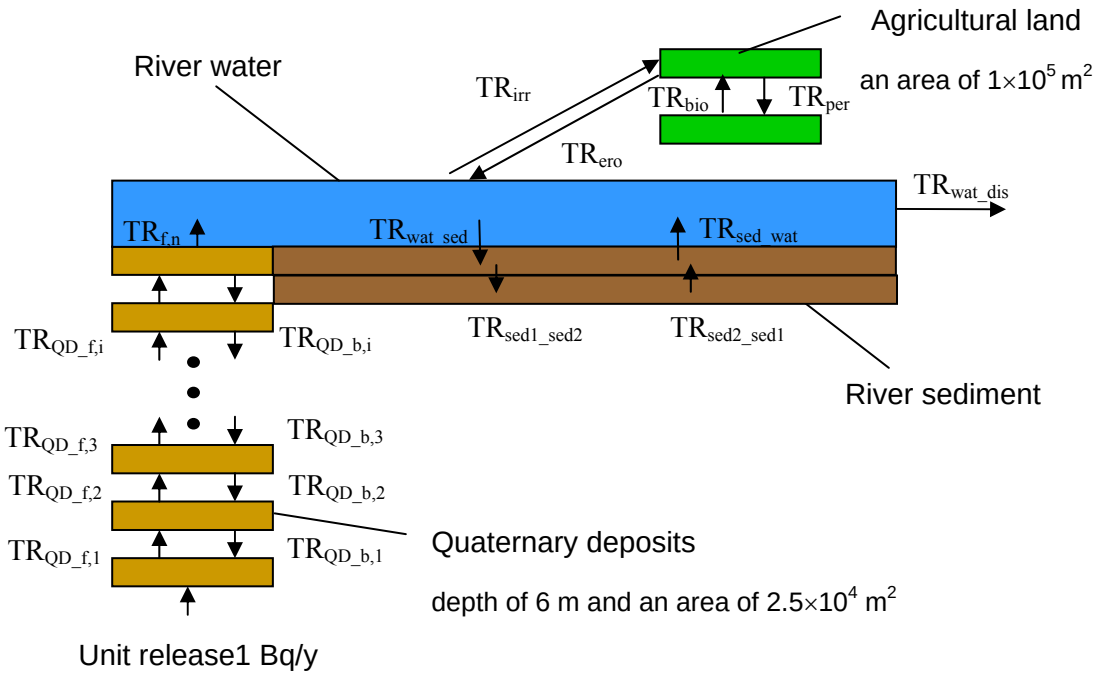

Figure 3-12. System of compartment models to describe transport through QD, river and irrigated agricultural land with unit release [1 Bq/y].

dictability. Here we use the ASP model to describe radionuclide transport in a stream. The governing equation of the ASP model (Wörman et al., 2002) is written as:

$$\frac{\partial C}{\partial t}+\frac{1}{A_T}\frac{\partial(AUC)}{\partial x}-D\frac{\partial^2 C}{\partial x^2}=J_S \qquad (3\text{-}11)$$

where C is the dissolved activity concentration of radionuclide in the stream water [Bq/m^3], A_T [m^2] is the cross-sectional area of the main stream including side pockets, A is the cross-sectional area of the main stream excluding side pockets [m^2], U is the flow velocity in the main stream [m/s], (Q=UA), Q is the discharge [m^3/s], and D is the main stream dispersion coefficient [m^2/s]. The effective flow velocity in the main stream channel corrected for side pockets with stagnant water is given by $U_e = Q/A_T$ (Wörman, 1998).

The net radionuclide flux [Bq/m^{3}s)] in the dissolved phase in the stream water can be written as integrating over the distribution of transport pathways:

$$J_S=\frac{1}{2}\int_0^\infty f(T)\frac{P}{A}\xi\left(-V_Z(\tau,T)\big|_{\tau=0}c_d+(V_Z(\tau,T))\big|_{\tau=T}g_d\right)dT\,. \qquad (3\text{-}12)$$

where g_d is solute mass per unit volume of water in the hyporheic zone [Bq/m^3], V_z is the infiltration velocity [m/s] into the bed in the direction of the streamlines denoted by $V_Z(\tau,T)\big|_{\tau=0}$ and exfiltration velocity out of the bed in the direction of the streamlines $V_Z(\tau,T)\big|_{\tau=T}$, $f(T)$ is the probability density function (PDF) of T weighted by the velocity component normal to the bed surface, V_n, T is the total residence time from inlet to exit of hyporheic flow path [s], τ is the exfiltration residence time [s] ($0<\tau<T$), P is the wetted perimeter [m], A is the cross-sectional area of the stream [m^2], and ξ is an area reduction factor equal to V_n/V_Z that accounts for the fact that the streamlines are not always perpendicular to the bed surface.

3.2.3 Model implementation and discretisation

There are similarities between a finite difference approximation of the advection-dispersion (A/D) type of equation and a compartmental model. Furthermore, when certain criteria are fulfilled compartmental models can provide identical solutions to those of the A/D equations (Xu et al., 2007). Here, a compartmental model is used to solve the two problems previously described since this allows radionuclide chain decay to be handled conveniently. The models are implemented in Ecolego Toolbox (Broed and Xu, 2008).

The transfer rates used in the compartmental model (Figure 3-12) for different paths in the system are given in Table 3-3 (definitions and values of parameters used to determine transfer rates are given in Appendix II). Radionuclide-dependent parameter values (K_d for soil and peat) are given inTable 3-4. In SR-Can K_d-peat was used to define the distribution between solids and water in lake sediments (Avila et al., 2006). Calculations were performed for selected radionuclides.

There are no site-specific data available for parameters such as the advective velocity into sediment V_z and the hydraulic radius, A/P, for the river model. Therefore, we employ data obtained from a tracer experiment performed in Säva Brook in Uppland County (Johansson et al., 2001) as a typical characterisation of an agricultural stream in a landscape type that is likely to exist if leakage occurs from the repository after a considerable land rise has occurred. In the experiment, moderately sorbing ^{51}Cr, was used as the tracer. The break-through curves were obtained at 8 stations along a distance of 30 km. The input data used in the modelling demonstration are based on the distance between station C and D, which is 3980 m and similar to the river length in the later assessment.

The lumped parameter TR_{wat_sed} was obtained by fitting the simulated breakthrough curves with experimental data using 250 compartments to represent the water course in the model (Figure 3-13). The calibrated lumped parameter value of TR_{wat_sed} is 0.033 h^{-1}, which is a factor of 0.55 of the value used in the ASP model. The reason for this is that the ASP model integrates the mass flux from water into sediment over the distribution of transport pathways (see Eq. (3-11)) while in the compartmental model framework the distribution function relates to the number of boxes used to represent the uptake zone in the stream sediment. Details of the determination of the transfer rate, $TR_{wat\_sed,}$ can be found in Broed and Xu, (2008). Once the transfer rate TR_{wat_sed} is obtained, one compartment is used to represent the water course in the river model for assessment purposes. This is because the transport residence time in rivers is rather short and the up-stream

Table 3-3. Description of transfer rates in compartmental models (definitions and values of the parameters in the descriptions are found in Appendix II).

Transfer rate	Description of transfer rate	References
$TR_{QD\_f,i}$	$\frac{(v/R_{QD})}{(L_{QD}/n_{QD})} + \frac{(D/R_{QD})}{(L_{QD}/n_{QD})^2}$, $v = u_{QD}/\varepsilon_{QD}$	Xu et al., (2007)
$TR_{QD\_b,i}$	$\frac{(D/R_{QD})}{(L_{QD}/n_{QD})^2}$, $R_{QD} = 1 + K_d \rho_{QD}/\varepsilon_{QD}$	Xu et al., (2007)
TR_{irr}	$\frac{V_{IRR} Nr_{IRR}}{VW} A_{IRR}$	Karlsson et al, (2001)
TR_{ero}	$\frac{Rem}{D_{ts}(1-\varepsilon_t)\rho_p}$	Karlsson et al, (2001)
TR_{per}	$\frac{R}{\varepsilon_t D_{ts}} Ret + \frac{BioT}{D_{ts}(1-\varepsilon_t)\rho_p}$, $Ret = \frac{1}{1+(1-\varepsilon_t)\rho_p K_d/\varepsilon_t}$	Karlsson et al, (2001)
TR_{bio}	$\frac{BioT}{D_{ds}(1-\varepsilon_d)\rho_p}$	Karlsson et al, (2001)
TR_{wat_sed}	$\frac{V_Z \xi}{2(A/P)}$	This report
TR_{sed_wat}	$\frac{(V_Z \xi/2)}{R_m(z/n_{riv})}$, $R_m = 1 + K_d \rho_{riv}/\varepsilon_{riv}$	This report
TR_{sed1_sed2}	$\frac{(V_Z \xi/2)}{R_m(z/n_{riv})}$	This report
TR_{sed2_sed1}	$\frac{(V_Z \xi/2)}{R_m(z/n_{riv})}$	This report
TR_{wat_dis}	$\frac{u_{riv}}{L_{riv}}$	This report

Table 3-4. Solid-liquid distribution coefficients (K_d) [m^3/kg] used in calculations (after Karlsson and Bergström, 2002).

	^{226}Ra	^{14}C	^{36}Cl	^{135}Cs	^{129}I	^{59}Ni	^{210}Pb	^{210}Po
K_d-soil	5×10^{-1}	1×10^{-3}	1×10^{-3}	1×10^{0}	3×10^{-1}	5×10^{-1}	1×10^{-1}	5×10^{-1}
K_d-peat	2×10^{0}	7×10^{-2}	1×10^{-2}	3×10^{-1}	3×10^{-2}	1×10^{0}	2×10^{1}	7×10^{0}

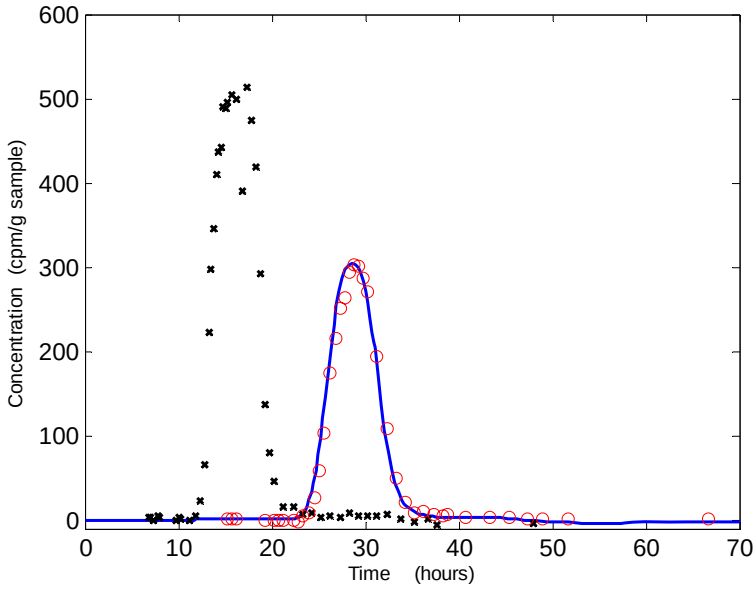

Figure 3-13. Measured concentration-time distribution for ^{51}Cr at stations C and D (marked with ' ×' and 'o', respectively) in the Säva Brook experiment (Johansson et al., 2001) and predicted curve (solid line) at station D using the compartmental river model with 250 compartments and a value of 0.033 h^{-1} for TR_{wat_sed}.

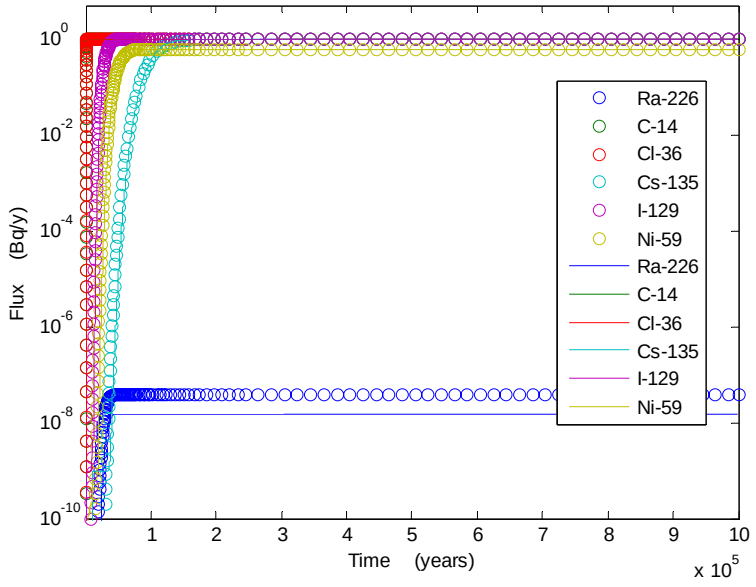

Figure 3-14. Fluxes through QD vs. time, based on unit release (1 Bq/y). Circles denote results from compartment QD model and solid lines denote analytical solutions from A/D equation (3-5).

boundary condition, with a continuous inflow, dominates the model behaviour. Thus, the number of compartments does not contribute significantly to the model error in a long term safety assessment (Xu et al., 2007).

In contrast to the river model a larger number of compartments are needed for the QD model because, for a moderately sorbing nuclide, the transport residence time through 6 metres of QD is about 150,000 years (Wörman et al., 2004). Figure 3-14 shows that, when 60 compartments are used in the QD compartment model, the simulated fluxes are close to those obtained from numerical inversion of the Laplace transform of (3-7).

Once the activity concentration in various media is determined we also use the Aggregated Transfer Factors (TF_{agg}) (Avila, 2006) to calculate dose rates for various media/ ecosystems in order to make our calculated results compatible with the LDF-values.

3.2.4 Results and discussion

Two calculations have been undertaken using SKB's K_d-peat values and K_d-soil values, respectively, for the distribution of radionuclides between solids and water in QD and river sediments. Calculated activity concentrations within the top 0.3 m layer of QD versus time are shown in Figure 3-15. As can be seen, the time taken for the activity concentrations to reach equilibrium in the top layer of QD ranges from 1,000 years to 100,000 years for different radionuclides and the result strongly depends on the K_d values. Figures 3-16 to 3-18 show the activity concentrations in different media as a function of time. They follow a similar pattern to that in the QD and, similarly, the calculated activity concentrations are sensitive to the K_d values.

It is noted that the K_d value for Cs used for river sediment in SR-Can (SKB, 2006c) is rather low. In freshwater, the organic matter content gives rise to high concentrations of fulvic acids that lead to a high sorption affinity for metals (Salomons and Förstner, 1984). The normal value of the ^{137}Cs K_d for freshwater sediments is in the range of 5 to 20 [m^3/kg] according to Wieland et al. (1993) and Crusius and Anderson (1995). The lowest K_d value for Cs in the these two studies is a factor of 17 times higher than that used in SR-Can. A review of the K_d database used in SR-Can is given in the next chapter.

Dose rates at equilibrium obtained from the two calculations are shown in Table 3-5 and Table 3-6. The results agree with our earlier study (Wörman et al., 2004), which showed that Quaternary deposits serve the function of both retarding and accumulating radionuclides. As can been seen, the latent dose rates are 2 to 4 orders of magnitude higher than those estimated using the LDF-concept (see Tables 3-5 and 3-6) when the Quaternary deposits are transformed to agricultural land. ^{226}Ra is the exception since it has a short half life.

This simple transport analysis using assumptions based on physical processes reveals that the discharge area is likely to be geographically limited. The discharge area used in SR-Can varies with time within the simulation period (Kautsky, 2006a). Reviewing the data, we found that the smallest discharge area during the entire simulation period was about 2.5 km^2 and the radiological consequences of canister leakage into this area was then analysed. According to our calculation, if a discharge area is 2.5 km^2 the estimated dose rates will be close to the LDF value because the dose rates are proportional to the discharge/contaminated area. It would be interesting to know if SKB can demonstrate that

the radionuclides leaking from a damaged canister spread out to an area as large as 2.5 km^2 at the surface environment.

Tables 3-5 and 3-6 show that dose rates from river water are comparable to SKB's LDFs. The lowest dose rates for all radionuclides, except for ^{36}Cl, are obtained for agricultural land irrigated by river water. Latent dose rates from river sediments are not negligible compared with LDFs and they depend very much on the K_d values used in the calculation, as mentioned above. This means that river sediments are a potential exposure source to individual humans.

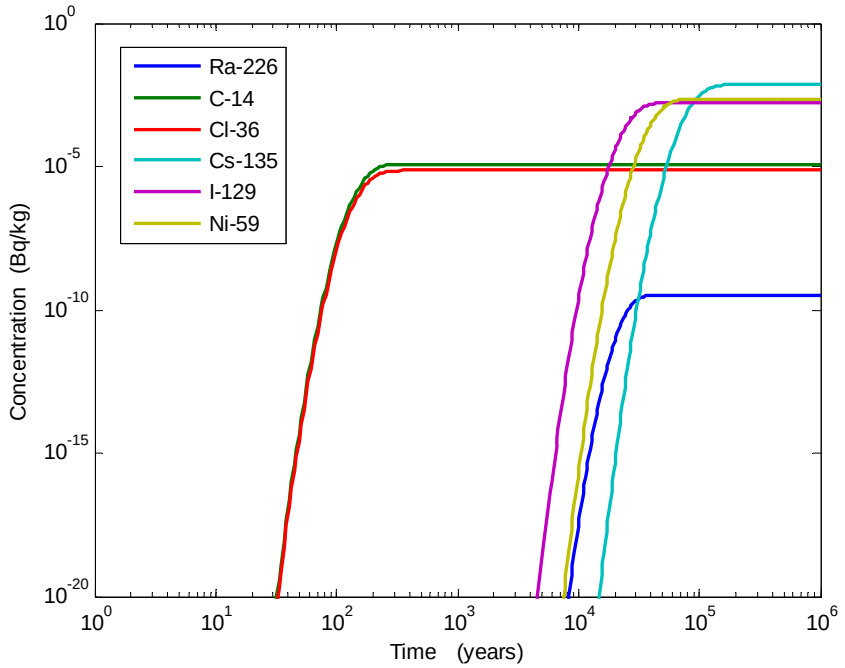

Figure 3-15. Activity concentrations of radionuclides in the top layer (0.3 m thick) of QD vs. time.

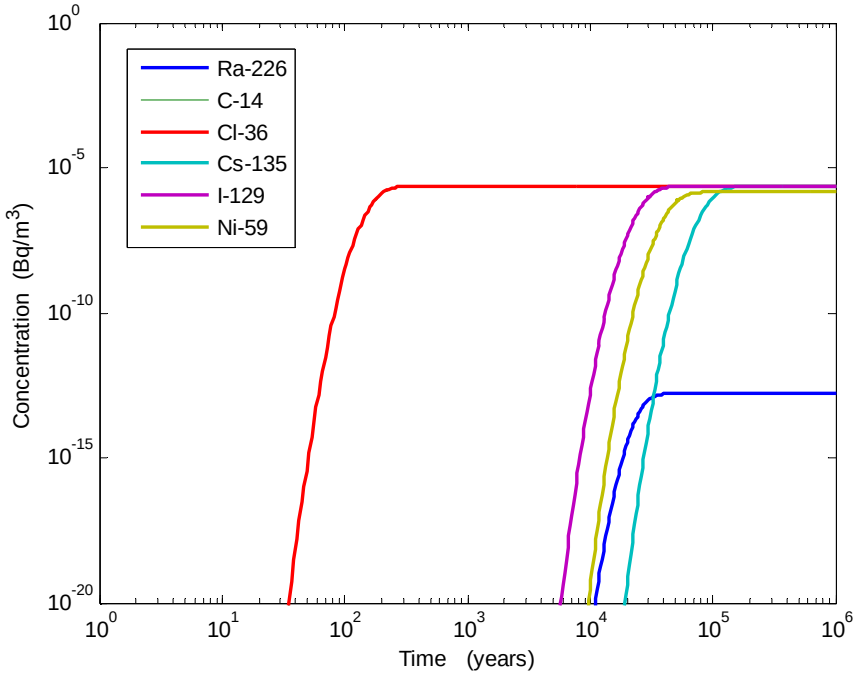

Figure 3-16. Activity concentrations of radionuclides in river water vs. time (the curve of concentration for ^{14}C overlaps that of ^{36}Cl).

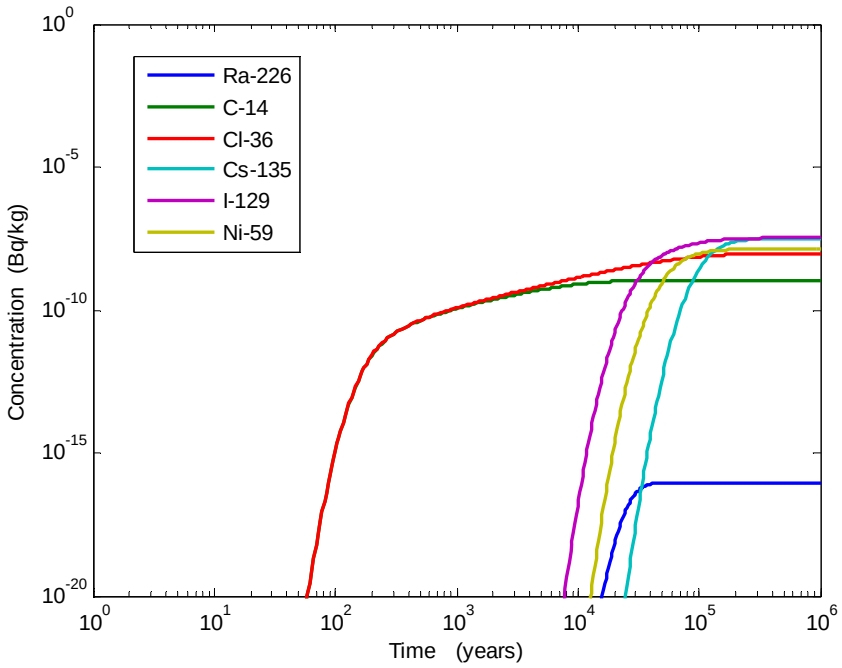

Figure 3-17. Activity concentrations of radionuclides in soil irrigated by river water vs. time.

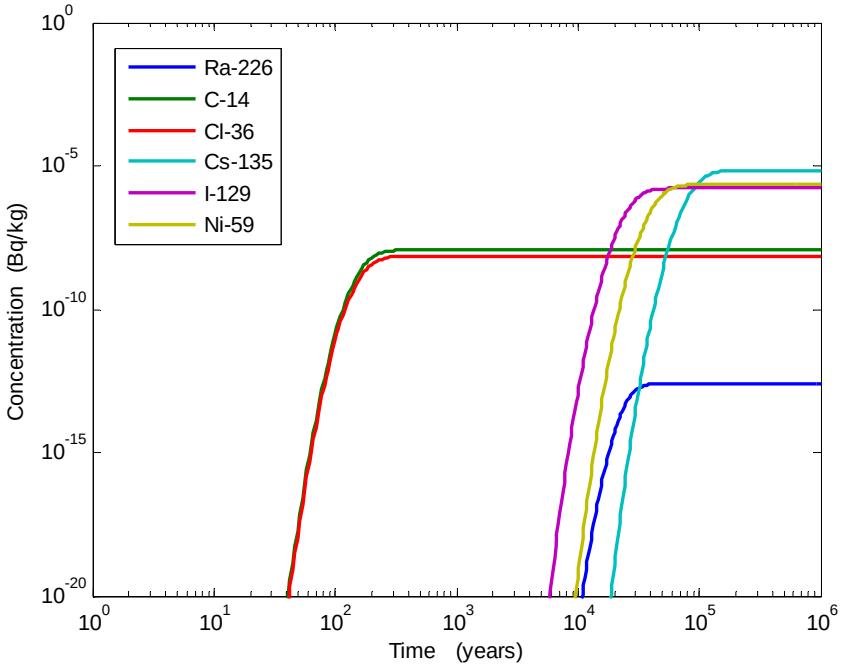

Figure 3-18. Activity concentrations of radionuclides in river sediment vs. time.

Table 3-5. Calculated dose rates [Sv/y per Bq/y] for various media by using $Kd_{\_peat}$ for the distribution between solids and water in the QD and river sediments comparing with the LDF [Sv/y per Bq/y].

Nuclides	QD latent	River water	Agricultural land	River latent	LDF
^{226}Ra	4.9×10^{-26}	2.5×10^{-29}	1.9×10^{-33}	2.2×10^{-29}	4.7×10^{-11}
^{14}C	-	2.2×10^{-11}	-	-	-
^{36}Cl	3.0×10^{-10}	8.6×10^{-14}	6.5×10^{-14}	2.8×10^{-13}	8.1×10^{-15}
^{135}Cs	1.8×10^{-10}	3.7×10^{-11}	2.6×10^{-15}	1.7×10^{-13}	2.3×10^{-12}
^{129}I	1.5×10^{-9}	4.3×10^{-11}	2.9×10^{-13}	1.5×10^{-12}	1.6×10^{-11}
^{59}Ni	7.6×10^{-12}	4.5×10^{-15}	2.2×10^{-17}	7.6×10^{-15}	4.4×10^{-15}

Table 3-6. Calculated dose rates [Sv/y per Bq/y] for various media by using k_{d_soil} for the distribution between solids and water in the QD and river sediments comparing with the LDF [Sv/y per Bq/y].

Nuclides	QD latent	River water	Agricultural land	River latent	LDF
^{226}Ra	2.0×10^{-15}	1.5×10^{-16}	5.5×10^{-22}	1.6×10^{-18}	4.7×10^{-11}
^{14}C	-	5.3×10^{-11}	-	-	-
^{36}Cl	5.1×10^{-11}	8.6×10^{-14}	6.5×10^{-14}	4.9×10^{-14}	8.1×10^{-15}
^{135}Cs	5.8×10^{-10}	3.6×10^{-11}	2.6×10^{-15}	5.5×10^{-13}	2.3×10^{-12}
^{129}I	1.5×10^{-8}	4.3×10^{-11}	2.9×10^{-13}	1.4×10^{-11}	1.6×10^{-11}
^{59}Ni	6.1×10^{-12}	7.3×10^{-15}	3.5×10^{-17}	5.8×10^{-15}	4.4×10^{-15}

4 Review of K_d database in SR-Can

4.1 Introduction

Following a review of SKB's 'SR-Can' safety assessment report (SKB, 2006a) by the INSITE/OVERSITE Site Investigation Group (SIG) several concerns have been raised over some aspects of the approach to the biosphere modelling component of the safety assessment. Specifically, questions have been raised concerning the K_d database used in the assessment. For the biosphere assessment, the 'SR 97' database (SKB report R-02-28; Karlsson & Bergström, 2002) has been used exclusively. One concern is that this database contains data which do not reflect the most recent scientific literature. Another is that, despite a large body of information being available on the biosphere characteristics of both the Forsmark and Laxemar repositories, the linkage between these site characteristics and the ranges of K_d values used in the assessment is not clear, or has not been demonstrated. A concern over the lack of site-specific radionuclide transfer and retention data is raised in the SR-Can report itself :

> "Also lacking is retention data of elements in regolith and biota (e.g. K_d for soil, sediments and peat, soil to plant transfer factors, animal transfer coefficients). Most of the required samples have been collected and chemical analyses and reporting is in progress. The ecosystem modelling of elemental transfers is, when finalised, to be used as a complement to transfer factors. This is in particular necessary in order to satisfactorily handle radionuclides such as C-14, for which current radionuclide transport models are associated with large uncertainties."

(Taken from page 560, section 13.7.7 – SKB, 2006a.)

Modelling carried out within the CLIMB project to date has demonstrated that simulations are sensitive to compartmental volume (ie. scale of discretisation) and solid-liquid K_d values for a small number of key radionuclides:

^{36}Cl, ^{99}Tc, ^{129}I, ^{79}Se, ^{59}Ni, ^{135}Cs, ^{226}Ra (and decay products, ^{210}Pb, ^{210}Po)

Several key questions have arisen with respect to the K_d values used in performance assessment (PA) calculations:

- Are the most relevant and up to date K_d values being used by SKB?
- Has selection of best estimate K_ds and ranges been appropriate?
- Can K_d value selection be demonstrably related to site characteristics (eg. organic soils versus sediment values).
- Could better and more defensible estimates of K_ds be obtained by site specific measurements?

This review addresses these questions, with specific reference to the parameters listed in *Nuclide documentation: element specific parameters values used in the biospheric models of the safety assessments SR97 and SAFE* (Karlsson & Bergström, 2002). Conclusions are drawn and recommendations made as to how, if necessary, K_d values used in PA calculations could be improved.

4.2 Structure and Approach

This review considers the K_d values for each of the key elements identified above in the order in which they appear in the database report (Karlsson & Bergström, 2002). A brief review is made of the behaviour of each element with respect to sorption in soils and sediments. This is not intended to be an exhaustive review of the literature, but rather a 'thumbnail sketch' on the basis of which some conclusions can be drawn about the key factors which are likely to control K_d for the element being considered. The absolute values of K_d from Karlsson & Bergström (2002) are then shown graphically in comparison with other acknowledged literature sources, plus some useful additional data (some unpublished) which help to place the SKB data in context.

An acknowledged feature of solid-liquid K_d values, whether for soils or sediments, is their uncertainty and emphasis is placed on this where relevant.

4.3 Review for selected elements

4.3.1 Chlorine (^{36}Cl)

K_d values within the literature are sparse for chlorine and ^{36}Cl, the most significant radionuclide of chlorine in waste safety assessments. This may be partly due to the fact that, until relatively recently, ^{36}Cl was not considered a key radionuclide in waste safety assessments, and partly due to the widespread assumption that chlorine behaves conservatively in soils, sediments and waters. The dominant chemical form of chlorine in waters is the chloride anion (Cl^-) which is known to be strongly repelled from negatively charged sediment particles. As a result its K_d is very low, approaching zero, and its mean travel velocity through porous media can be faster than tritiated water (Ogard et al., 1988), implying anion repulsion. However, some literature findings indicate that the retention of chlorine and ^{36}Cl in organic soils is significant, implying K_d values much higher than those expected for chloride. A significant body of work on this topic has been produced in Sweden by the research group of Öberg (1998, 2002) which has found that soil organic matter contains chlorine in comparable amounts to phosphorus. Lee et al. (2001) provided chromatographic evidence for the association of ^{36}Cl and chlorine with humic substances from soils and estuarine sediments. Furthermore, studies with soil lysimeters have shown that imbalances in chlorine budgets are most likely attributable to the storage of organic chlorine, which was estimated to be four times larger than the storage of chloride (Rodstedth et al., 2003). Finally, the direct measurement of cosmogenic and nuclear weapons derived ^{36}Cl in Canadian forest soils by Milton et al. (2003) has indicated that it behaves non-conservatively.

Sheppard et al. (2004), in summarizing parameters values for chlorine, used Milton's data to calculate K_d values for organic forest soils. These are shown in Figure 4-1 in comparison with K_d values for chlorine taken from the SKB data base. Also shown is the best estimate chlorine K_d for mineral soil, obtained from several literature sources. The mineral soil K_d value from Sheppard et al. (2004) can be seen to lie at the lower end of the range of K_d values used in SKB's calculations. Only a single K_d value was computed for mineral soil by Sheppard et al. since many zero values were encountered which prevented a geometric standard deviation being calculated. The very low best estimate of 10^{-4} m^3 kg^{-1} implies a 'close to zero' value for mineral soils, in keeping with the assumption that

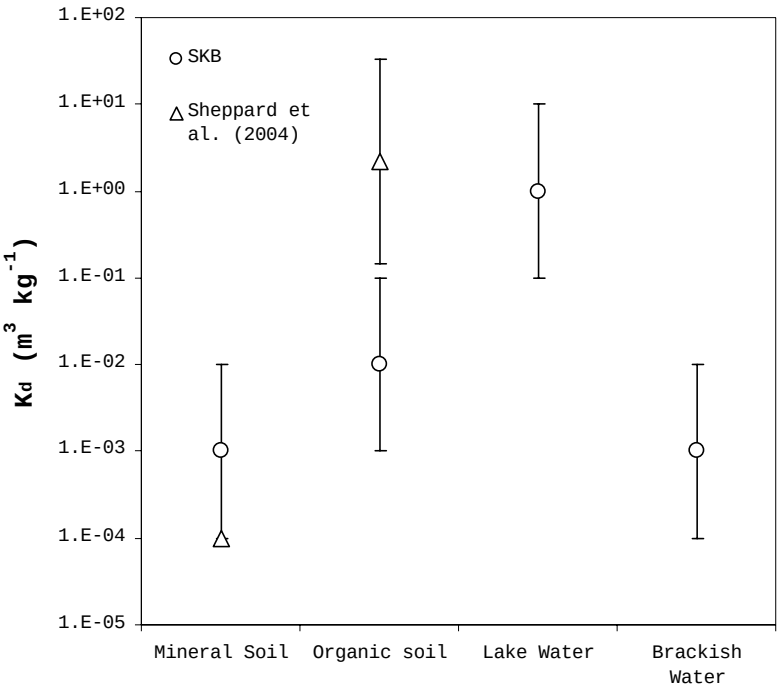

Figure 4-1. Comparison of K_d values for chlorine from the SKB database with those obtained from Sheppard et al. (1994). NB. The organic soil K_d values from Sheppard et al. are geometric means ± the 95% confidence range in the case of organic soil values.

dominant chemical form will be Cl^-. The SKB range extends two orders of magnitude above this value to a maximum of 10^{-2} m^3 kg^{-1}, which is probably realistic for inorganic chlorine (Cl^-) in mineral soils. In contrast, the range of organic soil K_d values provided by Sheppard et al. (2004) lies above the range used by SKB with no overlap of ranges. The authors of R-02-08 state on page 27 that "The root uptake (of chlorine) is very high whereas sorption to solid matter in soils, sediments and peat is very low." Given the evidence that exists within the literature for the non-conservative behaviour of chlorine in organic soils the range of K_d values assumed by SKB (10^{-3} to 10^{-1} m^3 kg^{-1}) would seem to be low. However, this is a case in which site specific measurements of K_d values in different soils from the Forsmark and Laxemar catchments would assist greatly in parameter selection.

On page 25 of R-02-28, Karlsson & Bergström state that the K_d values for chlorine in organic soils have been estimated *Assuming that chlorine behaves like iodine in reducing environments (pers. comm. P-O Aronsson, Ringhals NPP 2001-10-22) ...* and that *... a K_d-value close to that used for iodine has been used*. This assumption is unsafe since the chemistries of chlorine and iodine in reducing environments are significantly different. The K_d of iodine under reducing conditions is actually reduced with respect to oxidising conditions (see Section 4.3.5) whereas the K_d of chlorine in organic soils is expected to be increased in comparison with inorganic soils.

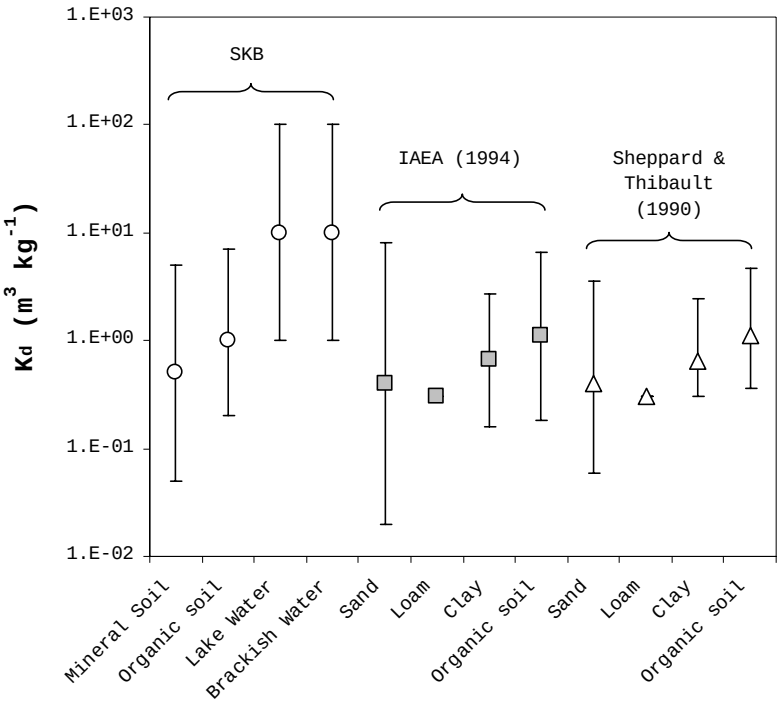

Figure 4-2. Comparison of K_d values for nickel from the SKB database with those obtained from IAEA (1994) and Sheppard and Thibault (1990).

4.3.2 Nickel (^{59}Ni)

Nickel is a transition metal element which has been widely studied in the context of plant and animal nutrition and phytotoxicity. However, studies of radionuclides of this element are very rare and, as a consequence, K_d values for radionickel are difficult to find in the literature. SKB has used soil K_d values for nickel obtained from IAEA (1994). The mineral soil value appears to be an average of values for sand, loam and clay soils (Figure 4-2). Individual uncertainties for Ni K_d values are given for each of these soil types in IAEA (1994). SKB has adopted an uncertainty range of ± one order of magnitude rather than combining the uncertainties for individual soil types. This seems a reasonable approach. The organic soil best estimate and uncertainty range used by SKB are the same as those presented in IAEA (1994), as expected. Figure 4-2 shows that the best estimate nickel K_d values in IAEA (1994) and Sheppard and Thibault (1990) are identical, since the 1990 publication by Sheppard and Thibault was the primary source of K_d data for the IAEA (1994) database. However, the uncertainty ranges presented for all soil types (except loam) are greater in IAEA (1994) than in Sheppard and Thibault. (1990). The reason for this is not known, but it may reflect the greater uncertainty associated with applying generic K_d values to soils outside of the geographical area for which they were originally derived. Thus, it could be argued that large uncertainty ranges should be used by SKB for K_d values derived from the literature for soils and ecosystems outside of Scandinavia. It also implies that site-specifc K_d values obtained specifically for the proposed repository sites could be used with greater precision, ie. less uncertainty.

4.3.3 Selenium (^{79}Se)

Selenium exhibits a complex geochemistry. The speciation and distribution of Se in soils is dependent upon a number of (often interacting) factors, including pH, chemical and mineralogical composition of the soil, microbial interactions and the nature of adsorbing surfaces (Neal, 1995). However, perhaps the most important influence on Se behaviour is soil redox potential. In natural systems, Se exists as an anion and in four possible oxidation states: selenate (+6); selenite (+4); elemental Se (0); and selenide (-2) (Fio et al., 1991). Therefore, in oxic systems, selenate would be expected to dominate, whereas in increasingly reduced systems, progressively reduced species would be expected to form. In general, sorption of reduced species of selenium is expected to be greater than sorption of oxidized species, as illustrated by Figure 4-3. Thus, as soil redox potential is reduced, K_d values for Se would be expected to increase.

Furthermore, biomethylation of Se is known to occur under conditions of low redox potential. This can lead to loss of volatile methyl selenide from soils and sediments although, in several experiments with radioselenium (^{75}Se), this has not been observed to occur to any significant degree (Ashworth and Shaw, 2006).

The Se K_d values used by SKB are plotted in Figure 4-4 alongside K_d values obtained from several other sources. The mineral soil and aquatic values used by SKB were obtained from Coughtrey et al. (1985) and, for the organic soil, from the IAEA (1994) data base. The best estimate mineral soil value used by SKB is one to two orders of magnitude lower than the best estimate K_d values for Se for sand, loam and clay soils from the IAEA (1994) database. The best estimate organic soil K_d used by SKB is, of course, identical to the best estimate Se K_d for organic soil from IAEA (1994). No uncertainty ranges are reported for Se K_d values within IAEA (1994) and it is concluded that SKB has simply assumed a one order of magnitude uncertainty range around the organic soil K_d. It is interesting that the IAEA K_d values for Se are approximately one order of magnitude higher than the best estimates reported by Sheppard and Thibault (1990), although much of the data contained in IAEA (1994) were originally drawn from the Sheppard and Thibault source. The reason for this difference is not known, but the older values are more in line with independent in situ measurements made by Ashworth and Shaw (unpublished). These latter measurements showed that ^{75}Se K_d values were not significantly different between sandy loam, clay loam and organic soils, although flooding, which induced anoxia in the soils, increased the K_d values, in line with the data shown in Figure 4-3.

It is not clear from R-02-28 why the K_d values for Se in suspended aquatic sediments are higher than for soil Kd values since no documentation is provided.

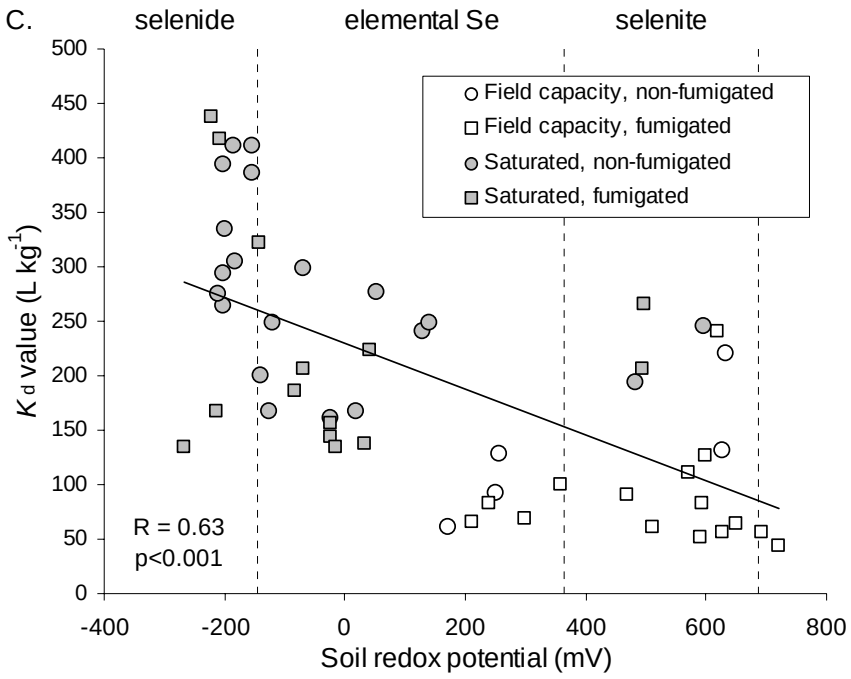

Figure 4-3. Effect of redox potential on in situ K_d for ^{75}Se in a sandy loam soil, showing redox thresholds for Se species (Ashworth and Shaw, unpublished).

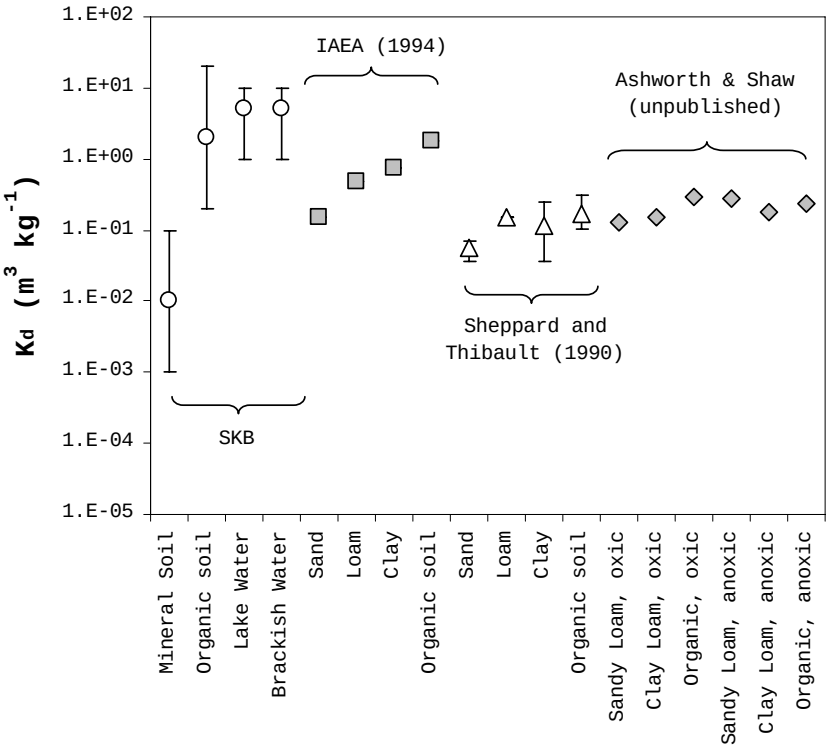

Figure 4-4. Comparison of K_d values for selenium from the SKB database with those obtained from IAEA (1994), Sheppard and Thibault (1990) and unpublished studies by Ashworth and Shaw.

4.3.4 Technetium (^{99}Tc)

The environmental chemistry of technetium is controlled to large degree by the redox potential of the surrounding medium, whether this is soil, sediment or water. Under oxic conditions the +7 oxidation state dominates, giving rise to the TcO_4^- anion which is thought to behave to some extent analogously to the NO_3^- anion in terms of its sorption and plant uptake. Repulsion of the TcO_4^- anion by electronegative surfaces of soils and sediments leads to low sorption and low K_d values, with consequently high mobility in soils and groundwaters. At low redox potentials, however, reduction to the +4 oxidation state (TcO_2) occurs. This form is insoluble and precipitates from solution at pH values greater than 3 or 4. The reduced form of Tc is associated with high K_d values, which may be relevant to periodically or permanently saturated soils or sediments. Both inorganic and organic substances have been found to complex Tc(IV) in the environment: these include halides, carbonates and phosphates (inorganic), sugars and polybasic acids (eg. humic acid) and polyhydric alcohols (Paquette et al., 1980). Of particular importance may be the interaction of Tc with humic substances, especially over the long term. Wildung et al. (1986) examined a large number of readily measurable soil variables and determined that Fe oxides were correlated strongly with early, short-term sorption of Tc, whereas organic C appeared to be the most significant soil component associated with Tc sorption over extended periods. Organic matter in soils and sediments has been identified by several authors as being of primary significance in the sorption of Tc.

Figure 4-5 shows the SKB K_d values for technetium alongside three other data sources. The first two are the IAEA (1994) and Sheppard and Thibault (1990) data bases for generic soil types, while the third (Wheater et al., 2007) shows average K_d estimates for a single soil type (loamy sand) under differing degrees of oxidation or reduction. The organic soil K_d value used by SKB is drawn from the IAEA (1994) publication. It is unusual that this K_d value should be lower than the values selected for the mineral soil and the lake sediments (presumably both assumed to be predominantly mineral sediments). The generic soil data from IAEA (1994) and Sheppard and Thibault (1990) indicate that the organic soil K_d for Tc would be expected to be generally higher than the K_d values obtained for mineral soils. The maximum K_d value for the loam soil (90 ml / g) within the IAEA data base is higher than the maximum for the organic soil (55 ml / g), although the Sheppard and Thibault (1990) K_d compendium, from which many of the data within the IAEA K_d data base are drawn, gives a maximum K_d for Tc in organic soil of 340 ml / g. This latter value is consistent with unpublished data from the BORIS 5th Framework study in which maximum K_d values of the order of 300 to >600 ml / g were observed in highly reduced soils, though values in excess of 300 were infrequent in this data set (Figure 4-6).

The three data points taken from Wheater et al. (2007) indicate the effect of increasing anoxic status of a soil on the K_d for Tc. The three values range from 0.01 to 35 ml / g and span a large portion of the range of K_d values indicated in the other data sets shown in Figure 4-5. This indicates that it may not be the soil type itself which dictates the major variation in Tc K_d, but the oxic/anoxic status of any soil.

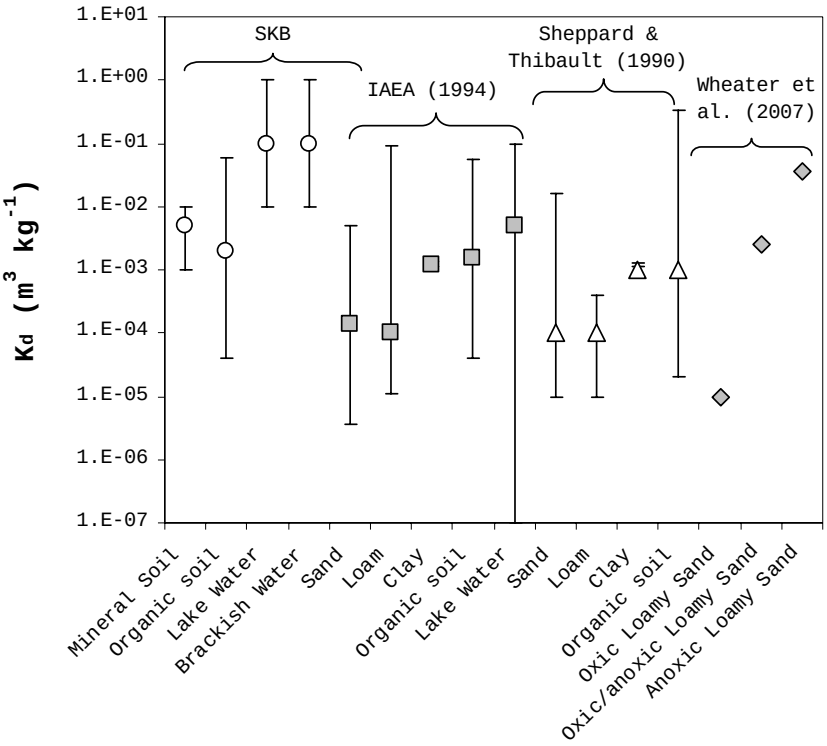

Figure 4-5. Comparison of K_d values for technetium from the SKB database with those obtained from IAEA (1994), Sheppard and Thibault (1990) and Wheater et al. (2007).

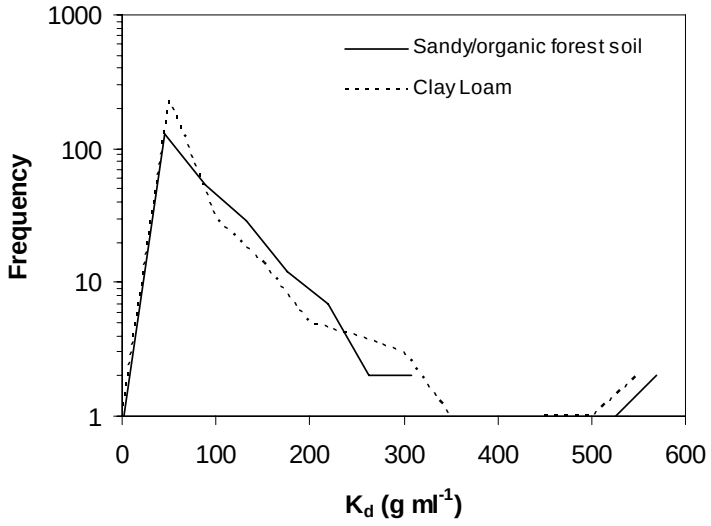

Figure 4-6. Frequency distributions of in situ Tc K_d values determined over a range of oxic and anoxic conditions in two soil types, obtained in the BORIS 5th Framework study.

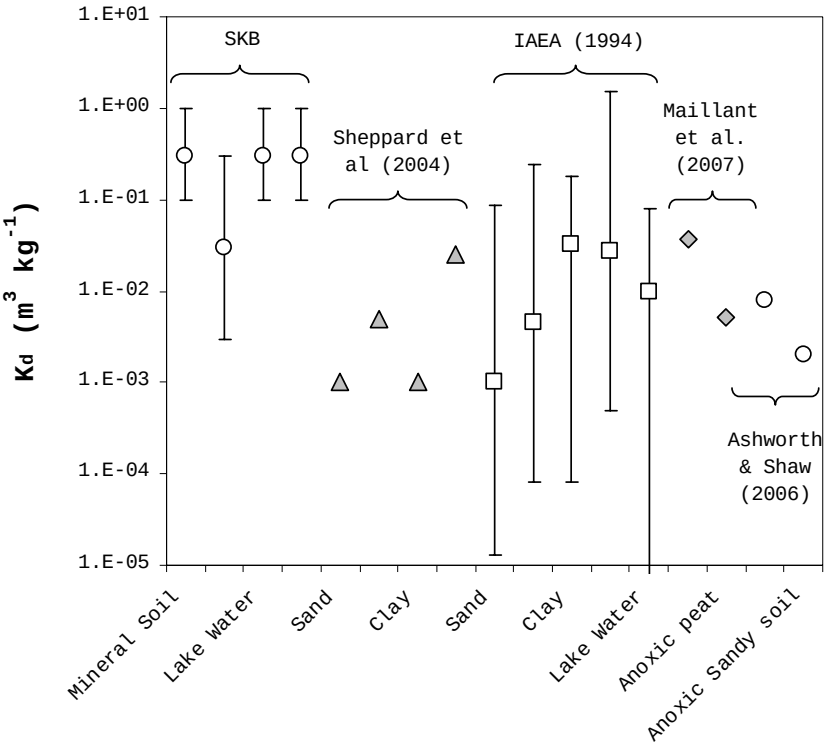

Figure 4-7**.** Comparison of K_d values for iodine from the SKB database with those obtained from Sheppard et al. (2004), IAEA (1994), Maillant et al. (2007) and Ashworth and Shaw (2006).

4.3.5 Iodine (^{129}I)

Unlike chlorine, many K_d data exist within the literature for iodine, which reflects a long-standing interest in environmental exposure pathways of this element and its associated radionuclides. The chemistry of iodine is likely to be controlled within the environment by transitions between oxidation states -1 (I^-, iodide), 0 (molecular iodine, I_2^0) and +5 (IO_3^-, iodate). Changes in redox potential in soils and waters are known to affect K_d values for iodine. Similarly, the sorption of iodine onto soils is known to be strongly affected by the presence of organic matter since iodine is an extremely organophilic element.

Figure 4-7 shows a comparison of K_d values for iodine taken from the SKB data base with those obtained from several other sources. Chief among the other literature sources used is the handbook of parameter values published by the IAEA (1994). As previously stated, the K_d database within this source is largely based on the K_d compendium published by Sheppard and Thibault (1990). K_d values for iodine have also been obtained from a more recent data review by Sheppard et al. (2002). Finally, data from two recent research papers which have provided K_d measurements for iodine under oxic and anoxic conditions are also included (Maillant et al., 2007; Ashworth and Shaw, 2006).

The first observation from Figure 4-7 is that the best estimate K_d values adopted by SKB are, in general, higher than those from the other sources listed. SKB have used the IAEA best estimate for iodine in organic soil, although the 'Low' and 'High' values they use

appear to be different from those in the IAEA publication. More important, however, is that the K_d values for mineral soil and aquatic sediments (presumably mainly mineral) are assumed to be higher than the K_d for organic soil. This is contradictory to all the other data sets summarized in Figure 4-7. As stated above, as an organophilic element iodine is known to sorb strongly to organic matter. On page 27 of R-02-28 it is stated that "Sorption to solid matter is intermediate for soil and suspended matter in fresh and brackish water but lower in peat". The available evidence (eg. Yoshida et al., 1998) suggests that the latter part of this statement (concerning peat) is incorrect. The best estimate K_d proposed by SKB for peat is in agreement with the other sources summarized in Figure 4-7. However, it is suggested that the three other K_d values proposed (for mineral soil and aquatic sediments) are probably too high and out of line with the other available data.

An important feature of iodine K_d values in soils and sediments, as described above, is the dependence on redox potential. Maillant et al. (2007) have recently made observations of aged iodine in a peat bog in Canada which indicate that in situ K_d values vary from approximately 38 ml / g in the oxic surface layers to 5 ml / g in the saturated and anoxic lower layers of peat. These observations of the effect of redox potential on iodine K_d are consistent with those of Ashworth and Shaw (2006) who studied in situ K_d values for iodine in small columns of mineral soil (loamy sand). Note (Figure 4-7) that the general effect of redox potential is the same in both studies, although the absolute K_d values are higher in the peat studied by Maillant et al. This further underlines the conclusion drawn above concerning the K_d values proposed by SKB for organic versus inorganic soils.

4.3.6 Caesium (^{135}Cs)

Radionuclides of caesium, notably ^{137}Cs and ^{134}Cs, are perhaps the most widely studied of all radionuclides due to their importance in the aftermath of the Chernobyl accident in 1986. Consequently, a very large body of evidence exists concerning the physico-chemical behaviour of radiocaesium in soils and sediments. Many of these studies are directly relevant to Sweden since much radioecological work was carried out in Swedish territories affected by Chernobyl deposition.

The behaviour of caesium in soils is controlled predominantly by interaction with clay minerals, especially illite which can selectively adsorb trace quantities of Cs in preference to other cations. K_d values for Cs are about 10^5 on illite and 10^3 L kg^{-1} on montmorillonite, another common clay mineral (Staunton and Roubaud, 1997). K_d values for caesium in soils may be as high as those for pure illite in sandy or highly organic soils, which may be due to the presence of only trace quantities of illite in such soils (Wauters et al., 1996). Sorption of Cs on organic matter such as humic substances is non-selective and, in general, an inverse correlation exists between the organic matter of a soil and Cs sorption, which is generally attributed to a reduction of clay content in increasingly organic soils. Furthermore, Staunton et al. (2002) have shown that soil organic matter can interfere with the sorption of Cs by clays.

The other major factors which influence Cs sorption in soil are the presence of cations, particularly K^+, NH_4^+ and H^+, which compete with Cs for sorption on both mineral and organic phases. Livens and Loveland (1988) established the concept of the 'immobilisation capacity' of a soil. Soils rich in clay (especially illite), low in organic matter and NH_4^+, with moderate to high pH, in general have a high immobilization capacity for Cs, and thus high K_d values. Conversely, acidic soils with relatively high organic matter, high

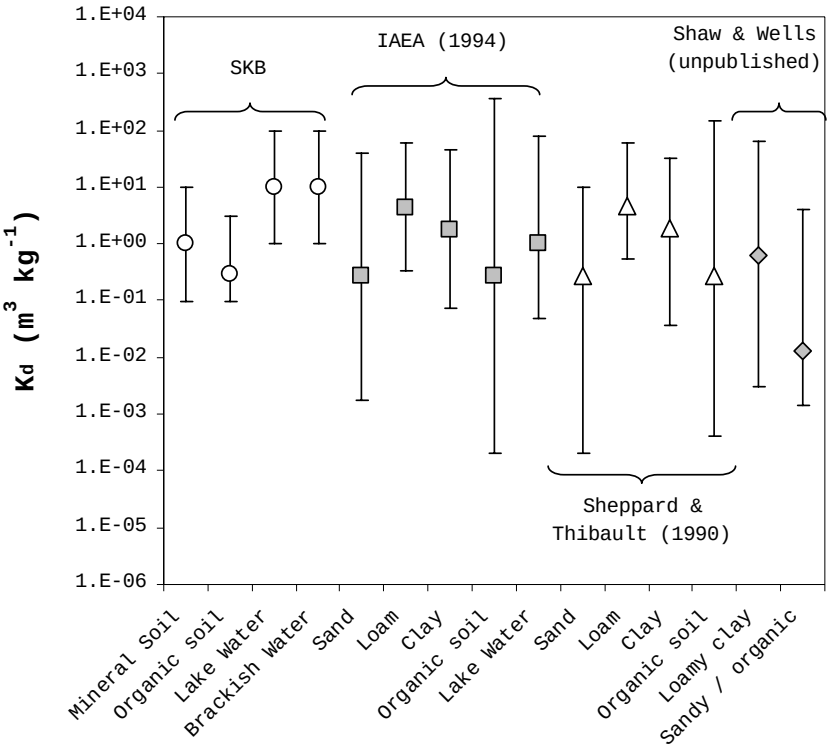

Figure 4-8. Comparison of K_d values for caesium from the SKB database with those obtained from IAEA (1994), Sheppard and Thibault (1990) and Shaw and Wells (unpublished).

NH_4^+ concentrations and low clay contents tend to have a low immobilization capacity and, therefore, low K_d values for Cs. In waters, increasing concentrations of dissolved cations, including Na^+ and K^+, will tend to desorb Cs from suspended solids. Hence, fresh waters with low base status would be expected to have high sediment-water K_d values, while estuarine and marine waters with high salt contents would be expected to have low sediment-water K_d values.

Figure 4-8 shows the K_d values for Cs used by SKB in comparison with K_d values from several other sources. The mineral soil K_d used by SKB appears to be intermediate between the sand, loam and clay values contained within the IAEA (1994) database. This seems appropriate, although the range of mineral soil values used by SKB is considerably less than the full range of values presented in IAEA (1994). The best estimate organic soil K_d used by SKB is drawn from the IAEA (1994) database, but the range of uncertainties adopted by SKB is substantially less than that presented by IAEA (1994). The soil K_d values used by SKB and presented in IAEA (1994) are in the same range as experimental estimates obtained in independent studies by Shaw and Wells (unpublished) although the best estimate K_d for a sandy/organic forest soil from the latter source is approximately one order of magnitude lower than the sand and organic best estimate K_d values drawn from IAEA (1994). This underlines the large variability in K_d values which is evident from one study to another, possibly due to methodological differences between studies.

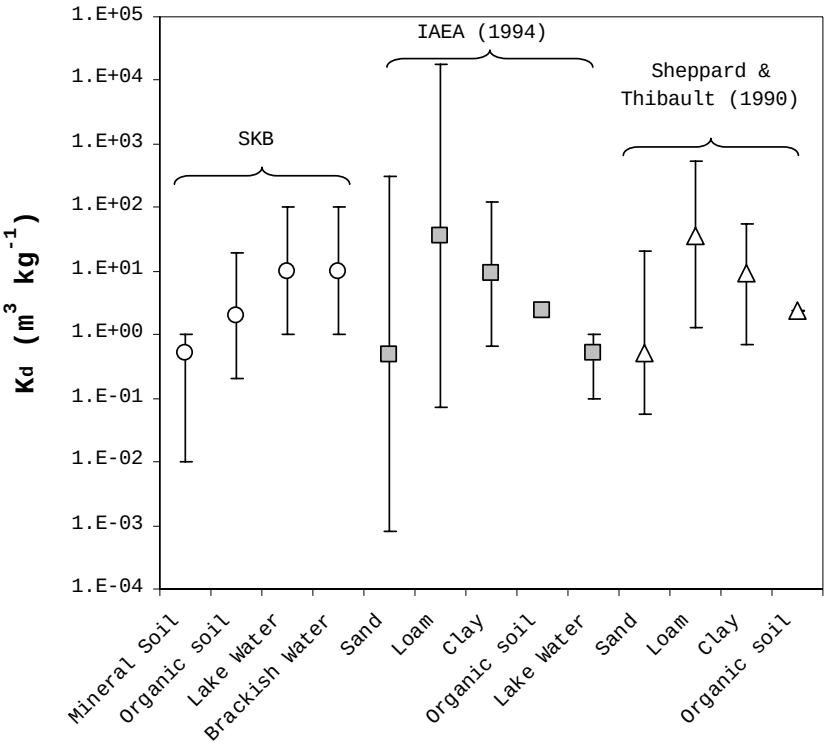

Figure 4-9: Comparison of K_d values for radium from the SKB database with those obtained from IAEA (1994) and Sheppard and Thibault (1990) .

The Shaw and Wells data is presented here as it was obtained using an in situ sampling method, which is preferable to batch methods on which many of the literature K_d estimates are based.

The two aquatic K_d values for Cs used by SKB (obtained from Coughtrey et al., 1985) are identical, with identical uncertainty ranges. Both best estimate values are one order of magnitude greater than the best estimate drawn from IAEA (1994). A lower best estimate value would certainly be expected for brackish waters, for the reasons briefly described above.

4.3.7 Radium (^{226}Ra)

Of all the elements reviewed in this document, the K_d values adopted by SKB for radium are best justified. The primary source of both mineral soil and aquatic K_d values for radium appears to be Bergstrom et al. (1984), although the organic soil value is derived from IAEA (1994). The K_d values used by SKB are shown in Figure 4-9 in comparison with soil K_d values from IAEA (1994) and Sheppard and Thibault (1990).

The best estimate mineral soil K_d value used by SKB reflects the lower end of the range of mineral soil values presented in IAEA (1994). It is almost two orders of magnitude lower than the loam soil K_d values from IAEA (1994), but almost equal to the IAEA's sandy soil K_d value. The best estimate IAEA K_d values are identical to the best estimate

values presented by Sheppard and Thibault (1990), for the reasons described in Section 4.3.2 above. Similarly, the uncertainty ranges given by Sheppard and Thibault (1990) are smaller than those in IAEA (1994).

The aquatic K_d values used by SKB are identical for both freshwater and brackish water, both in terms of best estimates and uncertainty ranges. Interestingly, these are approximately one order of magnitude greater than the freshwater K_d value for radium presented in IAEA (1994). A reasonably thorough justification of the selection of aquatic K_d values for radium is given on page 96.

4.4 Conclusions

As stated at the end of Section 4.2, K_d values for radionuclides in soils and sediments are notoriously uncertain and most compilations of K_d values will indicate large variations between upper and lower values with best estimates (usually geometric means or median values) somewhere in between these limits. For dose and risk assessment modeling, especially over long time scales during which the modeling of detailed physico-chemical processes is also subject to considerable uncertainties, the simplicity of the K_d approach is extremely useful. However, use of K_d values is only justifiable if the best estimates and ranges can be shown to apply to the systems being modelled, either by reference to appropriate literature sources or by using experimental or in situ sampling methods to obtain site specific values.

The major shortcoming of the K_d data in the SR-Can database is the lack of clear justification for selection of the values presented, either with reference to the literature or to the site specific data which has evidently been collected for Forsmark and Laxemar, reported elsewhere (SKB Reports R-04-08 and R-05-03). On close examination of individual K_d values some discrepancies are evident between values assumed by SKB and what would be expected from other published and unpublished sources (eg. chlorine and iodine K_d values in organic soils). In general, however, these discrepancies are probably small in relation to overall uncertainties in the assumed values. In order to make the selection of element-specific K_d values more defensible it is the linkage between the selected values (both absolute values and ranges of values) and the specific sites to which they are to be applied which needs to be strengthened.

4.5 Recommendations

On the basis of the conclusions above, three main recommendations can be made.

i) The K_d data base in R-02-28 should be brought up to date with reference to current literature[2].

ii) The linkage between sorption characteristics of specific elements and site

[2] One pending source of updated information will be the revised version of IAEA (1994), the publication of which is expected soon.

characteristics at the Forsmark and Laxemar sites should be made more explicit, especially with reference to updated K_d values resulting from i).

iii) SKB is encouraged to make in situ or laboratory determinations of site specific K_d values for the key elements of interest in biosphere assessments at the Forsmark and Laxemar sites. This would provide the strongest possible underpinning to i) and ii) above.

5 Conclusions

Results presented by SKB for near field and far field activity concentrations and dose rates can be reproduced when all the information is available. Since the radiological dose consequence is dominated by ^{226}Ra, further investigation and improved justification of site-specific K_d values for ^{226}Ra in the geosphere and biosphere is recommended.

SKB's development of the Landscape Dose Factor (LDF) is a welcome new approach which examines an evolving, integrated landscape instead of the single static biosphere object used in earlier assessments. However, if the approach is to be used in the safety assessment supporting the application for the construction of a geological repository, the approach requires further development in the following areas:

- The derivation of LDFs should be consistent with their use in different scenarios in the risk assessment.
- The existing method to calculate the mean dose rate from the landscape is not theoretically correct. This is because the unit release of radionuclides is distributed over all landscape objects, based on the assumption of equal probability of canister failure. Effectively this means that the releases are diluted. A revision might be considered in which this dilution did not take place. A further alternative might be to consider radionuclide release to a set of high-consequence single objects connected to a few objects further downstream. In this way a range of possible dose rates could be calculated.
- The size of the potentially contaminated area is an important issue. This review indicates that insufficient detail has been included when constructing the biosphere assessment model, leading to potentially excessive dilution. The procedure used to identify the sizes of biosphere objects should be clarified and improved.
- Models used to describe radionuclide transport and accumulation in various ecosystems should be validated as much as possible using site-specific data and process models to reflect understanding of the system and the dominant transport processes.
- Discretisation of compartmental models may affect predictions significantly, depending on factors such as boundary conditions and model parameters. Our independent modelling suggests how an appropriate discretisation can be determined for modelling radionuclide transport in water streams and QD for long-term safety assessment purpose. The independent modelling also indicates how the assessment models can be verified against the observations such as tracer experiments.
- A simulation period longer than 18 000 years might be considered to reflect uncertainty in the assumed period of temperate climate conditions, and the fact that equilibrium will not be reached for radionuclide transport though Quaternary deposits over a time period of 18 000 years.
- SKB is encouraged to make in situ or laboratory determinations of site-specific K_d values for the key radionuclides/elements of interest in biosphere assessments

at the Forsmark and Laxemar sites. This would provide more defensible estimations of K_d values.

6 References

Ashworth, D.J. and Shaw, G. (2005). Effects of moisture content and redox potential on in situ Kd values for radioiodine in soil. *Science of the Total Environment*. Doi:10.1016/j.scitotenv.2005.04.018.

Ashworth, D. J. and G. Shaw (2006). Soil migration, plant uptake and volatilisation of radio-selenium from a contaminated water table. Science of the Total Environment, 370, 506–514.

Avila R, (2006). The ecosystem models used for dose assessment in SR-Can, SKB R-06-81, Svensk Kärnbränslehantering AB

Avila, R., Ekström, P-A. Kautsky, U. (2006). Development of landscape dose factors for assessments in SR-Can. SKB TR-06-15. Svensk Kärnbränslehantering AB.

Bencala, K. E. (1983). Simulation of solute transport in a mountain pool- and-riffle stream with kinetic mass transfer model for sorption. *Water Resource Research*, 19(3), 732-738.

Bergström, U., K. Andersson and B. Rojder (1984) Variability of dose predictions for cesium-137 and radium-226 using the PRISM method. Studsvik Energiteknik AB, Sweden (STUDSVIK/NW-84/656).

Bergström, U., Nordlinder, S. and Aggeryd, I. (1999). Models for dose assessments Modules for various biosphere types. SKB TR-99-14. Svensk Kärnbränslehantering AB.

Bergström, U. and Barkefors, CM., (2004). Irrigation in dose assessments models, SKB Report R-04-26, SKB, Stockholm, Sweden

BIOMOVS, (1993), BIOMOVS Final Report, BIOMOVS Technical Report No. 15, published on behalf of the BIOMOVS Steering Committee by the Swedish Radiation Protection Institute, Stockholm Sweden

BIOMOVS II, (1996), "Biosphere Modelling for Dose Assessments of Radioactive Waste Repositories - Final Report of the Complementary Studies Working Group", Ed. R A Kłos, BIOMOVS II, Stockholm, Sweden, ISSN 11 03-8055, ISBN 91-972958

Broed, R. and Xu, S. (2008). Ecolego Toolbox version 1.0 user's manual. SSI report 2008:10. Statens strålskyddsinstitut, Sweden.

Brydsten, L, (2006). A model for landscape development in terms of shoreline displacement, sediment dynamics, lake formation, and lake choke-up processes, SKB Technical Report TR-06-40, SKB, Stockholm, Sweden

Cliffe, K. A. and Kelly, M. (2006). COMP23 version 1.2.2 user's manual. SKB R-04-64. Svensk Kärnbränslehantering AB.

Coughtrey, P. J., D. Jackson and M. C. Thorne (1985) Radionuclide distribution and transport in terrestrial and aquatic ecosystems. Rotterdam. (EUR-8115-VI).

Crawford, J., Neretniets, I. and Malmström, M. (2006). SR-Can data and uncertainty assessment for radionuclide K_d partitioning coefficients in granitic rock for use in SR-Can calculations. SKB R-06-75. Svensk Kärnbränslehantering AB.

Crusius, J. and R. F. Anderson, (1995). Evaluation of the Mobility of 137Cs, 239+240Pu and 210Pb from Their Distributions in Laminated Sediments. J. Palaeontology, 13, 119.

Elliott, A. H. and Brooks, N. H. (1997). Transfer of nonsorbing solutes to a streambed with bed forms: Theory. *Water Resource Research*, 33(1), 123-136.

Fischer, H. B., List, E. J., Koh, R. C. Y., Imberger, J. and Brooks, N. H. (1979). Mixing in inland and coastal waters. Academic Press INC. London.

Fio, J.L., R. Fujii and S. J. Deverel (1991) Selenium mobility and distribution in irrigated and nonirrigated alluvial soils. Soil Science Society of America Journal, 55, 1313 – 1320.

Global Mapper, (2007). Global Mapper 9.0, Global Mapper Software LLC, PO Box 3051, Olathe, KS 66063, USA, www.globalmapper.com

Hedin, A. (2001). Integrated analytic radionuclide transport model for a spent nuclear fuel repository in saturated fractured rock. Nuclear Technology. 138, 179-205.

Hedin, A. (2007a). E-mail to Björn Dverstorp and Bo Strömberg dated 19/3/07 on the

subject of input files for SR-Can calculations.

Hedin, A. (2007b). Letter to Bo Strömberg and Björn Dverstorp dated 29/06/07 on the subject of "Factual check of SIG report from the review of SR-Can".

Hollenbeck, K.J. (1998). INVLAP.M: A Matlab function for numerical inversion of Laplace transforms by De Hoog Algorithm, http://www.isva.dtu.dk/staff/karl/invlap.htm.

IAEA (1994). Handbook of parameter values for the prediction of radionuclide transfer in temperate environments. International Atomic Energy Agency, Vienna, Austria. (Technical Reports Series No. 364).

IAEA (2003). 'Reference Biospheres' for solid radioactive waste disposal: Report of BIOMASS Theme 1 of the BIOsphere Modelling and ASSessment (BIOMASS) Programme, 2003, IAEA-BIOMASS-6, IAEA, Vienna, Austria

Johansson, H., Jonsson, K., Forsman, K.J., Wörman, A. (2001). Retention of conservative and sorptive solutes in streams – simultaneous tracer experiment. *The Science of the Total Environment*. 266 (1–3), 229–238.

Jonsson, K. and Elert, M. (2005). Model for radionuclide transport in running water. SKB TR-05-03. Svensk Kärnbränslehantering AB.

Karlsson, S. and Bergström, U. (2002). Nuclide documentation Element specific parameter values used in the biospheric models of the safety assessments SR 97 and SAFE. SKB R-02-28. Svensk Kärnbränslehantering AB.

Karlsson, S., Bergström, U. and Meili, M. (2001). Models for dose assessments Models adapted to SFR-area, Sweden. SKB TR-01-04. Svensk Kärnbränslehantering AB.

Kautsky, U. (2006a). E-mail to Shulan Xu dated 04/12/06 on the subject of input files for SR-Can landscape model calculations.

Kautsky, U. (2006b). E-mail to Shulan Xu dated 22/12/06 on the subject of further description of landscape modelling in SR-Can.

Kłos, RA, Müller-Lemans, H, Van Dorp, F, and Gribi, P, (1996). TAME - The Terrestrial-Aquatic Model of the Environment: Model Definition, Nagra Technical Report NTB 93-04, NAGRA, Wettingen, Switzerland; PSI Technical Report No. 96-18, Würenlingen & Villigen, Switzerland, ISSN 1019-0643

Kłos, R A and Albrecht, A, (2005). The significance of agricultural vs natural ecosystem pathways in temperate climates in assessments of long-term radiological impact, Journal of Environmental Radioactivity. 83 (2005) 137 – 169

Kłos, R. (2008). The Generalised Ecosystem Modelling Approach in radiological assessment. SSI report 2008:09. Statens strålskyddsinstitut, Sweden.

Lee, R. T., G. Shaw, P. Wadey and X. Wang (2001) Specific association of ^{36}Cl with low molecular weight fractions of humic acids. Chemosphere, 43 (8), 1063-1070.

Lindborg T, (2005). Description of surface systems: Preliminary site description, Forsmark area – version 1.2, SKB R-05-03, Svensk Kärnbränslehantering AB, Stockholm, Sweden

Lindborg T, (2006). Description of surface systems - Preliminary site description, Laxemar area - version 1.2, SKB R-06-11, Svensk Kärnbränslehantering AB, Stockholm, Sweden

Lindgren, M. and Lindström, F. (1999). SR 97 Radionuclide transport calculations. TR-99-23. Svensk Kärnbränslehantering AB.

Livens, F. R. and P. J. Loveland (1988) The influence of soil properties on the environmental mobility of caesium in Cumbria. Soil Use and Management, 4, 69 – 75.

Maillant, S., M.I. Sheppard , G. Echevarria, S. Denys, G. Villemin, P. Tekely, E. Leclerc-Cessac, J.L. Morel (2007) Aged anthropogenic iodine in a boreal peat bog. Applied Geochemistry 22, 873–887.

Marklund, L., Wörman, A., Simić, E., Geier, J., Dverstorp, B. (2007). The impact of different geological parameters on transport of radionuclides. **(in press)**: *Nuclear Technology.*

Marsily, G. (1986). Groundwater Hydrology for Engineers. *Academic Press, Inc*.

Maul, P., Robinson, P., Avila, R., Broed, R., Pereira, A. and Xu, S. (2003). AMBER and Ecolego intercomparisons using calculations from SR-97. SKI report 2003:28, SSI report 2003:11.

Maul, P., Robinson, P., Bond, A. and Benbow, S. (2008). Independent calculations for the SR-Can assessment. SKI Report 2008:12, Statens kärnkrafinspektion.

Milton, G. M., J. C. D. Milton, S. Schiff, P. Cook, T. G. Kotzer and L. D. Cecil (2003) Evidence for chlorine recycling—hydrosphere, biosphere, atmosphere—in a forested wet zone on the Canadian Shield. Applied Geochemistry, 18, 1027-1042.

Neal, R.H. (1995) Selenium. In: Alloway, B.J. (ed) (1995) Heavy Metals in Soils 2nd Edition. London, Blackie Academic.

.

Norman, S. and Kjellbert, N. (1990). FARF31 – A far field radionuclide migration code for use with the PROPER package. SKB TR 90-01, Svensk Kärnbränslehantering AB.

Ogard, A.E., Thompson, J .L., Rundberg, R. S., Wolfsberg, K., Kubik, P. W., Elmore, D., Bentley, H.W. (1988) Migration of chlorine-36 and tritium from an underground nuclear test. Radiochimica Acta, 44/45, 213 - 217.

Öberg , G. (1998) Chloride and organic chlorine in soil. Acta Hydrochim. Hydrobiol., 26, 137 – 144.

Öberg , G. (2002) The natural chlorine cycle – fitting the scattered pieces. Applied Microbiology and Biotechnology, 58, 565 – 581.

Paquette, J., J. A. K. Reid and E. L. J. Rosinger (1980) Review of technetium behaviour in relation to nuclear waste disposal. Tech. Rec. TR-25, Atomic Energy of Canada Ltd., Pinawa, Manitoba, Canada.

Rodstedth, M., C. Ståhlberg, P. Sandén and G. Öberg (2003) Chloride imbalances in soil lysimeters. Chemosphere, 52, 381-389.

Romero, L., Thompson, A., Moreno, L., Neretnieks, I., Widén, H. and Boghammar, A. (1999). Comp23/Nuctran user´s guide – Proper version 1.1.6. SKB R-99-64, Svensk Kärnbränslehantering AB.

Salomons, W. and U. Förstner. (1984). *Metals in the Hydrocycle*, Springer-Verlag.

Sheppard, M. I., S. C. Sheppard and B. Sanipelli (2002) Recommended biosphere model values for iodine. Report No: 06819-REP-01200-10090. Ontario Power Generation, Nuclear Waste Management Division, 700 University Avenue, Toronto, Ontario, Canada, M5G 1X6.

Sheppard, M. I., S. C. Sheppard and B. Sanipelli (2004) Recommended biosphere model values for chlorine. Report No: 06819-REP-01200-10119-R00. Ontario Power Generation, Nuclear Waste Management Division, 700 University Avenue, Toronto, Ontario, Canada, M5G 1X6.

Sheppard., M. I. and D. H. Thibault (1990) Default soil solid/liquid partition coefficients, K_ds, for four major soil types: a compendium. Health Physics, 59, 471 – 482.

SKB, (2006a). Long-term safety for KBS-3 repositories at Forsmark and Laxemar — a first evaluation Main Report of the SR-Can project. SKB TR-06-09. Svensk Kärnbränslehantering AB.

SKB, (2006b). Data report for the safety assessment SR-Can. SKB TR-06-25. Svensk Kärnbränslehantering AB.

SKB, (2006c). The biosphere at Laxemar. Data, assumptions and models used in the SR-Can assessment. SKB R-06-83, Svensk Kärnbränslehantering AB.

SKB, (2006d). The biosphere at Forsmark: Data, assumptions and models used in the SR-Can assessment. SKB R-06-82, Svensk Kärnbränslehantering AB

Staunton, S. and M. Roubaud (1997) Adsorption of radiocaesium on montmorillonite and illite : effect of charge compensating cation, ionic strength, concentration of potassium, caesium and fulvic acid. Clays Clay Miner. 45, 251-260.

Staunton, S., C. Dumat and A. Zsolnay (2002). Possible role of soil organic matter in the availability of radiocaesium. J. Environmental Radioactivity 58, 163-173.

Vahlund, F. (2007). Personal communications during the SR-Can hearing.

Van Genuchten, M. Th. and Cleary, R. W. (1979). Movement of solutes in soil: computer-simulated and laboratory results. In: G.H. Bolt (Ed), *Soil Chemistry*, Part B. Physicochemical Models. Elsevier, Amsterdam, 349-386.

Vikström, M. and Gustafsson, L-G. (2006). Modelling transport of water and solutes in future wetlands in Forsmark. SKB R-06-46. Svensk Kärnbränslehantering AB.

Wauters, J., A. Elsen, A. Cremers, A. V. Konoplev, A.A. Bulgakov, A.A. and R. N. J. Comans (1996) Prediction of solid/liquid distribution coefficients of radiocesium in soils and sediments. Part one: a simplified procedure for the solid phase characterisation. Applied Geochemistry, 11, 589-594.

Wheater, H. S., J. N. B. Bell, A. P. Butler, B. M. Jackson, L. Ciciani, D. J. Ashworth, G. G. Shaw (2007) Biosphere implications of deep disposal of nuclear waste: the upwards migration of radionuclides in vegetated soils. Imperial College Press, series on Environmental Science and Management Vol. 5. ISBN-13 978-1-86094-743-8, ISBN-10 1-86094-743-3.

Wieland, E., P. H. Santchi, P. Höhener, and M. Sturm, (1993). Scavenging of Chernobyl 137Cs in Lake Sempach, Switzerland. *Geochim. Cosmochim. Acta*, 57, 2959.

Wildung et al. (1986) In 'Technetium in the Environment', edited by G. Desmet and C. Myttenaere. Elsevier Applied Science Publishers.

Wörman, A. (2000). Comparison of models for transient storage of solutes in small streams. *Water Resources Research*. 36(2), 455-468.

Wörman, A., Dverstorp, B. A., Kłos, R. A. and Xu, S. (2004). Role of the bio- and geosphere interface on migration pathways for 135Cs and ecological effects. *Nuclear Technology*. 148, 194-204.

Wörman, A., Packman, A. I., Johansson, H. and Jonsson, K. (2002). Effect of flow-induced exchange in hyporheic zones on longitudinal transport of solutes in streams and rivers. *Water Resources Research*. Vol. 38, N0. 1, 10.1029/2001WR000769.

Xu, S., Wörman, A. and Dverstorp, B. (2007). Criteria for resolution-scales and parameterisation of compartmental models of hydrological and ecological mass flow in watersheds. *J. of Hydrology.* 335, 364-373.

Yoshida, S., Y. Muramatsu and S. Uchida (1998) Soil-solution distribution coefficients, K_ds, of I^- and IO_3^- for 68 Japanese soils. Radiochimica Acta 82, 293-297.

Appendix I GEMA data for LF2:01 (northern Borholmsfjärden)

I.1 Characterising GEMA flowpath elements

This appendix provides an overview how GEMA models are configured using the example of flowpath element LF2:01 (Northern Borholmsfjärden). A more complete description of the Laxemar model is given by Kłos (2008).

The nature of the ecosystem type is a matter of judgement. As in SR-Can the assumption is that agricultural land is developed as soon as the possibility arises according to land rise. Table 3-2 lists the interpretation of the flowpath elements as they evolve in time. Global Mapper allows the cut and fill volumes for topographic areas to be calculated. Area features were generated from the -1m contour lines allowing for land rise. The contours in Figure 3-1 define successive objects as sea level falls.

Compartmental areas and volumes are derived from the topographic and QD thickness maps using GlobalMapper (2007). As a first approximation, the water body is assumed to follow sea level. At an interval of 1000 years the 1 m contours are used to define the volumes of the water body and sediments. As water level falls the area of emergent soil grows. The details derived using Global Mapper (2007) are shown in Table I-1.

Radionuclide transfer in GEMA are modelled by

QD, soils, sediments:
$$\lambda_{ij} = \frac{1}{V_i} \frac{F_{ij} + k_i M_{ij}}{\theta_i + (1-\varepsilon_i)\rho_i k_i} \ \text{y}^{-1}. \qquad \text{(I-1)}$$

Water column:
$$\lambda_{ij} = \frac{F_{ij} + k_i M_{ij}}{V_i} \ \text{y}^{-1}. \qquad \text{(I-2)}$$

Compartment volume is V_i [m^3], mineral density ρ_i [kg m^{-3}], porosity ε_i [-], volumetric moisture content θ_i [-] and radionuclide solid-liquid distribution coefficient (Kd) in the compartment is k_i.

Details of the interpretation of the Laxemar site were published after the finalisation of the GEMA dataset. For this reason some key data were taken from Bergström et al. (1999) rather than more recent sources. Similarly the values for precipitation and evapotranspiration were taken from Bergström and Barkefors (2004). These values are consistent with the ranges discussed by Lindborg (2006) and the values used in SR-Can (SKB 2006c).

Parameters characterising volumes and characteristics of compartments that change in time are given in Table I-2.. None varying parameters are listed in Table I-3. In determining the characteristics of streams in LF2:01 it was assumed that the depth was 0.1 m and width 2 m, based personal field observation of typical streams in the area. The length of the stream was based on an interpretation of the topography in the landscape element being modelled and derived using Global Mapper (2007).

Table I-1. Evolution of GEMA FPE LF2:01 Northern Borholmsfjärden. Volumes, areas and depths determined by 1 m contour intervals. Data derived using Global Mapper (2007) with the SKB topographic map SDEADM.UMEU_SM_HOJ_2102 and the QD map SDEADM.POS_SM_GEO_2653 (Lindborg 2006). For streams the width is assumed to be 2 m.

LF2:01 North Borholmsfjärden

Tot. area catchment	1466594	m^2				
Total QD	7.4	m	Water area	Water depth	Stream length	soil area
year AD	Δsealevel m	Type	m^2	m	m	m^2
2000	0	BCS	442534.4	1.0		27700
3000	-1	LNS	195386	0.5		274848.4
4000	-2	WNS	28105	0.3		442129.4
5000	-3	SAS	222	0.1	1110	470234.4
10000	-8	SAS	222	0.1	1110	470234.4

key	Aquatic	Terrestrial
BCS	Bay	Coastal / Natural soils
LNS	Lake	Natural soils
WNS	Wetland	Natural soils
WAS	Wetland	Agricultural soils
SAS	Streams	Agricultural soils

Table I-4 shows the fluxes calculated for the four phases of the evolution of northern Borholmsfjärden. These tables provide all the detail necessary to evaluate the transfer coefficients for a nuclide with the Kds from Table I-6, using Equations I-1 and I-2. Finally the transfer coefficients for ^{129}I and ^{226}Ra are reproduced in Table I-5.

With land rise there is a transition from marine to lacustrine, wetland and finally agricultural land. At some point drainage from the bays is assumed to take the form of a river system. The approximate location of the main drainage stream was approximated on the basis of the topographic maps.

At the transition from one ecosystem type to another a transition matrix **T** is used to partition the compartmental inventories. The matrix is case specific. In the GEMA calculations here the transitions are related to the changes in size of the aquatic and terrestrial compartments. Emergent soils are contaminated because the content of their parent material – the deep and top aquatic sediments – is distributed throughout the top soil, deep soil and deeper Quaternary material according to the transfer matrix **T**:

$$\mathbf{T} = \begin{pmatrix} f & 0 & 0 & 0 & 0 & 0 & 0 & 0 \\ 0 & f & 0 & 0 & 0 & 0 & 0 & 0 \\ 0 & 0 & 1 & 0 & 0 & 0 & 0 & 0 \\ 0 & 0 & 0 & 1 & 0 & 0 & 0 & 0 \\ (1-f)p_Q & (1-f)p_Q & 0 & 0 & 1 & 0 & 0 & 0 \\ (1-f)p_{DSoil} & (1-f)p_{DSoil} & 0 & 0 & 0 & 1 & 0 & 0 \\ (1-f)p_{TSoil} & (1-f)p_{TSoil} & 0 & 0 & 0 & 0 & 1 & 0 \\ 0 & 0 & 0 & 0 & 0 & 0 & 0 & 1 \end{pmatrix}, \qquad \text{(I-3)}$$

with $f = \dfrac{A_{LWat}\big|_k}{A_{LWat}\big|_{k-1}}$ and $p_i = \left.\dfrac{l_i\big|}{\sum_{\substack{t=Q,DSed,\\ TSed,Litt}} l_t}\right|_k$. This transfer is implemented at the end of each evolutionary timestep.

The details for LF2:01 illustrate the GEMA methodology. Data for the other ecosystem models use the same method and background material, e.g., Bergström et al. (1999), Bergström and Barkefors (2004), Kłos et al. (1996). The site specific characteristics are derived from the topographic maps and the evolutionary context. Data sets are discussed in greater detail in Kłos (2008).

Table I-2. Time varying parameters for LF2:01 Northern Borholmsfjärden as a function of time. Data derived from Global Mapper (2007) with the SKB topographic map SDEADM.UMEU_SM_HOJ_2102 and the QD map SDEADM.POS_SM_GEO_2653. For streams the width is assumed to be 2 m.

			Date AD				
			2000	3000	4000	5000	
Parameter		units	BCS	LNS	WNS	SAS	source
Local catchment area	ACatch	m^2	1024059.6	1024059.6	1024059.6	1024059.6	Derived
compartment areas	ADSed	m^2	442534.4	297611.1	28105	222	Derived
	ATSed	m^2	442534.4	297611.1	28105	222	Derived
	ALWat	m^2	442534.4	297611.1	28105	222	Derived
	AUWat	m^2	not used				
	AQ	m^2	n/a	144923.3	414429.4	442312.4	Derived
	ADSoil	m^2	n/a	144923.3	414429.4	442312.4	Derived
	ATSoil	m^2	n/a	144923.3	414429.4	442312.4	Derived
	ALitt	m^2	not used				
compartment volumes	VDSed	m^3	3230501.12	2172561.03	205166.5	44.4	Derived
	VTSed	m^3	44253.44	29761.11	2810.5	22.2	Derived
	VLWat	m^3	452181.6219	155708.8249	7479.85	44.4	Derived
	VUWat	m^3	not used				
	VQ	m^3	n/a	1036201.595	2963170.21	2830799.36	Derived
	VDSoil	m^3	n/a	21738.495	62164.41	309618.68	Derived
	VTSoil	m^3	n/a	14492.33	41442.94	132693.72	Derived
	VLitt	m^3	not used				
compartment thicknesses	LDSed	m	7.3	7.3	7.3	0.2	Derived
	LTSed	m	0.1	0.1	0.1	0.1	Assumed
	LLWat	m	1.021799937	0.523195623	0.266139477	0.2	Derived
	LUWat	m	not used				
	LQ	m	n/a	7.15	7.15	6.4	Derived
	LDSoil	m	n/a	0.15	0.15	0.7	Bergström et al. 1999
	LTSoil	m	n/a	0.1	0.1	0.3	Bergström et al. 1999
	LLitt	m	not used				
compartment porosity	EpsDSed	-	0.3	0.3	0.3	0.3	Bergström et al. 1999
	EpsTSed	-	0.6	0.6	0.6	0.6	Bergström et al. 1999
	EpsQ	-	n/a	0.3	0.3	0.3	Bergström et al. 1999
	EpsDSoil	-	n/a	0.3	0.3	0.5	Bergström et al. 1999
	EpsTSoil	-	n/a	0.3	0.3	0.8	Bergström et al. 1999
	EpsLitt	-	not used				
compartment volumetric moisture content	ThetaDSed	-	0.3	0.3	0.3	0.3	Saturated
	ThetaTSed	-	0.6	0.6	0.6	0.6	Saturated
	ThetaQ	-	n/a	0.3	0.3	0.3	Saturated
	ThetaDSoil	-	n/a	0.3	0.3	0.5	Saturated
	ThetaTSoil	-	n/a	0.3	0.25	0.6	Assumed
	ThetaLitt	-	not used				

Table I-3. Time invariant parameters for LF2:01.These parameters are applicable to all ecosystems.

Parameter		units	value	source
evapotranspiration	dETp	m y^{-1}	0.5	Bergström & Barkefors (2004)
precipitation	dppt	m y^{-1}	0.6	Bergström & Barkefors (2004)
mass deposition rate	mDep	kg m^{-2} y^{-1}	0.01	Assumed value
erosion rate	mEros	kg m^{-2} y^{-1}	0.01	Assumed value
groundwater velocity entering	vGBI	m y^{-1}	0.058	SKB (2006c)
biosphere	phiGBI	rad	1.570796	Assumed vertical
capillary rise	dcapil	m y^{-1}	0.1	Klos et al (1996)
active biomass	mDSoil	kg m^{-2}	0.1	Klos et al (1996)
biomass activity	wDSoil	y^{-1}	20	Klos et al (1996)
irrigation	dirri	m y^{-1}	0	No irrigation
suspended solid load	alphaDSed	kg m^{-3}	0.002	Assumed from Kłos et al. (1996)
	alphaTSed	kg m^{-3}	0.002	Assumed from Kłos et al. (1996)
	alphaLWat	kg m^{-3}	0.002	Assumed from Kłos et al. (1996)
	alphaUWat	kg m^{-3}	not used	
	alphaQ	kg m^{-3}	0.001	Assumed from Kłos et al. (1996)
	alphaDSoil	kg m^{-3}	0.001	Assumed from Kłos et al. (1996)
	alphaTSoil	kg m^{-3}	0.001	Assumed from Kłos et al. (1996)
	alphaLitt	kg m^{-3}	not used	
compartment density*	RhoLWat	kg m^{-3}	1000	
	RhoDSed	kg m^{-3}	2650	Density of parent mineral
	RhoTSed	kg m^{-3}	2650	
	RhoQ	kg m^{-3}	2650	
	RhoDSoil	kg m^{-3}	2650	
	RhoTSoil	kg m^{-3}	2650	
	RhoLitt	kg m^{-3}	2650	

* There is some debate about the use of density in the SR-Can models. The use of mineral density here means that bulk density can be readily expressed as $\rho_{bulk} = (1-\varepsilon)\rho_{mineral}$ if the sample is dried. For a wet sample this might become $\rho_{bulk} = (1-\varepsilon)\rho_{mineral} + \theta\rho_{water}$ might be used. The porosity of the medium is ε and volumetric moisture content θ.

Table I-4. Water and solid material fluxes in LF2:01 used in the evaluation of transfer coefficient.

Water fluxes $m^3\ y^{-1}$

	2000 AD – Bay with coastal soil		3000 AD – Lake with natural soil	
F_ATM_Catch	dppt*ACatch	6.14×10^5	dppt*ACatch	6.14×10^5
F_ATM_Lwat	dppt*ALWat	2.66×10^5	dppt*ALWat	1.79×10^5
F_ATM_Tsoil			dppt*ATsoil	8.70×10^4
F_Catch_Lwat	F_inflow_LWat+F_ATM_Catch-F_Catch_ATMOut	1.02×10^5		
F_Catch_ATMOut	dETp*ACatch	5.12×10^5	dETp*ACatch	5.12×10^5
F_Catch_Tsoil			F_ATM_Catch-F_Catch_ATMOut	1.02×10^5
F_Dsed_Tsed	F_GBI_Dsed	2.61×10^4	F_GBI_Dsed+F_Q_Dsed	1.34×10^5
F_Tsed_Lwat	F_Dsed_Tsed	2.61×10^4	F_Dsed_Tsed	1.34×10^5
F_Lwat_ATMOut	dETp*ALWat	2.21×10^5	dETp*ALWat	1.49×10^5
F_GBI_Dsed	ADSed*vGBI*SIN(phiGBI)	2.61×10^4	ADSed*vGBI*SIN(phiGBI)	1.76×10^4
F_GBI_Q				
F_Q_Dsed			F_Dsoil_Q-F_Q_Dsoil+F_GBI_Q	1.17×10^5
F_Q_Dsoil			dcapil*AQ	1.45×10^4
F_Dsoil_Q			F_Q_Dsoil+F_Tsoil_Dsoil-F_Dsoil_Tsoil	1.31×10^5
F_Dsoil_Tsoil			dcapil*ADSoil	1.45×10^4
F_Tsoil_ATMOut			dETTSoil*ATsoil	7.25×10^4
F_Tsoil_Dsoil			F_ATM_Tsoil+F_Catch_Tsoil+F_Dsoil_Tsoil-F_Tsoil_ATMOut	1.31×10^5
F_Lwat_EcoOutflow	F_ATM_Lwat-F_Lwat_ATMOut+F_Catch_Lwat+F_Tsed_Lwat	1.73×10^5	F_ATM_Lwat+F_Tsed_Lwat-F_Lwat_ATMOut	1.64×10^5

Solid material flux kg y-1

	2000 AD – Bay with coastal soil		3000 AD – Lake with natural soil	
M_ATM_Lwat	mdep*ALWat	4.43×10^3	mdep*ALWat	2.98×10^3
M_ATM_Tsoil			mdep * ATsoil	1.45×10^3
M_Catch_Lwat	M_inflow_LWat+alphaQ*F_Catch_Lwat	1.02×10^2		
M_Catch_Tsoil			M_inflow_TSoil+alphaTSoil*F_Catch_Tsoil	1.02×10^2
M_Dsed_Tsed	M_GBI_Dsed	5.22×10^1	M_Q_Dsed+M_GBI_Dsed	1.59×10^3
M_Dsed_GBI	M_Tsed_Dsed	4.58×10^3	M_Tsed_Dsed+M_GBI_Dsed+M_Q_Dsed-M_Dsed_Tsed	4.56×10^3
M_Tsed_Dsed	M_Lwat_Tsed	4.58×10^3	M_Dsed_Tsed+M_Lwat_Tsed-M_Tsed_Lwat	4.56×10^3
M_Tsed_Lwat	M_Dsed_Tsed	5.22×10^1	M_Dsed_Tsed	1.59×10^3
M_Lwat_Tsed	M_Tsed_Lwat+M_Catch_Lwat+M_ATM_Lwat	4.58×10^3	M_ATM_Lwat+M_Tsed_Lwat	4.56×10^3
M_GBI_Dsed	alphaDSed*F_GBI_Dsed	5.22×10^1	alphaDSed*F_GBI_Dsed	3.51×10^1
M_GBI_Q				
M_Q_Dsed			M_Dsoil_Q-M_Q_Dsoil+M_GBI_Q	1.55×10^3
M_Q_Dsoil			alphaQ*F_Q_Dsoil	1.45×10^1
M_Dsoil_Q			M_Q_Dsoil+M_Tsoil_Dsoil-M_Dsoil_Tsoil	1.57×10^3
M_Dsoil_Tsoil			alphaDSoil*F_Dsoil_Tsoil+wDsoil*mDSoil*ADSoil	2.90×10^5
M_Tsoil_Dsoil			M_ATM_Tsoil+M_Catch_Tsoil+M_Dsoil_Tsoil	2.91×10^5

Table I-4. Water and solid material fluxes in LF2:01 used in the evaluation of transfer coefficient. (Continued.)

Water fluxes $m^3\ y^{-1}$

	4000 AD – wetland with natural soil		5000 AD – Stream with agricultural soil	
F_ATM_Catch	dppt*ACatch	6.14×10^{5}	dppt*ACatch	6.14×10^{5}
F_ATM_Lwat	dppt*ALWat	1.69×10^{4}	dppt*ALWat	1.33×10^{2}
F_ATM_Tsoil	dppt*ATsoil	2.49×10^{5}	dppt*ATsoil	2.65×10^{5}
F_Catch_Lwat				
F_Catch_ATMOut	dETp*ACatch	5.12×10^{5}	dETp*ACatch	5.12×10^{5}
F_Catch_Tsoil	F_ATM_Catch-F_Catch_ATMOut	1.02×10^{5}	F_ATM_Catch-F_Catch_ATMOut	1.02×10^{5}
F_Dsed_Tsed	F_GBI_Dsed+F_Q_Dsed	1.46×10^{5}	F_GBI_Dsed+F_Q_Dsed	1.73×10^{5}
F_Tsed_Lwat	F_Dsed_Tsed	1.46×10^{5}	F_Dsed_Tsed	1.73×10^{5}
F_Lwat_ATMOut	dETp*ALWat	1.41×10^{4}	dETp*ALWat	1.11×10^{2}
F_GBI_Dsed	ADSed*vGBI*SIN(phiGBI)	1.66×10^{3}		
F_GBI_Q			AQ*vGBI*SIN(phiGBI)	2.61×10^{4}
F_Q_Dsed	F_Dsoil_Q-F_Q_Dsoil+F_GBI_Q	1.44×10^{5}	F_Dsoil_Q-F_Q_Dsoil+F_GBI_Q	1.73×10^{5}
F_Q_Dsoil	dcapil*AQ	4.14×10^{4}	dcapil*AQ	4.42×10^{4}
F_Dsoil_Q	F_Q_Dsoil+F_Tsoil_Dsoil-F_Dsoil_Tsoil	1.85×10^{5}	F_Q_Dsoil+F_Tsoil_Dsoil-F_Dsoil_Tsoil	1.91×10^{5}
F_Dsoil_Tsoil	dcapil*ADSoil	4.14×10^{4}	dcapil*ADSoil	4.42×10^{4}
F_Tsoil_ATMOut	dETTSoil*ATsoil	2.07×10^{5}	dETTSoil*ATsoil	2.21×10^{5}
F_Tsoil_Dsoil	F_ATM_Tsoil+F_Catch_Tsoil+F_Dsoil_Tsoil-F_Tsoil_ATMOut	1.85×10^{5}	F_ATM_Tsoil+F_Catch_Tsoil+F_Dsoil_Tsoil-F_Tsoil_ATMOut	1.91×10^{5}
F_Lwat_EcoOutflow	F_ATM_Lwat+F_Tsed_Lwat-F_Lwat_ATMOut	1.48×10^{5}	F_ATM_Lwat+F_Tsed_Lwat-F_Lwat_ATMOut	1.73×10^{5}

Solid material flux kg y-1

	4000 AD – wetland with natural soil		5000 AD – Stream with agricultural soil	
M_ATM_Lwat	mdep*ALWat	2.81×10^{2}	mdep*ALWat	2.22×10^{0}
M_ATM_Tsoil	mdep * ATsoil	4.14×10^{3}	mdep * ATsoil	4.42×10^{3}
M_Catch_Lwat				
M_Catch_Tsoil	M_inflow_TSoil+alphaTSoil*F_Catch_Tsoil	1.02×10^{2}	M_inflow_TSoil+alphaTSoil*F_Catch_Tsoil	1.02×10^{2}
M_Dsed_Tsed	M_Q_Dsed+M_GBI_Dsed	4.25×10^{3}	M_Q_Dsed+M_GBI_Dsed	4.55×10^{3}
M_Dsed_GBI	M_Tsed_Dsed+M_GBI_Dsed+M_Q_Dsed-M_Dsed_Tsed	4.53×10^{3}		
M_Tsed_Dsed	M_Dsed_Tsed+M_Lwat_Tsed-M_Tsed_Lwat	4.53×10^{3}		
M_Tsed_Lwat	M_Dsed_Tsed	4.25×10^{3}	M_Dsed_Tsed	4.55×10^{3}
M_Lwat_Tsed	M_ATM_Lwat+M_Tsed_Lwat	4.53×10^{3}		
M_GBI_Dsed	alphaDSed*F_GBI_Dsed	3.32×10^{0}		
M_GBI_Q			alphaQ*F_GBI_Q	2.61×10^{1}
M_Q_Dsed	M_Dsoil_Q-M_Q_Dsoil+M_GBI_Q	4.25×10^{3}	M_Dsoil_Q-M_Q_Dsoil+M_GBI_Q	4.55×10^{3}
M_Q_Dsoil	alphaQ*F_Q_Dsoil	4.14×10^{1}	alphaQ*F_Q_Dsoil	4.42×10^{1}
M_Dsoil_Q	M_Q_Dsoil+M_Tsoil_Dsoil-M_Dsoil_Tsoil	4.29×10^{3}	M_Q_Dsoil+M_Tsoil_Dsoil-M_Dsoil_Tsoil	4.57×10^{3}
M_Dsoil_Tsoil	alphaDSoil*F_Dsoil_Tsoil+wDsoil*mDSoil*ADSoil	8.29×10^{5}	alphaDSoil*F_Dsoil_Tsoil+wDsoil*mDSoil*ADSoil	8.85×10^{5}
M_Tsoil_Dsoil	M_ATM_Tsoil+M_Catch_Tsoil+M_Dsoil_Tsoil	8.33×10^{5}	M_ATM_Tsoil+M_Catch_Tsoil+M_Dsoil_Tsoil	8.89×10^{5}
M_Lwat_EcoOutflow			M_Tsed_Lwat+M_ATM_Lwat+M_Catch_Lwat	4.55×10^{3}

Table I-5. GEMA transfer coefficients for ^{129}I and ^{226}Ra in LF2:01 derived from the mass fluxes in Table I-4.

		Date AD			
Nuclide	Transfer coefficient y^{-1}	2000	3000	4000	5000
^{129}I	lambda_Dsed_Tsed	1.44E-04	1.11E-03	1.28E-03	6.96E+01
	lambda_Tsed_Dsed	9.58E-05	1.42E-04	1.49E-03	
	lambda_Tsed_Lwat	1.82E-02	1.39E-01	1.60E+00	2.40E+02
	lambda_Lwat_Tsed	3.04E-03	8.79E-03	1.82E-01	
	lambda_Lwat_EcoOutflow	3.82E-01	1.05E+00	1.98E+01	3.92E+03
	lambda_Q_Dsed		2.02E-03	8.80E-05	1.09E-03
	lambda_Q_Dsoil		2.50E-04	2.51E-05	2.79E-04
	lambda_Dsoil_Q		1.08E-01	5.39E-03	1.53E-02
	lambda_Dsoil_Tsoil		1.91E-02	8.38E-03	5.68E-03
	lambda_Tsoil_Dsoil		2.71E-02	9.08E-02	2.16E-02
^{226}Ra	lambda_Dsed_Tsed	2.19E-06	1.71E-05	2.02E-04	1.10E+00
	lambda_Tsed_Dsed	9.76E-05	1.45E-04	1.52E-03	
	lambda_Tsed_Lwat	2.79E-04	2.18E-03	2.58E-02	3.86E+00
	lambda_Lwat_Tsed	1.01E-01	2.93E-01	6.06E+00	
	lambda_Lwat_EcoOutflow	3.82E-01	1.05E+00	1.98E+01	4.92E+03
	lambda_Q_Dsed		3.12E-05	1.39E-05	1.73E-05
	lambda_Q_Dsoil		3.78E-06	3.78E-06	4.22E-06
	lambda_Dsoil_Q		1.67E-03	8.41E-04	2.44E-04
	lambda_Dsoil_Tsoil		7.37E-03	7.37E-03	2.21E-03
	lambda_Tsoil_Dsoil		2.06E-02	1.20E-02	1.80E-02

I.2 Radionuclide specific and dietary data in the GEMA calculations

The source data for radionuclides in the GEMA models of the Laxemar bays Borholmsfjärden and S Getbergsfjärden are those given by Karlsson & Bergström (2002). Additional data are used in the food web calculations taken from BIOMASS (IAEA 2003) and Kłos & Albrecht (2005) as noted below. Details of the exposure pathway database are given by Kłos (2008).

Table I-6. Solid – liquid distribution coefficients [m^3 kg^{-1}] Karlsson & Bergström (2002).

nuclide	Half life y	Soil m^3 kg^{-1}	Organic Soil m^3 kg^{-1}	susp solids lakes m^3 kg^{-1}	susp solids brackish water m^3 kg^{-1}
^{36}Cl	301000	0.001	0.01	1	0.001
^{59}Ni	76000	0.5	1	10	10
^{79}Se	1130000	0.01	2	5	5
^{99}Tc	211000	0.005	0.002	0.1	0.1
^{129}I	15700000	0.3	0.03	0.3	0.3
^{135}Cs	2300000	1	0.3	10	10
^{226}Ra	1600	0.5	2	10	10
^{210}Pb	22.3	0.1	20	0.05	0.05
^{210}Po	0.37891647	0.5	7	10	20

GEMA compartment	BCS	LNS	WNS	SAS	WAS
KLitt	-	-	-	-	-
KTSoil	organic	organic	organic	soil	soil
KDSoil	organic	organic	organic	organic	organic
KQ	organic	organic	organic	organic	organic
KUWat	-	-	-	-	-
KLWat	brackish	lake	lake	lake	lake
KTSed	organic	organic	organic	organic	organic
KDSed	organic	organic	organic	organic	organic

key	Aquatic	Terrestrial
BCS	Bay	Coastal / Natural soils
LNS	Lake	Natural soils
WNS	Wetland	Natural soils
WAS	Wetland	Agricultural soils
SAS	Streams	Agricultural soils

I.3 Ecosystem models in GEMA and SR-Can

A GEMA module consists of eight compartments not all of which may be active at all times. This gives the flexibility to model terrestrial and aquatic subsystems in the same module. This appendix compares the structure of key ecosystem types in the SR-Can review as represented in both GEMA and the SR-Can models. The GEMA emulation of the SR-Can models is based on an interpretation of SKB (2006cd).

Bays and lakes:

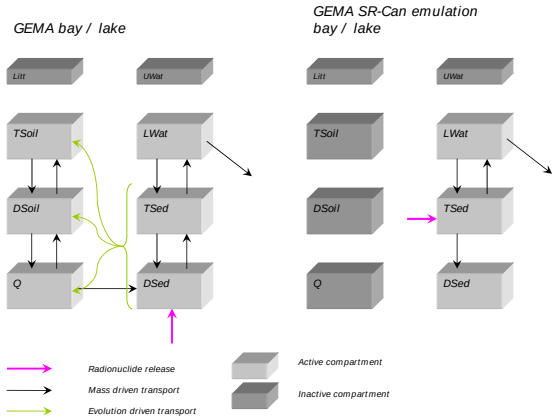

Wetlands / mires:

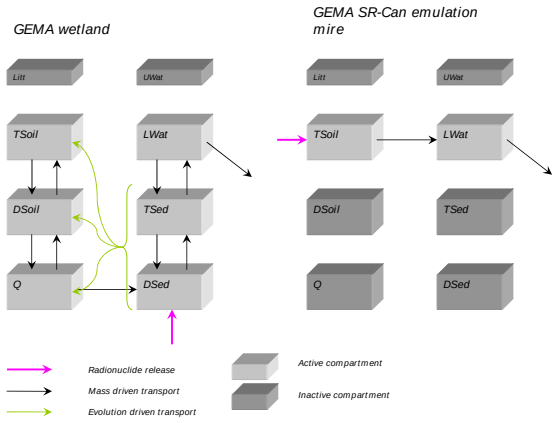

Agricultural land:

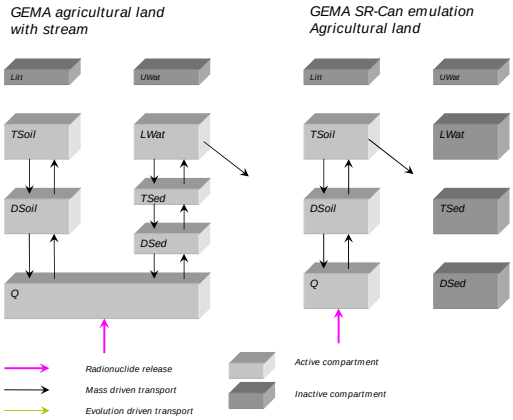

Appendix II Input data used in independent transport calculation

Table II-1 Parameter values in compartmental models

	Parameters	Definitions	Units	Values	References
Quaternary deposits model	u_{QD}	Darcy velocity in QD	[m/y]	0.058	SKB (2006c)
	D	Dispersion coefficient	[m^2/y]	0.0065	Assumed in this report
	L_{QD}	Thickness of QD	[m]	6	Assumed in this report
	ρ_{QD}	Density of QD	[kg/m^3]	1060	SKB (2006c)
	ε_{QD}	Porosity of QD	[-]	0.91	SKB (2006c)
	n_{QD}	Number compartments	[-]	60	This report
Irrigated agricultural land model	N_{IRR}	Number of irrigation	[number/y]	5	Karlsson et al, (2001)
	V_{IRR}	Water amount for each irrigation	[m]	0.03	Karlsson et al, (2001)
	A_{IRR}	Area of irrigated soil	[m^2]	1×10^5	Assumed in this report
	VW	Volume of irrigation water source	[m^3]	4.6×10^5	Kautsky (2006a)
	Rem	Removal of soil	[kg/(m^2y)]	0.005	Karlsson et al, (2001)
	ρ_p	Density of soil particles	[kg/m^3]	700	SKB (2006c)
	εt	Porosity of top soil	[-]	0.6	SKB (2006c)
	ε_d	Porosity of deep soil	[-]	0.6	SKB (2006c)
	R_{unoff}	Runoff	[m/y]	0.154	SKB (2006c)
	BioT	Bioturbation	[kg/(m^2y)]	2	Karlsson et al, (2001)
	D_{ts}	Depth of top soil	[m]	0.25	Karlsson et al, (2001)
	D_{ds}	Depth of deep soil	[m]	0.75	Karlsson et al, (2001)
River model	$<V>_z\xi/2$	Advective velocity into sediment	[m/y]	125	Wörman et al., (2002)
	A/P	Hydraulic radius (ratio of cross -section area and wetted perimeter)	[m]	0.77	Wörman et al., (2002)
	ρ_{riv}	Density of sediment	[kg/m^3]	1060	SKB (2006c)
	ε_{riv}	Porosity of sediment	[-]	0.91	SKB (2006c)
	z	Thickness of sediment	[m]	0.4	Johansson et al., (2001)
	n_{riv}	Number of sediment compartments	[-]	2	This report
	u_{riv}	Water velocity in river	[m/y]	4.7×10^6	Kautsky (2006a)
	L_{riv}	Length of the river	[m]	3812	Kautsky (2006a)

SSI-rapporter 2008

SSI reports 2008

2008:01 Myndigheternas granskning av SKB:s preliminära säkerhetsbedömningar för Forsmark och Laxemar
Avdelningen för kärnteknik och avfall och SKI
Maria Nordén, Öivind Toverud, Petra Wallberg, Bo Strömberg, Anders Wiebert, Björn Dverstorp, Fritz Kautsky, Eva Simic och Shulan Xu 90 SEK

2008:02 Patientstråldoser vid röntgendiagnostik i Sverige – 1999 och 2006
Avdelningen för personal- och patientstrålskydd
Wolfram Leitz och Anja Almén 110 SEK

2008:03 Radiologiska undersökningar i Sverige under 2005
Avdelningen för personal- och patientstrålskydd
Anja Almén, Sven Richter och Wolfram Leitz 110 SEK

2008:04 SKI:s och SSI:s gemensamma granskning av SKB:s Säkerhetsrapport SR-Can. Granskningsrapport
Avdelningen för kärnteknik och avfall
Björn Dverstorp och Bo Strömberg 110 SEK

2008:04 E SKI's and SSI's review of SKB's safety report SR-Can
Avdelningen för kärnteknik och avfall
Björn Dverstorp och Bo Strömberg 110 SEK

2008:05 International Expert Review of Sr-Can: Safety Assessment Methodology; External review contribution in support of SSI's and SKI's review of SR-Can
Avdelningen för kärnteknik och avfall
Budhi Sagar, et al 110 SEK

2008:06 Review of SKB's Safety Assessment SR-Can: –Contributions in support of SKI's and SSI's review by external consultants
Avdelningen för kärnteknik och avfall
Pierre Glynn et.al. 110 SEK

2008:07 Modelling of long term geochemical evolution and study of mechanical perturbation of bentonite buffer of a KBS-3 repository
Avdelningen för kärnteknik och avfall
Marsal F. et al. 110 SEK

2008:08 SSI's independent consequence calculations in support of the regulatory review of the SR-Can safety assessmenty
Avdelningen för kärnteknik och avfall
Shulan Xu, Anders Wörman, Björn Dverstorp, Richard Kłos, George Shaw och Lars Marklund 110 SEK

SSI report

STATENS STRÅLSKYDDSINSTITUT, SSI, är en central tillsynsmyndighet som verkar för ett gott strålskydd för människan och miljön, nu och i framtiden.

SSI sätter gränser för stråldoser till allmänheten och för dem som arbetar med strålning, utfärdar föreskrifter och kontrollerar att de efterlevs. SSI håller beredskap dygnet runt mot olyckor med strålning. Myndigheten informerar, utbildar och utfärdar råd och rekommendationer samt stöder och utvärderar forskning. SSI bedriver även internationellt utvecklingssamarbete.

Myndigheten, som sorterar under Miljödepartementet, har 110 anställda och är belägen i Solna.

THE SWEDISH RADIATION PROTECTION AUTHORITY (SSI) is a central regulatory authority charged with promoting effective radiation protection for people and the environment today and in the future.

SSI sets limits on radiation doses to the public and to those that work with radiation. SSI has staff on standby round the clock to respond to radiation accidents. Other roles include information, education, issuing advice and recommendations, and funding and evaluating research.

SSI is also involved in international development cooperation. SSI, with 110 employees located at Solna near Stockholm, reports to the Ministry of Environment.

Statens strålskyddsinstitut
Swedish Radiation Protection Authority

Adress: Statens strålskyddsinstitut; S-171 16 Stockholm
Besöksadress: Solna strandväg 96
Telefon: 08-729 71 00, **Fax**: 08-729 71 08

Address: Swedish Radiation Protection Authority
SE-171 16 Stockholm; Sweden
Visiting address: Solna strandväg 96
Telephone: + 46 8-729 71 00, **Fax**: + 46 8-729 71 08
www.ssi.se